To the Graduate Council:

I am submitting herewith a thesis written by Donald W. Brew entitled "Effects of Hypothetical NO_x Sources in East Tennessee on the Ozone Concentrations Impacting the GSMNP." I have examined the final copy of this thesis for form and content and recommend that it be accepted in partial fulfillment of the requirements for the degree of Master of Science, with a major in Environmental Engineering.

Terry L. Miller, Major Professor

We have read this thesis
and recommend its acceptance:

James L. Smoot

Wayne T. Davis

Accepted for the Council:

Associate Vice Chancellor and
Dean of the Graduate School

EFFECTS OF HYPOTHETICAL NO_X SOURCES IN EAST TENNESSEE ON THE OZONE CONCENTRATIONS IMPACTING THE GSMNP

A Thesis
Presented for the
Master of Science
Degree
The University of Tennessee, Knoxville

Donald W. Brew
May 1996

ABSTRACT

This thesis studied the effects of hypothetical NO_x sources located in East Tennessee on the ozone concentrations impacting the Great Smoky Mountains National Park (GSMNP). The product of this study is a technique of assessing the potential impact of a new or modified large NO_x source on ozone concentrations within a Class I area, without requiring an up-to-date detailed emissions inventory. The study evaluates the MAP-O3 model as a screening tool for selecting the day to be modeled by the Urban Airshed Model (UAM) for each hypothetical source location. The four source locations selected to be studied in East Tennessee were: Chattanooga, Crossville, Knoxville, and the Tri-Cities area. The results of MAP-O3 simulations were compared to UAM simulation results in determining that the MAP-O3 model was effective in selecting the modeling scenarios for which the UAM would predict incremental increases of ozone in the GSMNP due to the potential source. The study also investigates the effects of using EPA default concentrations along the boundary of the modeling domain on predicted ozone concentrations within the modeling domain. It was found that the use of default boundary conditions may significantly affect ozone concentration predictions in the domain, so a technique was developed to minimize these effects by utilizing temporally varying concentrations along the boundary that were predicted during modeling scenarios.

TABLE OF CONTENTS

CHAPTER PAGE

1. INTRODUCTION....1

2. LITERATURE REVIEW....5

2.1 Ozone Formation....5

2.2 Vegetation Damage Attributed to Ozone....7

2.3 Class I Areas....8

2.4 Great Smoky Mountains National Park (GSMNP)....10

2.5 UAM....11

2.6 MAP-O3....14

3. SELECTION OF MODELING SCENARIOS....17

3.1 MAP-O3 Runs....17

3.2 Selected Days to be Modeled at Knoxville....18

3.3 Selected Day to be Modeled at Crossville....18

3.4 Selected Day to be Modeled at Chattanooga....18

3.5 Selected Day to be Modeled at Tri-Cities....19

3.6 MAP-O3 Results....19

4. UAM INPUT FILES....20

4.1 Wind Files....20

4.2 Emissions File....27

4.2.1 Biogenic Emissions....27

4.2.2 Anthropogenic Emissions....28

4.3 Point Source Emission File....30

4.4 Mixing Height Input File....31

4.5 Temperature File....33

4.6 Meteorological Parameters File....34

4.7 Initial and Boundary Default Concentrations....40

5. PRELIMINARY RESULTS....42
5.1 Basecase Scenarios....42
5.2 July 07 & July 10 Point Source Scenarios....50
5.3 June 30 Point Source Scenarios....55
5.4 June 14 Point Source Scenarios....57
5.5 July 25 Point Source Scenarios....59
5.6 TVP Method....63

6. FINAL RESULTS....66
6.1 TVP Basecase Results....66
6.2 July 07 & July 10 TVP Scenarios....72
6.3 June 14 TVP Scenarios....73
6.4 June 30 TVP Scenarios....80
6.5 July 25 TVP Scenarios....81
6.6 Comparison to MAP-O3 Results....86

7. CONCLUSIONS....89
7.1 Basecase Scenarios....89
7.2 July 07 and July 10 Point Source Scenarios....90
7.3 June 14 Point Source Scenarios....90
7.4 June 30 Point Source Scenarios....91
7.5 July 25 Point Source Scenarios....91
7.6 Evaluation of MAP-O3 as an Appropriate Screening Model....92

REFERENCES....99

APPENDICES....103

APPENDIX A: Memorandum of Understanding....104
APPENDIX B: UAM Modeling Results....110

VITA....116

LIST OF TABLES

TABLE **PAGE**

3.1. Summary of MAP-O3 Results for Ozone Impacting the GSMNP on Days Selected....19

4.1. X and Y Components of Wind File for June 14 Simulation....22

4.2. X and Y Components of Wind File for June 30 Simulation....23

4.3. X and Y Components of Wind File for July 07 Simulation....24

4.4. X and Y Components of Wind File for July 10 Simulation....25

4.5. X and Y Components of Wind File for July 25 Simulation....26

4.6. Biogenic Emissions Used for UAM Simulations in Units of (gmol/hr)....28

4.7. NO and NO_2 UAM Point Source Emission File Input Values....31

4.8. Mixing Height Values for Five Days Simulated by the UAM....32

4.9. Temperature Input File Data for Five Days Simulated by the UAM....33

4.10. June 14 Metscalars Input File Data....36

4.11. June 30 Metscalars Input File Data....37

4.12. July 07 Metscalars Input File Data....38

4.13. July 10 Metscalars Input File Data....39

4.14. July 25 Metscalars Input File Data....40

4.15. Default Concentrations for Airquality, Boundary, and Topconc Files....41

6.1. Results from the NTVD and TVP Basecase Simulations....72

6.2. Maximum Predicted Ozone Concentrations for the July 07 and July 10 100,000 tpy NTVD and TVP Scenarios....73

6.3. Maximum Predicted Ozone Concentrations for the June 14 100,000 tpy NTVD and TVP Scenarios....80

6.4. Maximum Predicted Ozone Concentrations for the June 30 100,000 tpy NTVD and TVP Scenarios....81

6.5. Maximum Predicted Ozone Concentrations for the July 25 100,000 tpy NTVD and TVP Scenarios....83

6.6. Maximum Incremental Ozone Concentrations Impacting the GSMNP....86

LIST OF FIGURES

FIGURE **PAGE**

2.1. Urban Airshed Model Program with Input and Output Files....13

5.1. Modeling Domain; Including State, County, and Class I Area Boundaries....43

5.2. July 07 Basecase Simulation Using NTVD Concentrations....45

5.3. July 10 Basecase Simulation Using NTVD Concentrations....46

5.4. June 30 Basecase Simulation Using NTVD Concentrations....47

5.5. June 14 Basecase Simulation Using NTVD Concentrations....48

5.6. July 25 Basecase Simulation Using NTVD Concentrations....49

5.7. July 07 Point Source Simulation (6 p.m.) Using NTVD Concentrations....52

5.8. July 07 Point Source Simulation (8 p.m.) Using NTVD Concentrations....53

5.9. July 10 Point Source Simulation Using NTVD Concentrations....54

5.10. June 30 Point Source Simulation (5 p.m.) Using NTVD Concentrations....56

5.11. June 30 Point Source Simulation (8 p.m.) Using NTVD Concentrations....58

5.12. June 14 Point Source Simulation (6 p.m.) Using NTVD Concentrations....60

5.13. June 14 Point Source Simulation (8 p.m.) Using NTVD Concentrations....61

5.14. July 25 Point Source Simulation (5 p.m.) Using NTVD Concentrations....62

5.15. July 25 Point Source Simulation (8 p.m.) Using NTVD Concentrations....64

6.1. July 07 Basecase Simulation Using TVP Concentrations....67

6.2. July 10 Basecase Simulation Using TVP Concentrations....68

6.3. June 14 Basecase Simulation Using TVP Concentrations....69

6.4. June 30 Basecase Simulation Using TVP Concentrations....70

6.5. July 25 Basecase Simulation Using TVP Concentrations....71

6.6. July 07 Point Source Simulation (8 p.m.) Using TVP Concentrations....75

6.7. July 07 Point Source Simulation (6 p.m.) Using TVP Concentrations....76

6.8. July 10 Point Source Simulation Using TVP Concentrations....77

6.9. June 14 Point Source Simulation (6 p.m.) Using TVP Concentrations....78

6.10. June 14 Point Source Simulation (8 p.m.) Using TVP Concentrations....79

6.11. June 30 Point Source Simulation Using TVP Concentrations....82

LIST OF FIGURES (continued)

FIGURE **PAGE**

6.12. July 25 Point Source Simulation (7 p.m.) Using TVP Concentrations.....84

6.13. July 25 Point Source Simulation (8 p.m.) Using TVP Concentrations.....85

6.14. Comparison of MAP-O3 and UAM Ozone Concentration Predictions.....87

7.1. June 14 Point Source Simulation Showing Plume Progression at Noon.....93

7.2. June 14 Point Source Simulation Showing Plume Progression at 2 p.m.....94

7.3. June 14 Point Source Simulation Showing Plume Progression at 4 p.m.....95

7.4. June 14 Point Source Simulation Showing Plume Progression at 6 p.m.....96

7.5. June 14 Point Source Simulation Showing Plume Progression at 8 p.m.....97

1. INTRODUCTION

There are three Prevention of Significant Deterioration (PSD) Class I areas in East Tennessee: the Great Smoky Mountains National Park (GSMNP), Joyce Kilmer-Sliprock Wilderness Area (JKWA), and Cohutta Wilderness Area (CWA). In an effort to protect the air quality related values (AQRV) in these areas in accordance with the Tennessee Air Pollution Control Act and the Federal Clean Air Act, the Tennessee Division of Air Pollution Control (TDAPC) and the United States Department of the Interior (DOI) have developed a Memorandum of Understanding (Appendix A). Detailed in the memorandum are the policies and guidelines which are to be followed when permitting sources that may affect Class I areas. In general, it states that whenever a potential PSD source within 100 km of a Class I area (or at a greater distance for large PSD sources) is being planned, an AQRV analysis must be performed and submitted as part of a complete permit application. The AQRV analysis must include modeling results which will predict whether the proposed source could adversely impact the Class I area.

The AQRV of interest for this study is the minimization of air pollution that could potentially damage vegetation. Impacts on AQRV's are measured by both the deposition impacts of certain compounds, and the ambient impacts of criteria pollutants (TDAPC, 95). It has been found by many researchers that tropospheric ozone, which is considered a criteria pollutant, is harmful to vegetation (NRC, 92). Ozone is formed through a chemical reaction that involves nitrogen oxides ($NO_x = NO + NO_2$), hydrocarbons and other volatile organic compounds (VOCs), and sunlight (SOS, 95). NO_x and VOCs are often referred to as ozone precursors because it is photochemical reactions of the precursors that cause ozone to be formed. In areas that have an abundance of one of the precursors, ozone formation may be limited due to the lack of the other precursor. For instance, due to the large amount of naturally occurring biogenic VOC emissions in East Tennessee coupled with the area's rural nature (the limited number of large point sources

of NO_x), the region is considered to be NO_x limited (NRC, 92). Therefore, any new large NO_x source may cause an increase in ozone formation in the East Tennessee area.

In past studies associated with nonattainment issues the process of selecting days to model ozone occurrences was basically one in which the days chosen were the ones for which the area's monitors measured the highest values. However, in the event of modeling a proposed new source's impact on a Class I area, the old selection method is no longer useful. Now a method is needed which will both predict when that source will impact the PSD Class I area (or target), as well as identify the worst case days in terms of maximum incremental ozone production. This document presents a potential method of selecting the day(s) to be modeled, and predicting the ozone impacts in the GSMNP due to NO_x sources located in East Tennessee. The method utilizes two models referred to as the Mapping Areawide Predictions of Ozone model (MAP-O_3) (McIlvaine,1994) and the Urban Airshed Model (UAM).

The MAP-O_3 model is capable of assessing the magnitude and spatial impact of emissions from a single large point source and was used as a screening model that predicted which days a source would impact the GSMNP over an ozone season or seasons (90-92) (McIlvaine and Miller, 96). Four hypothetical source locations in East Tennessee were modeled: Knoxville Airport (McGhee Tyson), Tri-Cities Airport, Crossville, and Chattanooga. Once the worst case scenarios of ozone impact in the park were determined, the UAM was used to give a more refined analysis of the spatial and temporal ozone concentrations for that day's particular meteorological conditions. Four sizes of NO_x sources (100,000 tpy, 10,000 tpy, 1,000 tpy, and 100 tpy) were modeled for each day selected at each location (two days for McGhee-Tyson location). Also a basecase scenario using background emissions with no point sources was modeled. A comparison of the basecase scenario with the basecase scenario (with the point source added) allowed the determination of the incremental ozone which was formed by adding the potential point source. The results from the UAM were compared to the MAP-O_3 results in order to determine the laters effectiveness as a screening model for predicting:

(1) the days to be modeled (direct hits on the park), and (2) incremental ozone concentrations contributed by the hypothetical sources.

A secondary objective of this study was to investigate the influence of boundary conditions on predicted ozone concentrations. Previous State Implementation Plan (SIP) modeling of ozone with the UAM relied on the Regional Oxidant Model (ROM) for the data required by its boundary file for species concentrations. In the absence of ROM data (very few ROM simulations have been conducted past 88), an EPA non-temporally varying default (NTVD) concentration is generally used for the 23 species input into the UAM. Since Chattanooga, Crossville, and Tri-Cities are located relatively close to the UAM modeling domain boundary, it is possible that these default boundary conditions affect the results of the modeling scenarios. Two steps needed to be taken in order to minimize any boundary effect that was occurring. First, a single grid cell that was located sufficiently within the modeling domain such that it was unaffected by the boundary conditions was identified. This cell was also chosen as one which was representative of the basecase ozone and precursor concentrations within the entire modeling domain and throughout the modeling episode. Secondly, the concentrations of all the species were extracted from that grid cell and entered into the boundary cells of the domain for each hour. This procedure was done for each modeling scenario and was considered a temporally varying predicted (TVP) concentration.

The hypothesis was that using the TVP concentrations would provide a more realistic outcome than using the NTVD concentrations. For example, in one case this allowed up to 78 ppb of ozone to be advected in from the boundary cells in the afternoon instead of the constant 40 ppb default value found in the NTVD. The values of ozone in the TVP concentrations is essentially the background concentration of ozone being formed during basecase runs which varies throughout the day. An underlying assumption in the technique is that ozone and VOC precursor concentrations predicted within rural areas of the East Tennessee modeling domain should also be representative of domain boundary concentrations due to similar emissions and photochemical reactions that occur

in areas adjacent to the modeling domain. The results of the primary (NTVD) runs were compared to the secondary (TVP) runs confirming that the boundary conditions do play a significant role for sources located near the boundary.

2. LITERATURE REVIEW

2.1 Ozone Formation

Ozone (O_3) is a gaseous compound present in both the troposphere (0-10 km) and the stratosphere (11-50 km). In the troposphere, naturally occurring concentrations of ozone are believed to be between 20 - 30 ppbv, whereas, ozone concentrations in the stratosphere can be as high as 10,000 ppbv (NRC, 1991). In addition to background ozone concentrations found in the lower atmosphere, ozone concentrations levels have increased over the past century due the reactions of sunlight with anthropogenic emissions of NO_x (NO_2 + NO) and volatile organic compounds (VOCs) from both stationary and mobile sources. Clinical research has shown that increases in ozone concentrations up to or below 120 ppbv in the troposphere can produce significant changes in respiratory functions in humans, and also have serious impacts on crop yields and forest ecosystems. Stratospheric ozone has a different effect on humans and the environment. This ozone, in fact, acts as a shield against biologically harmful solar ultraviolet radiation, and transforms it into mechanical energy of heat and atmospheric winds (Krupa and Manning, 1988).

Finlayson-Pitts & Pitts (1986), and Krupa and Manning (1988), have summarized information which is relevant to the formation of ozone in the troposphere. As stated earlier, ozone is formed through the reactions of NO_x, VOCs, and sunlight. This reaction is based on a chain reaction initiated by hydroxyl radicals (OH) formed from the interaction of monotomic oxygen, the product of photolysis of O_3, with water, shown in the following two reactions:

1. $$O_3 + h\nu(\lambda \leq 310 \text{ nm}) \rightarrow O_2 + O$$

2. $$O + H_2O \rightarrow 2OH$$

In equation 1, $h\nu$ represents energy from the sun, where h is 6.62E-34 J·s (Plank's constant) and ν is the photon wavelength emitted from the sun (Wark, 1981).

VOC's major purpose in the formation of tropospheric ozone is the oxidation of combustion emissions (NO) to NO_2. This can be shown by the reaction of the hydroxyl radical with methanol (CH_3OH) to produce a hydroperoxyl radical:

3. $OH + CH_3OH \rightarrow CH_3O + H_2O$

4. $CH_3O + O_2 \rightarrow CH_2O + HO_2$

Then the hydroperoxyl radical rapidly oxidizes NO to NO_2:

5. $HO_2 + NO \rightarrow OH + NO_2$

Finally, photodissociation of NO_2 by sunlight is what controls the actual production of ozone:

6. $NO_2 + h\nu\ (\lambda < 430\ nm) \rightarrow NO + O$

7. $O + O_2 \rightarrow O_3$

Ozone production is therefore a function of the ratio of NO_2 to NO in the atmosphere as well as sunlight intensity. Therefore, it is easy to understand why NO_x emission plumes from large point sources are of such concern in terms of ozone production, which leads to increasing ambient ozone concentrations.

Equation 8 is the terminating step in the process of ozone formation.

8. $NO + O_3 \rightarrow NO_2 + O_2$

This step, an ozone scavenging reaction, competes with the ozone production reactions in equations 6 and 7, resulting in the ambient concentrations of ozone in the troposphere at any instant during the day.

Equation 9 represents another ozone scavenging reaction that occurs at night in the presence of nitrogen dioxide.

9. $NO_2 + O_3 \rightarrow NO_3 + O_2$

This equation represents the decrease in ambient ozone concentrations near the earth's surface, which allows for lower concentrations in the early morning hours.

2.2 Vegetation Damage Attributed to Ozone

Ozone is a strong oxidant that damages plant tissue. The National Ambient Air Quality Standards (NAAQS) for ozone is 0.120 ppm (parts per million), over a one hour averaging time, and is not to be exceeded more than three times in any consecutive three year period. However, Eastern white pines show visible ozone injury from concentrations of 0.07 ppm for 4 hour exposures (Krupa and Manning, 1988; Costonis and Sinclair, 1969). The first signs of vegetation damage due to photochemical pollutants in the air were observed in the 1940's in the Los Angeles basin (NRC, 1992). However, it wasn't until the late 1950's that the damage was shown to be related to ozone (Wark, 1981). Haagen-Smit's work in the 1950's was key in establishing the roles that NO_x and VOCs played in the formation of ozone, as well as in determining the damaging effects ozone had on vegetation (NRC, 1992).

Ozone enters the plant through stomata during normal gas exchange between the leaf and its environment. The amount of ozone entering the plant varies depending on the plant's ability to restrict entry by closing the stomata when sensing the presence of ozone. Once inside the plant, ozone attacks cell membranes, wherein leaf cells active in photosynthesis appear to be the most sensitive. Ozone oxidizes the plant cells it contacts, which results in injury if the plant's biochemical detoxification cannot offset oxidation (Musselman et. al, 1994). Indications that repair mechanisms in the cell cannot keep up with this cellular injury appear as chlorosis or oxidant stipple on leaf tissue. Damage occurs to the plant when enough tissue is destroyed. This is evidenced by either reductions in aesthetic value of the plant from lesions, or a loss of foliage, or by reductions in plant productivity and yield (Musselman et. al, 1994).

There are many factors that influence how a plant will respond to ozone. Some factors which are necessary for ozone injury to occur are: warm temperatures, high relative humidity, sunlight, good nutrition, and adequate soil moisture. Factors which determine the types of symptoms that will occur on plants include the concentration of ambient ozone, duration of exposure, and type of plant (Krupa & Manning, 1988). The

degree of injury to a plant can either be chronic or acute. Chronic injury results from long-term exposure to low ozone concentrations. Acute injury to plants occurs when they are exposed to high ozone concentrations for short periods of time resulting in cell death. Due to the fluctuating nature of ambient ozone concentrations, both types of symptoms may occur on the same plant at different times in the plant's life cycle. Experimental studies have compared "equivalent ozone dose" of constant concentration exposure versus peak concentration exposure to plants, and have shown that the greatest detrimental effect on plant growth was a result of peaks in ozone concentration during exposure (Lefon & Foley, 1993; Musselman et. al, 1994).

2.3 Class I Areas

The Clean Air Act (CAA) passed by Congress in 1970 established a national policy of protecting, and in some cases enhancing air quality. In 1977, the act was amended and established "Class I" areas which included all national parks exceeding 6,000 acres, and wilderness areas at least 5,000 acres in size. This amendment established the PSD (prevention of significant deterioration) program which was to protect air quality in regions of the country where the air is cleaner than is required by the National Ambient Air Quality Standards (NAAQS). Within this program Congress developed a classification approach for controlling the increase of air pollution in these "clean" regions as Class I, Class II and Class III areas. Class I areas are given the greatest degree of air quality protection. Only very small increases in air pollutant concentrations are allowed in these areas (Bunyak, 1993).

Congress established Class I pollution "increments" which are the allowed increases in pollutant concentrations for certain pollutants: sulfur dioxide, particulate matter, and nitrogen oxides. In order to obtain a permit to construct a new or expand an existing facility which emits air pollutants that may affect air quality in a Class I area, they must show that their emissions will not cause or contribute to pollutant concentrations in excess of the Class I increments (Shaver et. al, 1994).

However, in recognizing that air pollution levels even below Class I increments can be harmful to sensitive park resources, Congress charged the federal land managers (FLMs) with the affirmative responsibility to protect the air quality related values (AQRV) of the Class I areas from adverse effects (Shaver et. al, 1994). AQRVs include visibility, flora, fauna, surface waters, ecosystems, and geological, cultural, and historical resources. Under the CAA, it is mandatory for the FLM to participate in the review of potential impacts from new or modified pollution sources before construction permits are issued. This participation during the permitting phase is the main way the FLM is able to carry out it's responsibility to protect AQRVs. For instance, if the FLM can demonstrate to the permitting authority that a proposed facility's emissions would adversely affect the AQRVs of the Class I area, even if these emissions would not cause pollutant concentrations to exceed Class I increments, then the permitting facility cannot authorize the proposed project (Shaver et. al, 1994). The FLM is directed through the legislative history of the CAA to "assume an aggressive role in protecting the air quality values of land areas under his jurisdiction.... In cases of doubt the land manager should err on the side or protecting the air quality-related values for future generations" (U.S. Senate, 1977).

The secretary of the interior has delegated the authority of the FLM to the assistant secretary for Fish and Wildlife and Parks for areas under National Park Service (NPS) and Federal Wildlife Service (FWS) jurisdiction (Bunyak, 1993). The Fish and Wildlife service has stated that air pollution effects on resources in Class I areas constitute an unacceptable adverse impact if such effects: (1) diminish the national significance of the area, (2) impair the quality of the visitor experience, and/or (3) impair the structure and functioning of ecosystems (Federal Register, 1982 [40 FR 30223]). The magnitude, duration, location, projected frequency, and reversibility of the impact are factors that are considered when determining whether an effect is unacceptable, and therefore adverse (Shaver et. al, 1994).

2.4 Great Smoky Mountains National Park (GSMNP)

The GSMNP is located in the southern Appalachians on the border of Tennessee and North Carolina, and was designated a Class I area by Congress in 1977. The park encompasses 800 square miles of deep-cleft valleys and mountain ridges. It is world renowned for the beauty of its ancient mountains, and the diversity of its plant and animal resources. The US Congress first delegated the Great Smoky Mountains a national park in 1926 in order to protect these special natural and cultural resources for future generations. In 1990, over eight million visits were made to the GSMNP, and it is one of the nation's most popular national parks. This popularity is in part due to the accessibility of the park, which is located within driving distance of two thirds of the United States population. However, it is the park's accessibility that makes it very susceptible to one of civilization's negative effects - pollution. The park is located downwind of many urban and industrial areas that generate millions of tons of air pollution annually (Shaver et. al, 1994).

Since 1980, gaseous pollutant, fine particle, visibility, meteorological, and precipitation chemistry monitoring have taken place at GSMNP. An ozone and meteorological monitoring station was established at a mid-elevation site in the park (823 m above sea level) in 1980. In 1986 an ozone monitor was installed at a high elevation site (1,250 m) and in 1987 a low elevation site (600m) was chosen (Shaver et. al, 1994). Researchers have observed foliar symptoms indicative of ozone injury on plants and hardwood leaves in GSMNP, even though there have been no recorded exceedences of the ozone NAAQS of 120 ppb (0.120 parts per million) since 1984, which supports the suspicion that the NAAQS for ozone exceeds the level at which plant injury occurs (Renfro, 1990).

These observations led to a four year NPS Air Quality Division funded project, beginning in 1987, which included ozone chamber fumigation studies on suspected sensitive species, as well as field surveys and establishing permanent monitoring plots of sensitive hardwood species. The overall goal of the project was to establish whether

there were effects of ambient ozone on native plant species in their natural habitat in GSMNP, and to relate any observed effects to experimental ozone fumigations of known ozone exposures (Renfro, 1990). Documented from these projects were adverse physiological effects and foliar injury on vegetation from ozone at concentrations lower than the NAAQS. Forty-six species were tested in the fumigation studies of which twenty-five were identified as being sensitive to ozone, including the common hardwoods, black cherry and yellow poplar, and a native conifer, table-mountain pine (Hacker and Renfro, 1992; Shaver et. al, 1994).

The permanent monitoring plots located adjacent to sensitive hardwood species were used to correlate ambient ozone concentrations with foliar injury in the field. Black cherry, yellow-poplar, white ash, and sassafras all exhibited foliar injury at the sites where the species occurred. Even though the severity of injury was low, the number of trees showing some degree of injury was high. NPS researchers then conducted a survey of black cherry trees along specified intervals of trails in GSMNP in order to further document the extent of foliar injury under field conditions during August and September of 1992. Over 50% of the 1,200 trees evaluated showed some degree of foliar injury due to ozone at ambient concentrations (Shaver et. al, 1994). Alarmingly, other studies in North America and Europe have shown that these types of injury to vegetation, such as growth reductions and leaf damage, in GSMNP can lead to ecosystem changes (Woodman 1987; Shaver et. al 1994).

2.5 UAM

In an effort to evaluate the impact of ozone formation and its related effects, photochemical models have been developed. The Urban Airshed Model (UAM) is a three dimensional photochemical model that simulates ozone formation in a gridded modeling domain. The model calculates the concentrations of chemically inert and reactive species throughout the domain which are dependent of emission rates and meteorological conditions specific to each modeling scenario. The model is effective in

accounting for temporal and spatial variations of each scenario including emission variations. The ozone formation is simulated by the Carbon Bond-IV chemical kinetic mechanism. This mechanism estimates the ozone forming potential of air pollutants by classifying the ozone precursors into 23 separate species depending on their particular characteristics. A species continuity equation then estimates the time rate of change of ozone concentration by calculating the diffusion, emission, reaction, removal, and transport of the species in the modeling domain (OAQPS, 1993).

The model inputs consist of initial and boundary conditions, meteorological, emissions data from sources of precursor pollutants, chemical reaction rates, and simulation control files for each particular episode to be modeled. The model has four output files, which consist of two concentration files (instantaneous or average), a deposition file, and an execution trace file. Figure 2.1 shows a flowchart of all UAM input and output files.

The input files that are classified as air quality files include: (1) Airquality, (2) Boundary, (3) Topconc, and (4) Terrain. The Airquality file contains instantaneous background concentrations of the 23 species modeled by the UAM at the beginning of the simulation. The Boundary file specifies the concentrations of the 23 species around the perimeter of the modeling domain for the duration of the modeling scenario. The Topconc file also contains species concentrations for the duration of the modeling scenario, but it is for the top layer of the domain. The terrain file consists of surface roughness and deposition factors for each grid cell.

The input files classified as meteorological data files consist of: (1) Diffbreak, (2) Regiontop, (3) Temperature, (4) Wind, and (5) Metscalars. These files are all based on day specific meteorological conditions and were constructed using UAM preprocessors as is described in Volume IV of the UAM User's Guide, with the exception of the Wind file for which a uniform wind field based on lower level readings from the airport nearest the source location was used. Since there were no ROM simulations available for the days

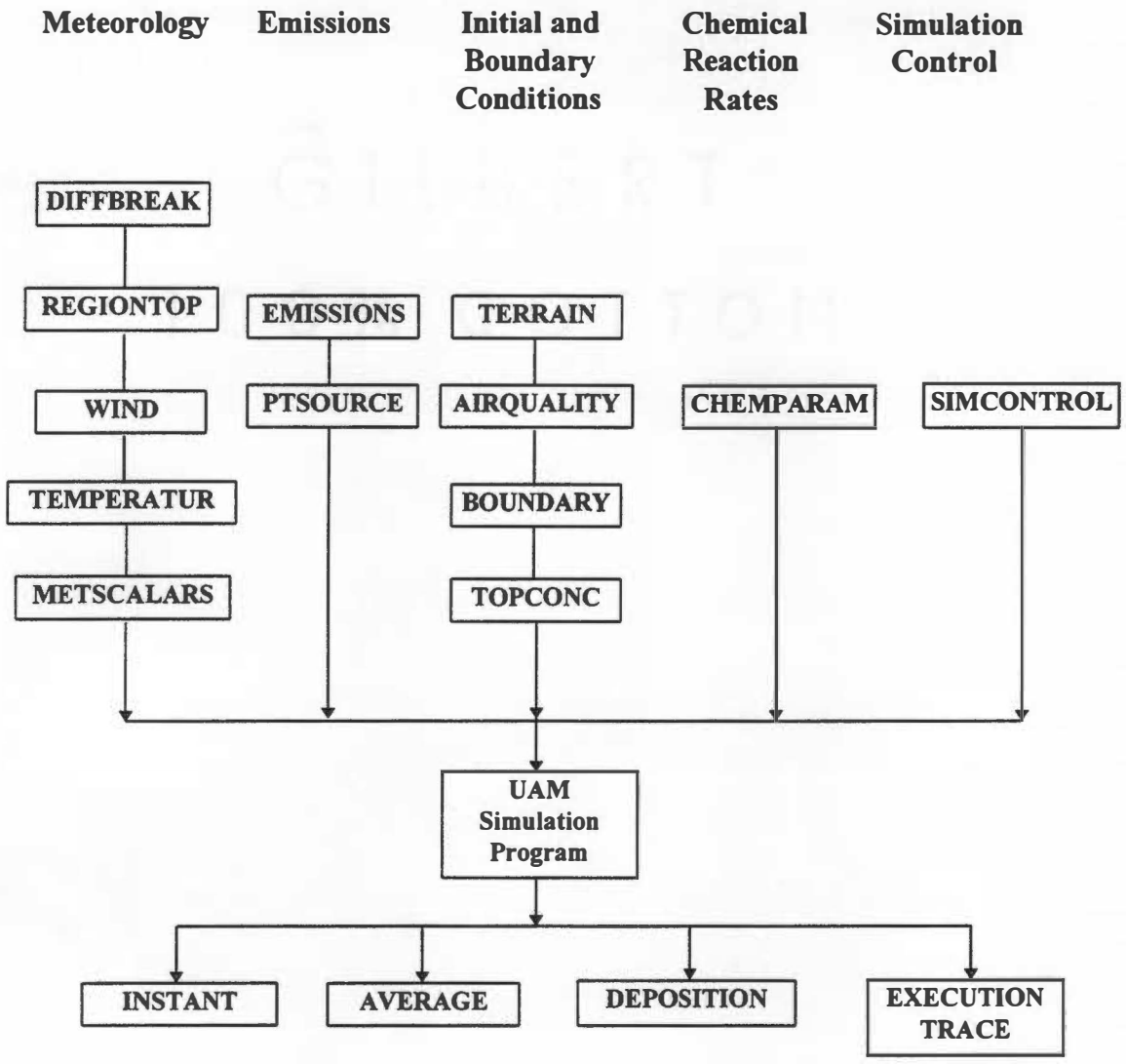


Figure 2.1. Urban Airshed Model program with input and output files.

that were selected to be modeled is why no ROM-UAM preprocessors were used to construct these files.

The files that are considered emission files include (1) Ptsource, and (2) Emissions. The Ptsource file is a gridded elevated point source emission file that specifies stack parameters, such as stack height, flow rate, and temperature, and the grid cell location of each point source. The Emissions file specifies the temporally gridded information of all other ground-level biogenic and anthropogenic emissions.

A chemical reaction rate file (Chemparam), and simulation control file (Simcontrol) are the final input files required by the UAM. The Chemparam file contains information on the chemical species to be simulated, such as reaction rate constants, and the Simcontrol file is used to specify the duration of the modeling scenario and any flags that are to be set for each modeling episode (OAPQS, 1990).

Because of the complexity of the files and the lengthy execution time of the UAM, it is not practical to run it for every day of an ozone season. Therefore it is necessary to pre-select specific dates for which such a model will be run. These are generally chosen to be dates of highest observed ozone. In cases where the objective is to evaluate the impact of specific sources on specific receptors, other screening procedures may be needed to identify dates to be modeled.

2.6 MAP-O3

One screening model which has been developed for use in identifying dates in which meteorological conditions might cause an interaction between specific sources and receptors is the Mapping Areawide Predictions of Ozone model (MAP-O3). This model is made up of two parts, a meteorological based trajectory mapping program and a photochemical reaction program. The trajectory mapping program supplies the photochemical program with plume trajectories derived by daily meteorological observations of wind direction and speed. The trajectory program disperses the plume horizontally over a polar grid with 10 kilometer ring spacing and 22.5° radicals.

Essentially, ozone concentrations from the photochemical program are "mapped" over the polar grid for each hour of each day of the ozone season (May 1 to September 30 for East Tennessee) (McIlvaine and Miller 1996).

The photochemical program that predicts instantaneous or hourly average ozone concentrations over time is the Environmental Protection Agency (EPA) Ozone Isopleth Mechanism (OZIP-4) lagrangian model. This model combines a chemical kinetic mechanism with simplified meteorological assumptions to mathematically simulate chemical and physical processes taking place in the atmosphere (EPA, 1989a, 1989b). Time has two components when dealing with point source plumes; the time that the plume originates from the stack, which is referred to as the birth hour, and the time over which the plume has traveled downwind, which is called the plume age. The result of the two models is a map of hourly ozone concentrations occurring over the ozone season in the vicinity of the source (McIlvaine and Miller, 1996).

The input data required by the MAP-O3 is relatively basic as compared to more intense air dispersion models. However, the extent of meteorological data required is very large since the MAP-O3 model is designed to successively calculate ozone concentrations for each day within an entire ozone season. The input data required includes: latitude and longitude, time zone, date, morning and afternoon mixing heights, hourly temperature variation, hourly atmospheric moisture estimates, concentrations of non-methane organic compounds (NMOC), NO_x, CO, and O_3 in the air above the mixed layer due to transport aloft, concentrations of NMOC, NO_x, CO, and O_3 transported in the surface layer, anthropogenic NMOC and NO_x emissions for each hour, organic reactivity, and biogenic emission rates and speciation. Once these input files are constructed and run, the NO_x emissions from a potential point source can be added to the input files and run. Subtracting the temporally and spacially varying ozone concentrations obtained in the first run (basecase) from those obtained in the second run (with a point source included) will give the maximum incremental ozone concentration that could be formed

due to the potential point source for the duration of the meteorological files used (McIlvaine and Miller, 1996).

3. SELECTION OF MODELING SCENARIOS

The goals of this project were to identify a method of selecting the day(s) to be modeled, and to predict the ozone impact on the GSMNP due to NO_x sources located in East Tennessee. Therefore, the first step was to identify a technique that would predict which day(s) a hypothetical point source in East Tennessee could have the greatest impact on a particular target. The MAP-O3 model was designed for such a task and was used as a screening technique to select the days for which more advanced modeling, using the UAM, would be conducted.

3.1 MAP-O3 Runs

The MAP-O3 model is capable of assessing the magnitude and spacial impact of emissions from single large point sources over an ozone season or seasons. The MAP-O3 model was, therefore, used as a screening model to decide which days the largest incremental increase of ozone due to a point source could impact the GSMNP from different locations. These days were then selected for further analysis and were to be modeled with the UAM. In fact, the MAP-O3 model was run for the entire 1990-1992 ozone seasons with NO_x sources located at two locations (Knoxville, and Crossville), and run for the 1990 ozone season for the other two locations (Tri-Cities, and Chattanooga). The dates that gave the highest incremental ozone concentrations in the GSMNP due to the potential point sources were considered to be the worst case days and were used as the dates to be modeled using the UAM. The results of all the MAP-O3 runs are summarized in Chapter 5 of the document: Development and Application of a Screening Model for Predicting Ozone Formation Due to Major Point Source Emissions in East Tennessee (McIlvaine and Miller, 1996).

3.2 Selected Days to be Modeled at Knoxville

Both July 7, and July 10 predicted values of 53 ppb (parts per billion) of ozone to impact the GSMNP due to a 10,000 tpy NO_x source located at the McGhee Tyson airport. The meteorological data inputs for these days were from 1990 data recorded at the McGhee Tyson airport. Since these two days gave the highest potential ozone increment hitting the park, the plume trajectories for these days were analyzed, based on wind speed and direction from surface data from the McGhee Tyson airport, to see if they looked realistic (McIlvaine and Miller, 1996). Since both plume trajectories appeared reasonable, both days were kept and modeled with the UAM.

3.3 Selected Day to be Modeled at Crossville

MAP-O3 modeling of a 10,000 tpy NO_x source located at Crossville, Tennessee yielded an incremental ozone increase of 20 ppb in the GSMNP for June 30. This was the largest increment for any day for the three years of meteorological data modeled. The meteorological data for this day were from 1990 and from the McGhee Tyson airport since it is the closest airport to the site. Analyzing the plume trajectory, it was concluded that the centerline of the plume did not appear to impact the park, but it was within the 22.5° range of the park's boundary that MAP-O3 considers a "hit" (McIlvaine, 1994). Since it was considered a hit by MAP-O3 the day was selected to be modeled by the UAM, with additional interest to see how close the UAM would model the ozone plume with respect to the park.

3.4 Selected Day to be Modeled at Chattanooga

The largest incremental increase of ozone due to a 10,000 tpy NO_x source located at the Chattanooga airport was 48 ppb on September 7 using 1990 meteorological data. However, this day gives a very unrealistic plume trajectory (the plume was meandering across the mountains to the east, then back toward the park) and was therefore deleted from further consideration (McIlvaine and Miller 1996). The second highest incremental

ozone day was selected instead, due to its realistic (almost a straight line) plume trajectory toward the park. This day was June 14 using 1990 meteorological data from the Chattanooga airport, and gave an incremental ozone increase of 36 ppb on the GSMNP. Therefore, June 14 was modeled using the UAM.

3.5 Selected Day to be Modeled at Tri-Cities

An incremental ozone increase of 19 ppb in the GSMNP due to a 10,000 tpy NO_x source located at the Tri-Cities airport was the largest increment found using 1990 meteorological data (McIlvaine and Miller, 1996). This increment occurred on July 25 using meteorological data from the Tri-Cities airport. The plume trajectory for this day was analyzed and considered to be reasonable. Therefore, July 25 was modeled using the UAM.

3.6 MAP-O3 Results

As previously discussed, the MAP-O3 was used to predict which days a source at each location was most likely to cause high ozone concentrations in the GSMNP. Table 3.1 shows the incremental ozone formed (ppb) in the GSMNP for the days selected above. Runs were made for 10000, 1000, and 100 tpy NO_x sources for each of the simulations.

Table 3.1. Summary of MAP-O3 results for ozone impacting the GSMNP on days selected.

Date Selected	NO_x Emission Rate (tpy)		
	100	1000	10000
	Incremental Ozone (ppb) Impacting the GSMNP		
June 14	0.74	6.4	36
June 30	0.35	3.0	20
July 07	0.90	8.0	53
July 10	0.75	8.0	53
July 25	0.40	3.4	19

4. UAM INPUT FILES

In order to achieve the goal of assessing the effectiveness of MAP-O3 as a screening model, the input files to the UAM were constructed with the intent of simulating MAP-O3's input data. The main inputs required to match UAM input to MAP-O3 input are in the wind and emissions input files. The UAM wind files were constructed from surface meteorological readings from the airport closest to the location of the potential point source, and the emissions file was constructed using a constant domain emissions of both anthropogenic and biogenic emissions. Another similarity between the MAP-O3 and UAM runs is in the length of the simulations. Normally the UAM would be run for a 24 hour simulation, but due to the way MAP-O3 handles emissions and how the simulations are run, the UAM runs for comparison purposes were set for 18 hours.

In order to determine the incremental ozone which could be attributed to a large NO_x source, a basecase scenario was run. The basecase scenario was executed with all the input files required by the UAM, including an emissions file, but without a point source file. Next, the UAM was executed with the same files used for the basecase scenario plus a point source file containing the NO_x emissions due to the potential source. To determine the ozone formed due to this point source, the basecase run was subtracted from the second run. The UAM input files of interest are discussed in the following sections, and the MAP-O3 input files are summarized in Chapter 4 of the document: Development and Application of a Screening Model for Predicting Ozone Formation Due to Major Point Source Emissions in East Tennessee (McIlvaine and Miller, 1996).

4.1 Wind Files

The wind files used for each day simulated by the UAM were based on surface wind data collected at the airport closest to the location of the potential point source which was to be modeled. In particular, McGhee Tyson airport data was used for both

the Knoxville and Crossville simulations, the data used for the Cleveland simulation were from Lovell Field in Chattanooga, and the Tri-Cities airport data were used for the Tri-Cities simulation. The wind speed and direction data collected at a particular airport was used over the entire domain and for each of the five vertical layers simulated by the UAM. This means that a temporally varying, non-spacially varying windfield was used for each modeling scenario. These were the same data used to construct the wind trajectories discussed in chapter 2.

The UAM wind input file requires that wind speed and direction be converted to distance components of meters traveled per hour. Tables 4.1 - 4.5 show the x and y components of wind speed and direction for the five days which were simulated by the UAM and the location where the readings were taken. The UAM requires wind components to be greater than zero, therefore, the values for calm hours were set to be 500 meters, which is relatively small compared to the 5000 meter grid cells.

Table 4.1. X and Y components of wind file for June 14 simulation.

Station	Date	Hour	Wind Direction (deg)	Wind Speed (m/sec)	Distance (m)	X-comp (m)	Y-comp (m)
Lovell Field	June 14	06	00	0.0	707.1	500.0	500.0
		07	00	0.0	707.1	500.0	500.0
		08	00	0.0	707.1	500.0	500.0
		09	160	2.1	7560.0	-2585.7	7104.1
		10	00	0.0	707.1	500.0	500.0
		11	250	5.2	18720.0	17591.0	6402.6
		12	250	3.6	12960.0	12178.4	4432.6
		13	260	4.7	16920.0	16662.9	5787.0
		14	250	2.6	9360.0	8795.5	3201.3
		15	200	3.6	12960.0	4432.6	12178.4
		16	250	2.6	9360.0	8795.5	3201.3
		17	230	2.6	9360.0	7170.2	6016.5
		18	240	4.1	14760.0	12782.5	7380.0
		19	230	2.6	9360.0	7170.2	6016.5
		20	240	2.6	9360.0	8106.0	4680.0
		21	210	3.6	12960.0	6480.0	11223.7
		22	00	0.0	707.1	500.0	500.0
		23	00	0.0	707.1	500.0	500.0

Table 4.2. X and Y components of wind file for June 30 simulation.

Station	Date	Hour	Wind Direction (deg)	Wind Speed (m/sec)	Distance (m)	X-comp (m)	Y-comp (m)
McGhee-Tyson	June 30	06	230	3.1	11160.0	8549.1	7173.5
		07	240	3.1	11160.0	9664.8	5580.0
		08	230	4.6	16560.0	12685.7	10644.6
		09	220	3.6	12960.0	8330.5	9927.9
		10	260	2.6	9360.0	9217.8	1625.3
		11	240	2.6	9360.0	8106.0	4680.0
		12	250	3.1	11160.0	10487.0	3816.9
		13	260	3.6	12960.0	12763.1	2250.5
		14	250	3.6	12960.0	12178.4	4432.6
		15	260	5.1	18360.0	18081.1	3188.2
		16	270	2.6	9360.0	9360.0	500.0
		17	330	4.1	14760.0	7380.0	-12782.5
		18	340	3.6	12960.0	4432.6	-12178.4
		19	260	2.6	9360.0	9217.8	1625.3
		20	260	2.6	9360.0	9217.8	1625.3
		21	240	3.1	11160.0	9664.8	5580.0
		22	210	3.1	11160.0	5580.0	9664.8
		23	290	2.1	7560.0	7104.1	-2585.7

Table 4.3. X and Y components of wind file for July 07 simulation.

Station	Date	Hour	Wind Direction (deg)	Wind Speed (m/sec)	Distance (m)	X-comp (m)	Y-comp (m)
McGhee-Tyson	July 07	06	20	2.6	9360.0	-3201.3	-8795.5
		07	30	2.1	7560.0	-3780.0	-6547.1
		08	360	2.1	7560.0	500.0	-7560.0
		09	130	2.1	7560.0	-5791.3	-4859.5
		10	80	2.1	7560.0	-7445.1	-1312.8
		11	330	2.1	7560.0	3780.0	-6547.1
		12	180	2.6	9360.0	500	9360.0
		13	50	2.6	9360.0	-7170	-6016.7
		14	50	2.1	7560.0	-5791.3	-4859.5
		15	240	3.1	11160.0	9664.8	-5580.0
		16	310	3.1	11160.0	8549.1	-7173.5
		17	20	2.1	7560.0	-2585.7	-7104.1
		18	10	2.1	7560.0	-1312.8	-7445.1
		19	00	0.0	707.1	500.0	500.0
		20	50	2.6	9360.0	-7170.2	-6016.5
		21	40	2.1	7560.0	-4859.5	-5791.3
		22	360	1.5	5400.0	500.0	-5400.0
		23	20	2.3	9360.0	-3201.3	-8795.5

Table 4.4. X and Y components of wind file for July 10 simulation.

Station	Date	Hour	Wind Direction (deg)	Wind Speed (m/sec)	Distance (m)	X-comp (m)	Y-comp (m)
McGhee-Tyson	July 10	06	250	2.1	7560.0	7104.1	2585.7
		07	210	2.1	7560.0	3780.0	6547.1
		08	190	2.6	9360.0	1625.3	9217.8
		09	230	4.1	14760.0	11306.8	9487.5
		10	220	3.1	11160.0	7173.5	8549.1
		11	200	4.1	14760.0	5048.2	13869.8
		12	220	4.1	14760.0	9487.5	11306.8
		13	240	4.1	14760.0	12782.5	7380.0
		14	320	2.6	9360.0	6016.5	-7170.2
		15	300	2.6	9360.0	8106.0	-4680.0
		16	360	3.1	11160.0	500.0	-11160.0
		17	260	1.5	5400.0	5317.9	937.7
		18	230	3.6	12960.0	9927.9	8330.5
		19	230	4.6	16560.0	12685.7	10644.6
		20	230	2.6	9360.0	7170.2	6016.5
		21	230	5.1	18360.0	14064.6	11801.6
		22	260	3.6	12960.0	12763.1	2250.5
		23	300	2.6	9360.0	8106.0	-4680.0

Table 4.5. X and Y components of wind file for July 25 simulation.

Station	Date	Hour	Wind Direction (deg)	Wind Speed (m/sec)	Distance (m)	X-comp (m)	Y-comp (m)
Tri-Cities	July 25	06	00	0.0	707.1	500.0	500.0
		07	60	1.6	5760.0	-4988.3	-2880.0
		08	90	3.6	12960.0	-12960.0	500.0
		09	100	2.1	7560.0	-7445.1	1312.8
		10	70	4.1	14760.0	-13869.9	-5048.2
		11	90	3.6	12960.0	-12960.0	500.0
		12	40	3.6	12960.0	-8330.5	-9927.9
		13	30	3.6	12960.0	-6480.0	-1123.7
		14	50	3.6	12960.0	-9927.9	-8330.5
		15	60	4.1	14760.0	-12782.5	-7380.0
		16	20	4.1	14760.0	-5048.2	-13869.9
		17	20	4.1	14760.0	-5048.2	-13869.9
		18	40	4.1	14760.0	-9487.5	-11306.8
		19	20	4.1	14760.0	-5048.2	-13869.9
		20	20	3.1	11160.0	-3816.9	-10487.0
		21	120	2.1	7560.0	-6547.1	3780.0
		22	30	2.1	7560.0	-3780.0	-6547.1
		23	40	3.6	12960.0	-8330.5	-5791.3

4.2 Emissions File

An up to date emissions inventory was essential for UAM simulations in the past dealing with attainment and nonattainment issues. However, the goal of this project was not to predict the ambient ozone concentrations in East Tennessee, but rather to predict the incremental ozone increases in the GSMNP due to the addition of hypothetical NO_x sources in East Tennessee. We have attempted to do this without a detailed emissions inventory by constructing UAM emissions input files from simplified, uniform biogenic and anthropogenic emissions used for the MAP-O3 simulations.

4.2.1 Biogenic Emissions

The biogenic emissions used are based on PC-BEIS2 model results using a representative East Tennessee county (Campbell). Campbell county's emissions are approximately equal to the average daily biogenic emissions for 36 East Tennessee counties. MAP-O3 speciates biogenic emissions into isoprene (ISOP) and monoterpene (TERP), and the values are input as (kg/km^2·hr). Monoterpene is simulated as 1 mole of olefins (OLE) and 8 moles of paraffins (PAR). The UAM uses units of (g·mol/hr). Therefore, to convert MAP-O3 values to UAM values the following conversions were made: (The following is an example of emissions from 6 - 7 am)

Isoprene:

Molecular weight of Isoprene = 68 g/gmol

$$\frac{0.297 \text{ kg ISOP}}{\text{km}^2 \cdot \text{hr}} \cdot \frac{25 \text{ km}^2}{\text{grid}} * = \frac{7.425 \text{ kg ISOP}}{\text{grid} \cdot \text{hr}}$$

$$\frac{7.425 \text{ (kg ISOP / grid} \cdot \text{hr)}}{68 \text{ (g/gmol)}} \cdot \frac{1000 \text{ g}}{\text{kg}} = \frac{109.19 \text{ g·mol ISOP}}{\text{hr}} \quad \text{(per grid)}$$

* The 25 km^2 values represent the area of one UAM grid cell which is 5 km by 5 km.

Monoterpene:

1 mole of OLE has a molecular weight = 26 g/gmol; 1mol · 26 g/gmol = 26 g

1 mole of PAR has a molecular weight = 14 g/gmol; 8mol · 14 g/gmol = 112 g

$$\%\ \text{mass of OLE} = \frac{26\ g}{138\ g} = 18.8\% \qquad \%\ \text{mass of PAR} = \frac{112\ g}{138\ g} = 81.2\%$$

$$\frac{0.236\ kg\ TERP}{km^2 \cdot hr} \cdot \frac{25\ km^2}{grid} = \frac{5.9\ kg\ TERP}{grid \cdot hr}$$

$$5.9\ \frac{kg\ TERP}{grid \cdot hr} \cdot \frac{0.188\ mol\ (OLE)}{mol\ (TERP)} \cdot \frac{1000\ g}{kg} = \frac{42.66\ g \cdot mol\ (OLE)}{hr} \quad \text{(per grid)}$$

$$5.9\ \frac{kg\ TERP}{grid \cdot hr} \cdot \frac{0.812\ mol\ (PAR)}{mol\ (TERP)} \cdot \frac{1000\ g}{kg} = \frac{342.30\ g \cdot mol\ (PAR)}{hr} \quad \text{(per grid)}$$

Biogenic emissions vary hourly due to changes in temperature, wind speed, relative humidity, and cloud cover. Table 4.6 shows the hourly biogenic emissions used for the UAM simulations.

Table 4.6. Biogenic emissions used for UAM simulations in units of (gmol / hr).

	6-7 a.m.	**7-8 a.m.**	**8-9 a.m.**	**9-10 a.m.**	**10-11 a.m.**	**11-noon**	**12-1 p.m.**	**1-2 p.m.**	**2-3 p.m.**
OLE	42.66	47.00	57.85	66.70	77.73	94.72	99.97	110.45	115.51
PAR	342.20	377.00	464.00	535.05	623.50	759.80	801.85	885.95	926.55
ISOP	109.19	716.18	1326.8	1830.1	2372.4	3102.9	3340.4	3704.0	3826.1
	3-4 p.m.	**4-5 p.m.**	**5-6 p.m.**	**6-7 p.m.**	**7-8 p.m.**	**8-9 p.m.**	**9-10 p.m.**	**10-11 p.m.**	**11p.m. 12a.m.**
OLE	115.51	110.45	104.67	94.72	73.57	63.81	57.85	54.77	52.42
PAR	926.55	885.95	839.55	759.80	590.15	511.85	464.00	439.35	420.50
ISOP	3732.3	3408.1	2917.6	2094.9	677.21	0.0	0.0	0.0	0.0

4.2.2 Anthropogenic Emissions

The anthropogenic emissions were also uniformly distributed over the entire modeling domain. These emissions are for all mobile, area, and stationary point sources from 6 a.m. to 6 p.m. in order to be consistent with MAP-O3 inputs. The emission values were estimated by population density using an existing 1988 emissions inventory for 17

counties in Middle Tennessee. The anthropogenic emissions are divided into two groups: oxides of nitrogen (NO_x), and non-methane organic compounds (NMOC). The average emission factor for Middle Tennessee was 0.180 kg/capita-day for NO_x and 0.298 kg/capita-day for NMOC (McIlvaine and Miller 1996). These values were multiplied by the population of the counties in East Tennessee and divided by the land area yielding a regional emission density of 0.758 kg/km^2-hr for NO_x and 1.255 kg/km^2-hr for NMOC.

MAP-O3 requires that anthropogenic emissions be input as 10 different species. These species include ethane (ETH), olefins, aldehydes (ALD2), formaldehyde (FORM), toluene (TOL), xylene (XYL), paraffins, non-reactive (NR) species, nitric oxide (NO), and nitrogen dioxide (NO2). The first eight species make up the NMOC, and the last two represent NO_x. MAP-O3 also has a default speciation profile based on measurements of urban air pollution. Converting the emission density to units used by the UAM (gmol/hr) is as follows:

$$\frac{1.255\ \text{kg NMOC}}{\text{km}^2 \cdot \text{hr}} \cdot \frac{25\ \text{km}^2}{\text{grid}} \cdot \frac{1000\ \text{g}}{\text{kg}} = \frac{31375\ \text{g}}{\text{grid} \cdot \text{hr}}$$

$$\frac{0.778\ \text{kg NOx}}{\text{km}^2 \cdot \text{hr}} \cdot \frac{25\ \text{km}^2}{\text{grid}} \cdot \frac{1000\ \text{g}}{\text{kg}} = \frac{19450\ \text{g}}{\text{grid} \cdot \text{hr}}$$

Emissions are then multiplied times the default mass fraction for each specie and divided by the molecular weight of that specie to determine the (gmol/hr) emission rate for each specie.

$$\frac{31375\ \text{g}}{\text{hr}} \cdot 0.037 \,/\, \frac{28\ \text{g ETH}}{\text{g} \cdot \text{mol}} = \frac{41.46\ \text{g} \cdot \text{mol}}{\text{hr}}\ \text{ETH}$$

$$\frac{31375\ \text{g}}{\text{hr}} \cdot 0.035 \,/\, \frac{26\ \text{g OLE}}{\text{g} \cdot \text{mol}} = \frac{42.24\ \text{g} \cdot \text{mol}}{\text{hr}}\ \text{OLE}$$

$$\frac{31375\ \text{g}}{\text{hr}} \cdot 0.052 \,/\, \frac{29\ \text{g ALD2}}{\text{g} \cdot \text{mol}} = \frac{56.26\ \text{g} \cdot \text{mol}}{\text{hr}}\ \text{ALD2}$$

$$\frac{31375\ \text{g}}{\text{hr}} \cdot 0.021 \,/\, \frac{30\ \text{g FORM}}{\text{g} \cdot \text{mol}} = \frac{21.96\ \text{g} \cdot \text{mol}}{\text{hr}}\ \text{FORM}$$

$$\frac{31375\ g}{hr} \cdot 0.089 \;/\; \frac{92\ g\ TOL}{g \cdot mol} = \frac{30.35\ g \cdot mol\ TOL}{hr}$$

$$\frac{31375\ g}{hr} \cdot 0.117 \;/\; \frac{106\ g\ XYL}{g \cdot mol} = \frac{34.63\ g \cdot mol\ XYL}{hr}$$

$$\frac{31375\ g}{hr} \cdot 0.564 \;/\; \frac{14\ g\ PAR}{g \cdot mol} = \frac{126.40\ g \cdot mol\ PAR}{hr}$$

The remaining 0.085 % of NMOC is NR. The conversion of NO_x emissions to (gmol/hr) of NO and NO_2 is as follows:

$$\frac{19450\ g}{hr} \cdot 0.750 \;/\; \frac{30\ g\ NO}{g \cdot mol} = \frac{486.25\ g \cdot mol\ NO}{hr}$$

$$\frac{19450\ g}{hr} \cdot 0.250 \;/\; \frac{46\ g\ NO_2}{g \cdot mol} = \frac{105.71\ g \cdot mol\ NO_2}{hr}$$

4.3 Point Source Emission File

The emissions file described above is used for determining ozone formation during the basecase simulations. The point source emission file is used when simulating the ozone formed by all biogenic and anthropogenic sources in addition to the potential large NO_x source. Therefore, the point source emission file is not used when the basecase simulations are run. The point source emission file is constructed from the NO_x produced from a certain source size (100, 1000, 10000, and 100000tpy) as if it were emitting 24 hours a day for 365 days a year. The initial NO to NO_2 ratio is 3 to 1 based on MAP-O3 ratios of NO_2 to NO_x. To determine the impact of the hypothetical source on ozone formation, which is simulated by the point source file, the results of the basecase run are subtracted from the results of the run with the point source file. The emissions for the hypothetical point source are from 6 a.m. to 6 p.m. based on the MAP-O3 input file. The conversion of tons per year (tpy) of NO_x to (gmol / hr) of NO and NO_2 is as follows:

$$\frac{100\ ton\ NO_x}{yr} \cdot \frac{yr}{365\ day} \cdot \frac{day}{24\ hr} \cdot \frac{907.18\ kg}{ton} \cdot \frac{0.75\ NO}{NO_x} = \frac{7.77\ kg\ NO}{hr}$$

$$\frac{100 \text{ ton } NO_x}{\text{yr}} \cdot \frac{\text{yr}}{365 \text{ day}} \cdot \frac{\text{day}}{24 \text{ hr}} \cdot \frac{907.18 \text{ kg}}{\text{ton}} \cdot \frac{0.25 \ NO_2}{NO_x} = \frac{2.59 \text{ kg } NO_2}{\text{hr}}$$

$$\frac{7.77 \text{ kg NO}}{\text{hr}} \cdot \frac{1000\text{g}}{\text{kg}} \cdot \frac{\text{gmol}}{46\text{g}} = \frac{168.85 \text{ g} \cdot \text{mol NO}}{\text{hr}}$$

$$\frac{2.59 \text{ kg } NO_2}{\text{hr}} \cdot \frac{1000\text{g}}{\text{kg}} \cdot \frac{\text{gmol}}{46\text{g}} = \frac{56.28 \text{ g} \cdot \text{mol } NO_2}{\text{hr}}$$

The reason the molecular weight of NO was set at 46 g/gmol (the same as for NO_2) is because all NO_x is measured and reported as NO_2. Table 4.7 shows the input values of NO and NO_2 used for the UAM point source file for each of the modeling scenarios.

Table 4.7. NO and NO_2 UAM Point Source Emission File Input values.

Emission Rate (tpy NO_x)	Emission Rate NO (g·mol/hr)	Emission Rate NO_2 (g·mol/hr)
100	168.85	56.28
1000	1688.47	562.82
10000	16884.68	5628.23
100000	168846.78	56282.26

4.4 Mixing Height Input File

The UAM input file named *Diffbreak* is the file that specifies the daytime mixing height and the nighttime inversion height for each column of cells throughout the modeling domain on an hourly basis. The hourly mixing heights are constructed from the twice daily mixing height data collected for each day to be modeled at the closest upper-air station to the modeling domain (Nashville) plus the mixing height data for the day before and after the day to be simulated. The morning and afternoon mixing heights retrieved from the SCRAM bulletin board are converted to hourly mixing heights by the RAMMET-X (version 3.0) preprocessor, and then converted to an acceptable format which can be input into the UAM using the DFSNBK preprocessor. The values input

into the UAM are uniformly distributed across the modeling domain. Table 4.8 shows the hourly mixing heights for each of the five days simulated by the UAM.

Table 4.8. Mixing height values for five days simulated by the UAM.

Mixing Heights (meters)					
Hour	**June 14**	**June 30**	**July 07**	**July 10**	**July 25**
1	297.0	256.0	343.0	338.0	140.0
2	297.0	256.0	343.0	338.0	140.0
3	297.0	256.0	343.0	338.0	140.0
4	297.0	256.0	343.0	338.0	140.0
5	454.6	388.8	451.4	485.1	220.1
6	716.7	629.3	668.0	795.7	477.9
7	978.7	869.8	884.5	1106.4	735.8
8	1240.8	1110.4	1101.1	1417.0	993.7
9	1502.8	1350.9	1317.7	1727.6	1251.5
10	1764.9	1591.4	1534.3	2038.2	1509.4
11	2026.9	1831.9	1750.8	2348.8	1767.3
12	2289.0	2072.5	1967.4	2659.4	2025.1
13	2551.0	2313.0	2184.0	2970.0	2283.0
14	2551.0	2313.0	2184.0	2970.0	2283.0
15	2551.0	2313.0	2184.0	2970.0	2283.0
16	2551.0	2313.0	2184.0	2970.0	2283.0
17	2551.0	2313.0	2184.0	2970.0	2283.0
18	2551.0	2313.0	2184.0	2970.0	2283.0
19	2462.0	2260.3	2110.7	2963.9	2283.8
20	2029.5	1888.0	1618.5	2238.9	1694.1
21	1597.0	1515.6	1126.3	1608.3	1231.7
22	1164.5	1143.3	634.2	977.6	769.4
23	732.0	771.0	142.0	347.0	307.0
24	732.0	771.0	142.0	347.0	307.0

4.5 Temperature File

Another meteorological input file utilized by the UAM is the surface temperature file named *Temperatur*. This file simply contains the hourly surface temperature for each grid cell. The temperature data employed by this file were obtained from the National Climatic Data Center (NCDC) from the airport site nearest the location of the potential point source, as was described in section 4.1. Table 4.9 shows the surface temperatures used as input to the UAM for the five scenarios. The temperatures listed in the table for each hour were kept spatially constant for the entire modeling domain for each day simulated.

Table 4.9. Temperature input file data for five days simulated by the UAM.

Temperature Input Values (°K)					
Time	June 14	June 30	July 07	July 10	July 25
6-7 am	293.0	296.9	293.6	296.3	292.4
7-8 am	295.8	298.6	294.7	298.6	294.7
8-9 am	297.4	300.2	295.2	299.1	297.4
9-10 am	300.2	301.9	298.6	301.9	298.0
10-11 am	300.8	303.6	301.3	304.1	299.7
11-noon	301.3	304.7	303.0	306.3	301.3
12-1 pm	302.4	305.8	305.8	306.3	302.4
1-2 pm	300.8	305.8	306.9	308.0	302.4
2-3 pm	300.4	306.9	307.4	308.0	303.6
3-4 pm	300.2	306.0	307.4	306.3	303.6
4-5 pm	302.4	306.9	308.0	304.1	303.0
5-6 pm	301.3	305.2	308.0	303.0	301.9
6-7 pm	300.2	303.6	307.4	301.3	300.2
7-8 pm	299.1	302.4	305.2	299.7	299.7
8-9 pm	298.6	300.8	303.0	299.1	298.0
9-10 pm	296.9	299.1	301.3	298.0	297.4
10-11 pm	296.9	298.6	299.7	297.4	295.8
11-midnite	296.3	298.0	298.6	297.4	296.3

4.6 Meteorological Parameters File

The input file containing the spacially non-varying meteorological parameters for each modeling scenario is the *Metscalars* file. The parameters included in this file are the concentration of water vapor, the NO_2 photolysis rate constant, the temperature gradient below and above the mixing height, the exposure class, and the atmospheric pressure for each hour simulated (OAQPS Vol 1, 1990).

Two programs are required to obtain the information and format required by the UAM. The first program is the SUNFUNC4, which calculates the solar zenith angle and the NO_2 photolysis rates (Radfactor) for each hour. The information needed to execute the SUNFUNC4 program are the location in terms of latitude and longitude, the time zone, the date, and the hours of the simulation. The SUNFUNC4 program was run for each different modeling scenario.

The next program which is required to give us the proper UAM input files is the METSCL program. This preprocessing program is used to format the information input into the UAM. The parameters required by this program are the output parameters from the SUNFUNC4 program in addition to the temperature gradient below (TGRADEBELOW) and above (TGRADEABOVE) the mixing height, the concentration of water vapor (CONCWATER), the exposure class (EXPCLASS), and the atmospheric pressure (ATMOSPRESS). The default value of 1 atm was used for the atmospheric pressure values. TGRADEBELOW and TGRADEABOVE are found by using the following equations:

$$\text{TGRADEBELOW} = (T_{mix}\ (^{\circ}K) - T_{surf}\ (^{\circ}K)) \,/\, \text{Mixing Height (m)}$$

$$\text{TGRADEABOVE} = (T_{top}\ (^{\circ}K) - T_{mix}\ (^{\circ}K)) \,/\, (\text{Regiontop} - \text{Mixing Height})$$

T_{mix} and T_{top} are the temperatures at the mixing height and the region top height respectively. T_{mix} values were obtained from available data from the Nashville upper-air station, and T_{top} was set at 283.3 $^{\circ}K$ for the modeling domain. The regiontop height was set at 3420 meters for the modeling domain, which is the maximum mixing height (2970m) plus 450 meters. The hourly surface temperatures (T_{surf}) were obtained from the

National Climatic Data Center (NCDC) at the proper airport location as described in section 4.5.

The CONCWATER values were computed utilizing a psychrometric chart and surface T_{dry} (same as T_{surf} °F) and T_{wet} (°F) which are obtained from the NCDC. The psychrometric chart gives CONCWATER as lb of water per lb of air. To convert to ppm the following relations were used:

$$\text{CONCWATER } (\mu g/m^3) = \text{CONCWATER} \frac{\text{lb water}}{\text{lb air}} \cdot 453.6 \times 10^6 \frac{\mu g \text{ water}}{\text{lb water}} \cdot \frac{2.611 \text{ lb air}}{m^3 \text{ air}}$$

$$\text{CONCWATER (ppm)} = 8.314 \times 10^{-2} \cdot \frac{\text{Tdry (K)}}{1013.25 \text{ mbar}} \cdot \frac{\text{CONCWATER } (\mu g/m^3)}{18 \text{ g/gmol}}$$

EXPCLASS was found using Table 6-9 in section 6.3 of the UAM User's Guide, volume II. The table lists the EXPCLASS based on solar zenith angle (output from SUNFUNC4 program), and cloud cover. The cloud cover was obtained from NCDC surface meteorological data from the proper airport. Tables 4.10 - 4.14 show the values of the Metscalar files for the five days simulated by the UAM.

Table 4.10. June 14 Metscalars input file data.

Metscalars Input Data for June 14					
Time	TGRADEBELOW	TGRADEABOVE	EXPCLASS	RADFACTOR	CONCWATER
6 - 7	0.0053	-0.0045	1.0	0.2360	21720.0
7 - 8	0.0041	-0.0042	1.0	0.3867	22846.0
8 - 9	0.0028	-0.0036	1.0	0.4887	22041.0
9 - 10	0.0015	-0.0028	2.0	0.5578	24133.0
10 - 11	0.0003	-0.0017	2.0	0.6025	24776.0
11 - 12	-0.0001	-0.0013	2.0	0.6254	23811.0
12 - 13	-0.0022	-0.0012	2.0	0.6289	24294.0
13 - 14	-0.0035	0.0003	2.0	0.6131	23811.0
14 - 15	-0.0048	0.0003	3.0	0.5770	25098.0
15 - 16	-0.0061	0.0003	2.0	0.5170	25902.0
16 - 17	-0.0073	0.0003	1.0	0.4285	24133.0
17 - 18	-0.0086	0.0003	0.0	0.2985	25098.0
18 - 19	-0.0073	0.0003	1.0	0.1247	25098.0
19 - 20	-0.0061	-0.0002	1.0	0.0	26224.0
20 - 21	-0.0048	-0.0023	-2.0	0.0	25581.0
21 - 22	-0.0035	-0.0037	-2.0	0.0	27350.0
22 - 23	-0.0022	-0.0047	-1.0	0.0	26546.0
23 - 24	-0.0001	-0.0054	-1.0	0.0	26707.0

Table 4.11. June 30 Metscalars input file data.

Metscalars Input Data for June 30					
Time	TGRADEBELOW	TGRADEABOVE	EXPCLASS	RADFACTOR	CONCWATER
6 - 7	0.0054	-0.0055	0.0	0.2432	21720.0
7 - 8	0.0042	-0.0055	1.0	0.3906	22202.0
8 - 9	0.0030	-0.0052	1.0	0.4906	23811.0
9 - 10	0.0017	-0.0048	2.0	0.5585	23972.0
10 - 11	0.0005	-0.0044	2.0	0.6023	24455.0
11 - 12	-0.0007	-0.0039	3.0	0.6246	24133.0
12 - 13	-0.0020	-0.0047	3.0	0.6276	24937.0
13 - 14	-0.0032	-0.0041	3.0	0.6114	24133.0
14 - 15	-0.0045	-0.0041	3.0	0.5751	22524.0
15 - 16	-0.0057	-0.0041	2.0	0.5150	23972.0
16 - 17	-0.0069	-0.0041	2.0	0.4246	24133.0
17 - 18	-0.0082	-0.0041	1.0	0.2967	23972.0
18 - 19	-0.0069	-0.0041	0.0	0.1242	22041.0
19 - 20	-0.0057	-0.0042	0.0	0.0	20432.0
20 - 21	-0.0045	-0.0051	1.0	0.0	21720.0
21 - 22	-0.0032	-0.0056	-1.0	0.0	21237.0
22 - 23	-0.0020	-0.0055	-1.0	0.0	23811.0
23 - 24	-0.0007	-0.0058	-1.0	0.0	22524.0

Table 4.12. July 07 Metscalars input file data.

Metscalars Input Data for July 07					
Time	TGRADEBELOW	TGRADEABOVE	EXPCLASS	RADFACTOR	CONCWATER
6 - 7	0.0079	-0.0052	1.0	0.2348	20915.0
7 - 8	0.0064	-0.0051	1.0	0.3852	21398.0
8 - 9	0.0048	-0.0050	1.0	0.4870	20915.0
9 - 10	0.0032	-0.0049	2.0	0.5560	22524.0
10 - 11	0.0017	-.00046	2.0	0.6006	23007.0
11 - 12	0.0001	-0.0042	3.0	0.6234	22363.0
12 - 13	-0.0015	-0.0041	3.0	0.6269	19145.0
13 - 14	-0.0030	-0.0035	3.0	0.6111	17376.0
14 - 15	-0.0046	-0.0035	3.0	0.5749	18019.0
15 - 16	-0.0062	-0.0035	2.0	0.5149	16732.0
16 - 17	-0.0077	-0.0035	2.0	0.4216	16088.0
17 - 18	-0.0093	-0.0035	1.0	0.2960	18984.0
18 - 19	-0.0077	-0.0035	1.0	0.1228	19306.0
19 - 20	-0.0062	-0.0037	1.0	0.0	19628.0
20 - 21	-0.0046	-0.0046	-2.0	0.0	19628.0
21 - 22	-0.0030	-0.0084	-2.0	0.0	20915.0
22 - 23	-0.0015	-0.0056	-2.0	0.0	21719.0
23 - 24	0.0001	-0.0061	-2.0	0.0	22524.0

Table 4.13. July 10 Metscalars input file data.

Metscalars Input Data for July 10					
Time	TGRADEBELOW	TGRADEABOVE	EXPCLASS	RADFACTOR	CONCWATER
6 - 7	0.0074	-0.0060	1.0	0.2306	23007.0
7 - 8	0.0062	-0.0058	1.0	0.3825	24133.0
8 - 9	0.0049	-0.0053	1.0	0.4852	23972.0
9 - 10	0.0037	-0.0052	1.0	0.5547	24937.0
10 - 11	0.0025	-0.0048	2.0	0.5998	26868.0
11 - 12	0.0013	-0.0041	3.0	0.6228	27029.0
12 - 13	0.0001	-0.0066	3.0	0.6245	25581.0
13 - 14	-0.0011	-0.0067	3.0	0.6107	26546.0
14 - 15	-0.0023	-0.0067	3.0	0.5745	23811.0
15 - 16	-0.0036	-0.0067	1.0	0.5144	23007.0
16 - 17	-0.0048	-0.0067	1.0	0.4254	21237.0
17 - 18	-0.0060	-0.0067	0.0	0.2947	22846.0
18 - 19	-0.0048	-0.0067	0.0	0.1211	23328.0
19 - 20	-0.0036	-0.0068	0.0	0.0	23007.0
20 - 21	-0.0023	-0.0055	-1.0	0.0	24133.0
21 - 22	-0.0011	-0.0060	-1.0	0.0	24937.0
22 - 23	0.0001	-0.0065	-1.0	0.0	24133.0
23 - 24	0.0013	-0.0063	-1.0	0.0	24615.0

Table 4.14. July 25 Metscalars input file data.

Metscalars Input Data for July 25					
Time	TGRADEBELOW	TGRADEABOVE	EXPCLASS	RADFACTOR	CONCWATER
6 - 7	0.0076	-0.0037	-2.0	0.2273	17697.0
7 - 8	0.0062	-0.0034	1.0	0.3806	19306.0
8 - 9	0.0047	-0.0030	1.0	0.4833	19628.0
9 - 10	0.0032	-0.0024	1.0	0.5523	19467.0
10 - 11	0.0018	-0.0020	2.0	0.5965	22524.0
11 - 12	0.0003	-0.0013	3.0	0.6182	19789.0
12 - 13	-0.0012	-0.0005	3.0	0.6202	17697.0
13 - 14	-0.0026	0.0011	3.0	0.6025	17376.0
14 - 15	-0.0041	0.0011	3.0	0.5632	16088.0
15 - 16	-0.0056	0.0011	2.0	0.4995	16893.0
16 - 17	-0.0070	0.0011	2.0	0.4043	14480.0
17 - 18	-0.0085	0.0011	1.0	0.2628	15284.0
18 - 19	-0.0070	0.0011	1.0	0.8910	18663.0
19 - 20	-0.0056	0.0011	1.0	0.0	18502.0
20 - 21	-0.0041	-0.0019	-2.0	0.0	17376.0
21 - 22	-0.0026	-0.0034	-2.0	0.0	17697.0
22 - 23	-0.0012	-0.0044	-2.0	0.0	17376.0
23 - 24	0.0003	-0.0052	-2.0	0.0	17697.0

4.7 Initial and Boundary Default Concentrations

The UAM input files that contain the initial and boundary species' concentrations are the Airquality, Boundary, and Topconc files. The Airquality file contains the initial concentrations, for each grid cell, of the 23 species modeled by the UAM at the beginning of a simulation. For each hour simulated, the Boundary and Topconc files contain the 23 species' concentrations along the perimeter and top of the modeling domain respectively. As previously stated, due to the lack of ROM data these concentrations could not be extracted from previous ROM runs. Therefore, the default concentrations were used for

each species in each file constructed. Table 4.15 shows the 23 species and their default concentrations.

Table 4.15. Default concentrations for Airquality, Boundary, and Topconc files.

Default Concentrations for Carbon-Bond-IV Species		
Species	Species Name	Concentration (ppbC)
OLE	Olefins	0.60
PAR	Paraffins	14.94
TOL	Toluene	1.26
XYL	Xylene	0.78
FORM	Formaldehyde	2.1
ALD2	Higher aldehydes	1.11
ETH	Ethene	1.02
CRES	Cresol, higher phenols	0.01
MGLY	Methyl glyoxal	0.01
OPEN	Aromatic ring fragment acid	0.01
PNA	Peroxynitric acid	0.01
NXOY	Total nitrogen compounds	0.01
PAN	Peroxyacyl nitrate	0.01
HONO	Nitrous acid	0.01
H2O2	Hydrogen peroxide	0.01
HNO3	Nitric acid	0.01
MEOH	Methanol	0.1
ETOH	Ethanol	0.1
O3	Ozone	40.0 (ppb)
NO2	Nitrogen dioxide	2.0 (ppb)
NO	Nitric oxide	0.0 (ppb)
CO	Carbon monoxide	350.0 (ppb)
ISOP	Isoprene	0.1 (ppb)

5. PRELIMINARY RESULTS

The UAM was executed with the input data summarized above for the five days selected from MAP-O3 results. Simulations for each day included a basecase plus four NO_x source sizes (100, 1000, 10000, and 100000 tpy). The following sections summarize the results for each simulation beginning with the basecase simulations, followed by the point source simulations. Results are presented by source location, beginning with Knoxville, then Crossville, Chattanooga, and finally Tri-Cities.

A major concern to this project was whether or not the default boundary concentrations placed at the boundary of our modeling domain would interact with the hypothetical NO_x source emissions being modeled, and in turn alter the UAM's predicted ozone concentrations in the domain or within the park. In order to get an understanding of the effect of the boundary conditions, the preliminary simulations were executed using the non-temporally varying default (NTVD) boundary concentrations. Isopleth maps were constructed for each hour of each simulation using Tecplot™ (version 6.0) software. Each map shows the predicted ozone concentration in each cell of the 66km by 46km modeling domain. Although maps were constructed for each hour simulated, only selected hourly maps are in this report. Figure 5.1 shows the modeling domain used for this study, including county and state lines and Class I areas.

5.1 Basecase Scenarios

The Knoxville simulations (July 07 & July 10) were conducted first, using surface meteorological input data from the McGhee-Tyson airport. The July 07 simulation resulted in a maximum ozone concentration of 77.6 ppb in the GSMNP at 6 p.m., and the July 10 simulation resulted in a maximum ozone concentration of 73.3 ppb in the park at 4 p.m.

It was anticipated that ozone concentrations formed throughout the study domain would be uniform since a constant domain emissions inventory was used. In order to visually see whether this was occurring in these first simulations, Tecplot™ was used to

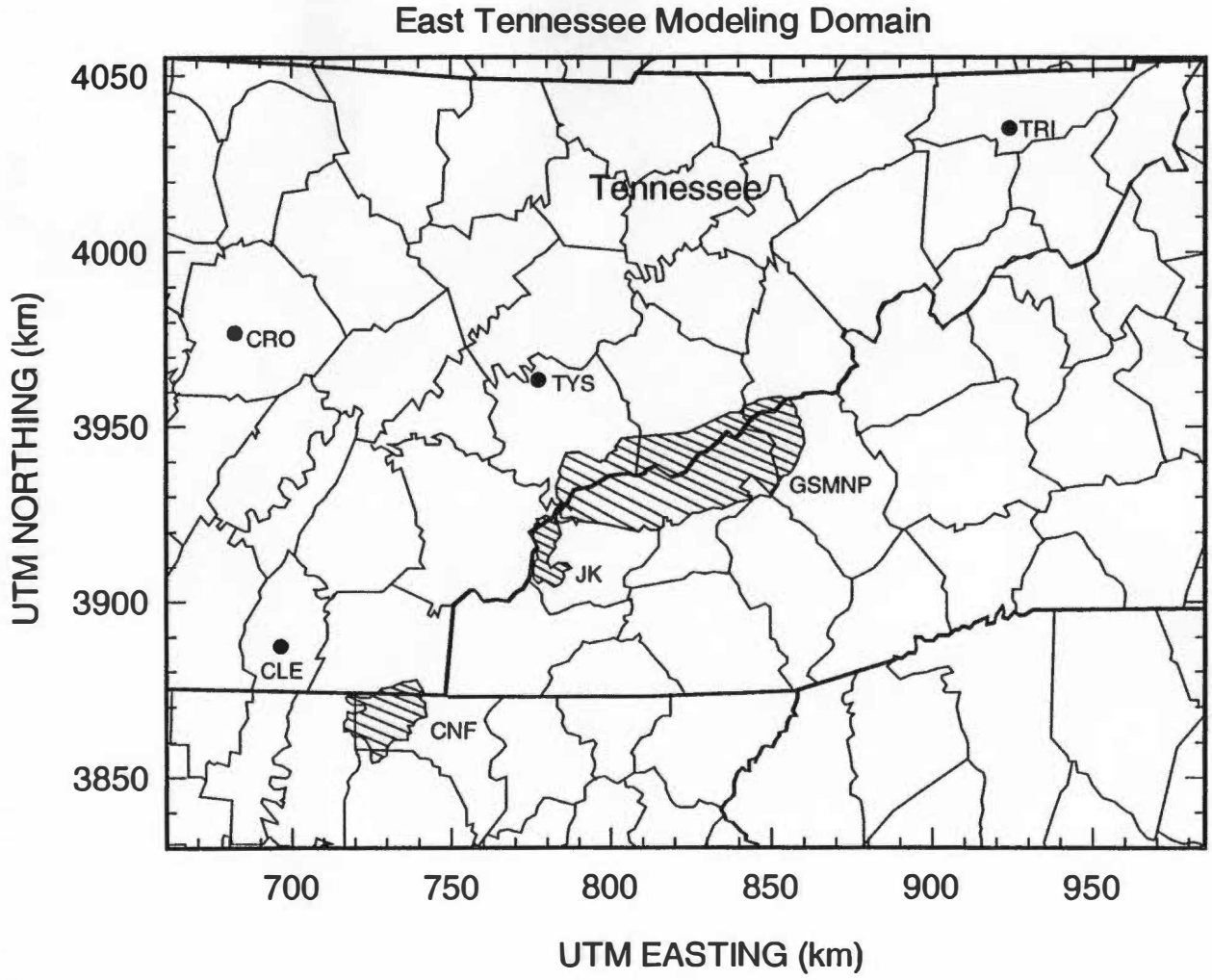


Figure 5.1. Modeling Domain; Including State, County, and Class I Area Boundaries

create isopleth maps for each hour. After constructing the maps an interesting pattern was observed while examining them. As expected, the constant domain emissions inventory was giving a uniform prediction of ozone concentrations, however this was not the case for the entire domain. An ozone concentration discrepancy could be seen coming in from the domain boundary, and becoming more distinct as the time progressed, apparently following each day's wind patterns. The ozone concentration values coming into the modeling domain from the boundary appeared to be lower than what was being formed from the uniform emissions. This was evidently due to the fact that the ozone concentrations predicted inside the modeling domain, with values up to 77.6 ppb, were formed by emissions and sunlight, whereas the default value of 40 ppb used for the boundary was being blown into the domain causing the discrepancy and giving the isopleth maps an unrealistic, rectangular appearance. This phenomena was referred to as a discrepancy wave, because when viewing in sequence all 18 isopleth maps constructed for a day in Tecplot, the boundary concentrations appear as a wave being blown into the modeling domain. Figure 5.2 and 5.3 are isopleth maps of the July 07 & 10 basecase simulations showing the influence of the default boundary concentrations on predicted ozone concentrations within the modeling domain.

In order to confirm that this phenomena was not isolated to the Knoxville runs, the basecase scenarios were executed and examined for the final three days selected by MAP-O3. The isopleth maps of these days confirmed that the occurrence of the ozone concentration discrepancy was not due to isolated meteorological events on July 7 and 10, but due to the NTVD concentrations used along the modeling domain boundary. The maximum ozone formed in the park for the June 30, June 14, and July 25 simulations was 73.3 ppb, 67.6 ppb, and 72.5 ppb respectively. The isopleth maps constructed for these days showed results similar to those for July 7 and 10 with lower ozone concentration values advecting into the modeling domain, and from different directions on the different days, confirming our hypothesis that each day's discrepancy followed that day's wind pattern. Figures 5.4, 5.5, and 5.6 are the isopleth maps for the June 30, June 14, and July

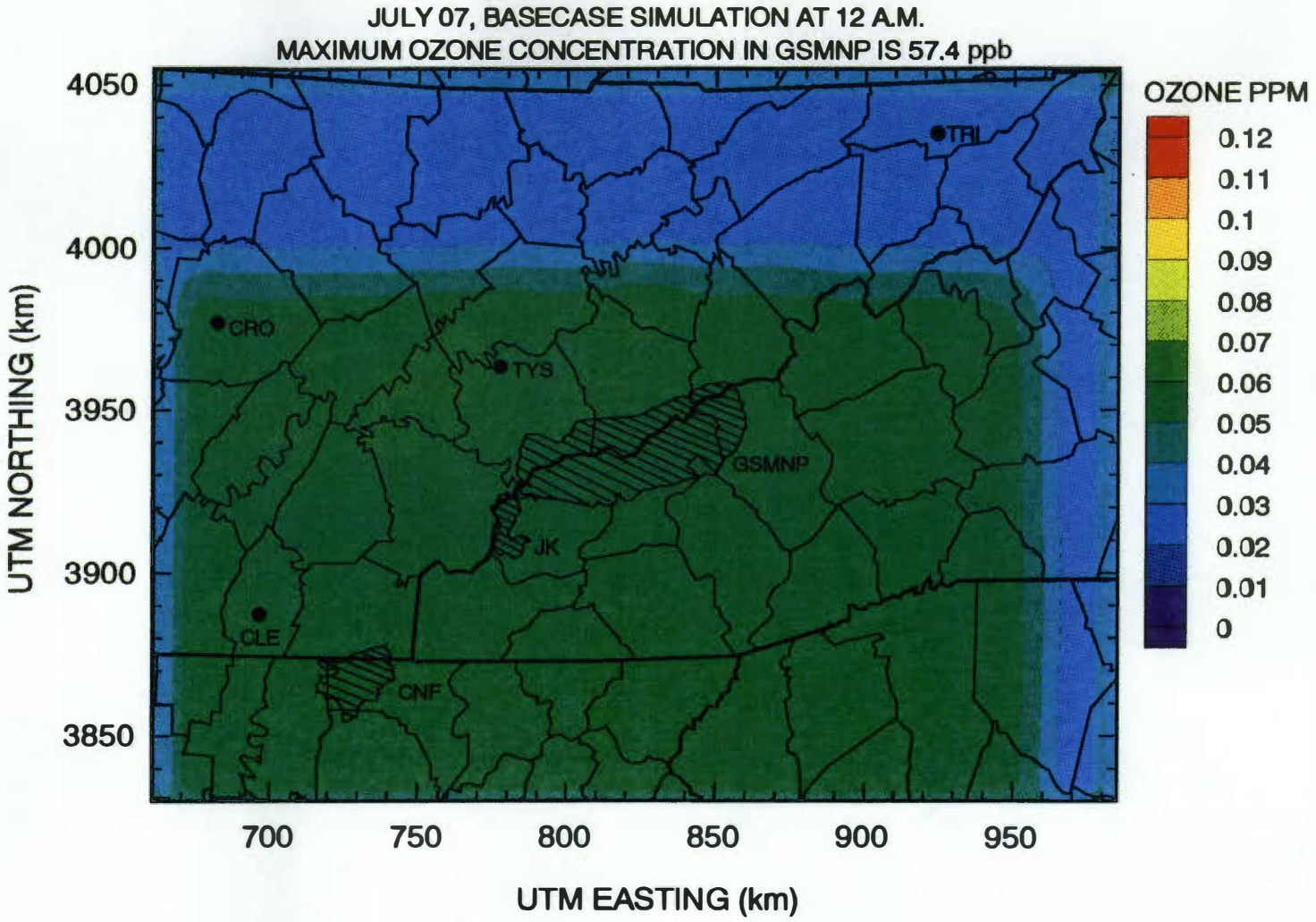


Figure 5.2. July 07 Basecase Simulation Using NTVD Concentrations.

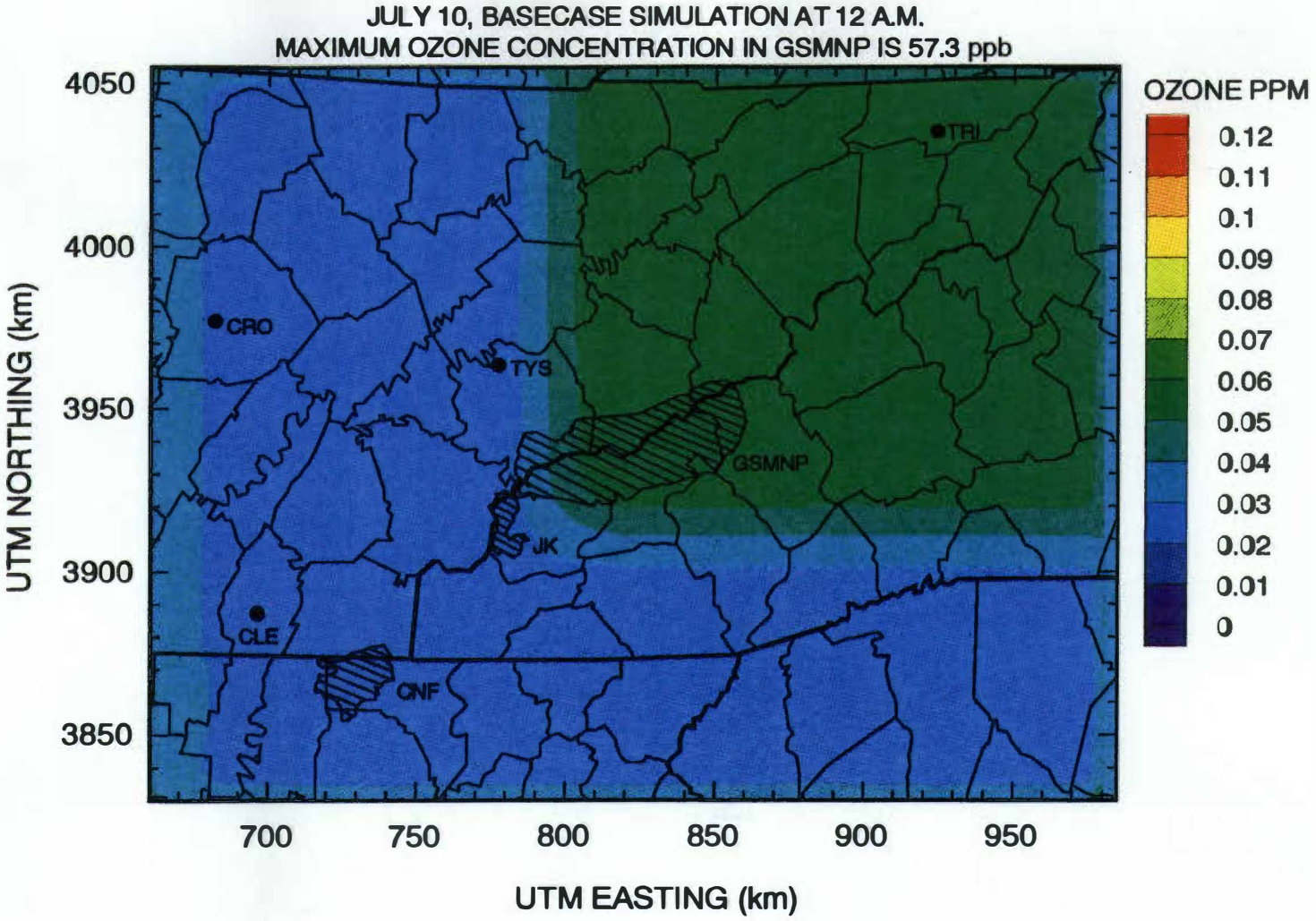


Figure 5.3. July 10 Basecase Simulation Using NTVD Concentrations.

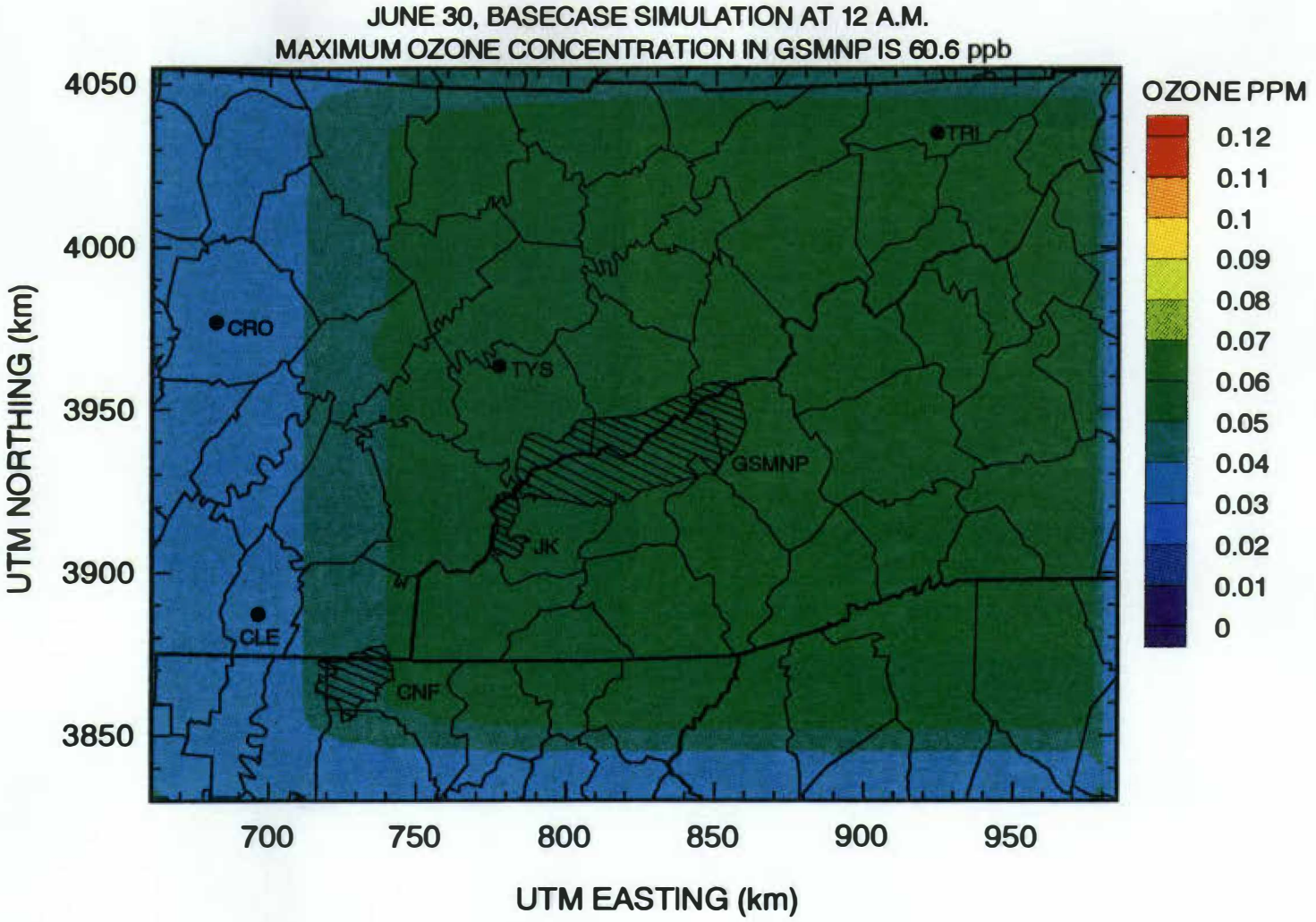


Figure 5.4. June 30 Basecase Simulation Using NTVD Concentrations.

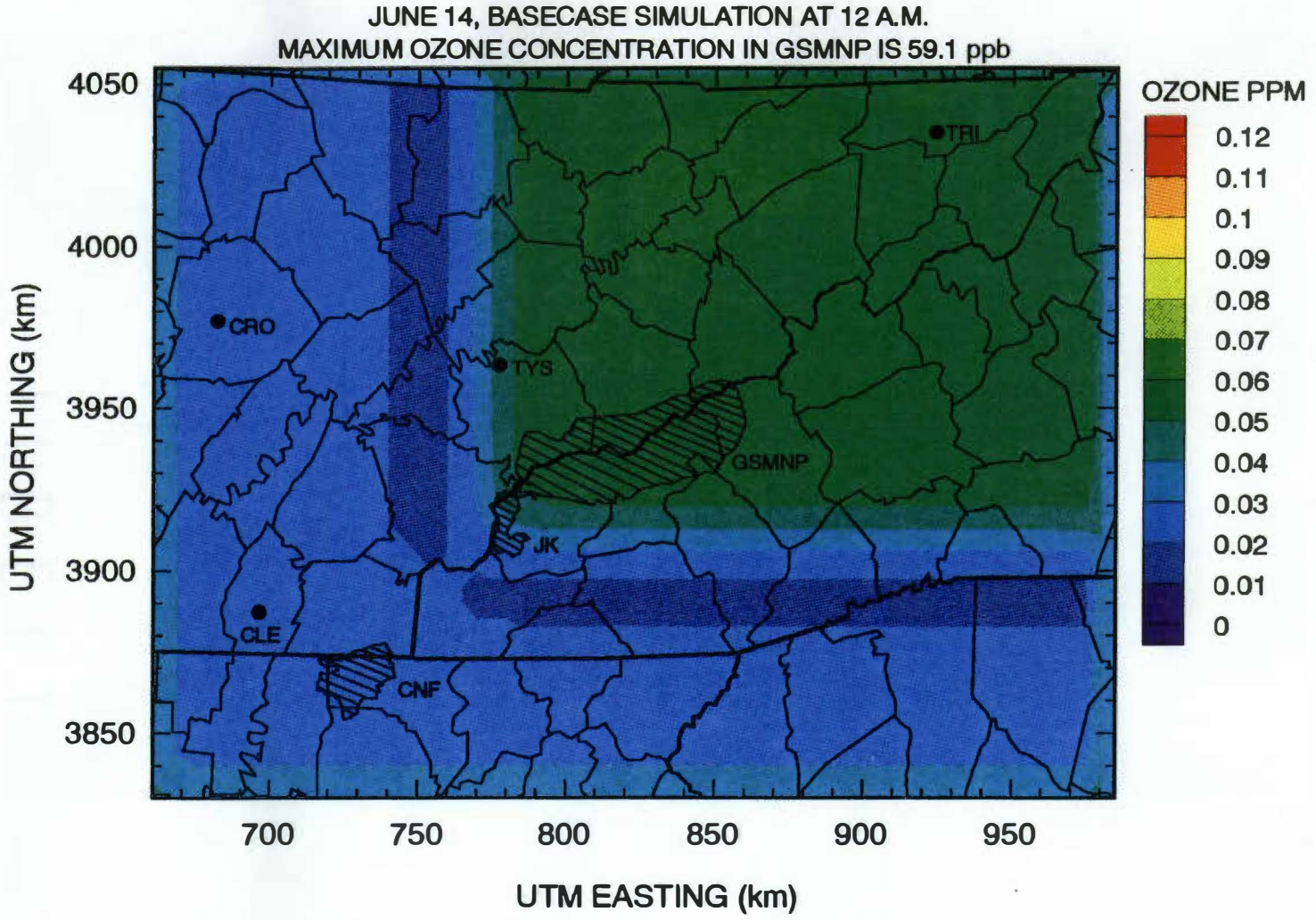


Figure 5.5. June 14 Basecase Simulation Using NTVD Concentrations.

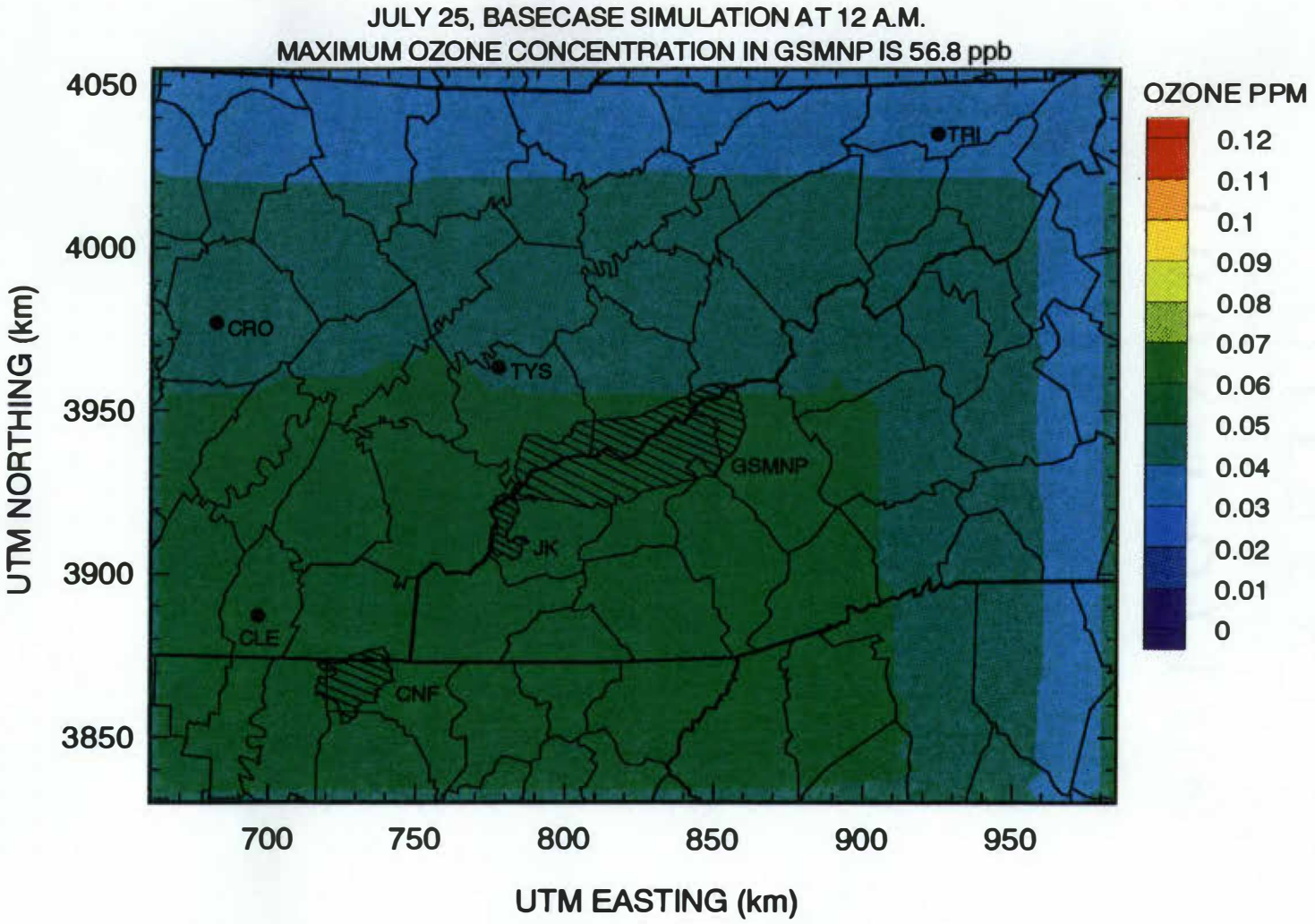


Figure 5.6. July 25 Basecase Simulation Using NTVD Concentrations.

25 basecase simulations showing the lower ozone concentrations advecting into the modeling domain from the boundary.

The reason the basecase scenarios' isopleth map resulted in a rectangular appearance was due to the lack of hourly varying boundary conditions. Previous modeling exercises had utilized EPA developed ROM runs to provide temporally and spatially varying boundary conditions. Since ROM runs were not available for the region and dates to be modeled, NTVD concentrations for species along the domain boundary had to be used. Although the predicted ozone concentrations in areas where boundary conditions were blown into the modeling domain appeared to affect the model's accuracy, the predicted ozone concentrations due to emissions away from the boundary did not appear to be significantly affected.

5.2 July 07 & July 10 Point Source Scenarios

The July 07, and July 10 simulations were executed with the hypothetical NO_x source located at the McGhee-Tyson airport. For each of the source sizes for both days, an increase in ozone concentrations from basecase values occurred in the modeling domain as well as in the GSMNP. The July 07 simulations resulted in ozone incremental increases in the park of 65.0 ppb, 44.5 ppb, 8.6 ppb, and 0.5 ppb for the source sizes of 100,000, 10,000, 1,000, and 100 tpy respectively. The July 10 simulations resulted in incremental ozone increases in the park of 48.0, 12.4, 1.6, and 0.2 ppb for the four source sizes.

July 07's wind trajectory showed calm or variable (swirling) winds early in the morning, causing the emissions from the NO_x source to be blown around the airport for several hours, allowing them to accumulate until they are finally blown toward the GSMNP. This resulted in giving the emission plume a very puff-like appearance. The maximum ozone concentration due to the 100,000 tpy source occurred in the park at 6 p.m., whereas the maximum ozone contributions due to the 10,000 and 1,000 tpy sources did not occur in the park until 8 p.m. The maximum ozone contribution due to the 100

tpy source occurred in the park at 7 p.m. All source sizes for July 07 impacted the GSMNP at the same location, but the time at which the maximum increment occurred in the park differs due to the size of the plumes for each scenario and how they were affected by the wind and dilution effects. Figure 5.7 is the isopleth map of the July 07, 100,000 tpy source simulation at 6 p.m., showing the maximum ozone increment impacting the GSMNP due to the potential source.

The maximum predicted ozone concentration for this simulation occurred in the modeling domain outside the GSMNP, and in turn resulted in the maximum incremental ozone increase in the domain. The maximum incremental increase due to the 100,000 tpy source occurred at 8 p.m., whereas the maximum incremental increases due to the other size sources each occurred at 6 p.m. The maximum incremental ozone concentrations were 68.5, 46.0, 9.2, and 1.06 ppb for the four source sizes in descending order. These values were slightly larger than the increments that occurred within the GSMNP. Figure 5.8 is the isopleth map of the July 07, 100,000 tpy simulation at 8 p.m. when the maximum incremental ozone occurs within the modeling domain.

On July 10 the wind blew primarily north-east early in the morning and then blew south-east for three hours in the afternoon resulting in a hit on the park. Since there were no calm hours or swirling effects by the wind on this day, the emissions were evenly dispersed throughout the day which resulted in an evenly dispersed plume, unlike the puff of July 07. The maximum predicted ozone concentration occurred for each source size at 6 p.m. and all occurred within the boundary of the GSMNP. Figure 5.9 shows the 100,000 tpy source for the July 10 simulation impacting the park at 6 p.m.

At this point it was still unclear whether the ozone concentration discrepancy caused by using default boundary concentrations was influencing the predicted ozone concentrations within the modeling domain when simulating the hypothetical NO_x sources. In order for this to occur, the grid cell that is allocated to receive the hypothetical point source's emissions would have to be overcome by the 'discrepancy wave' moving across the modeling domain that was caused by the NTVD boundary

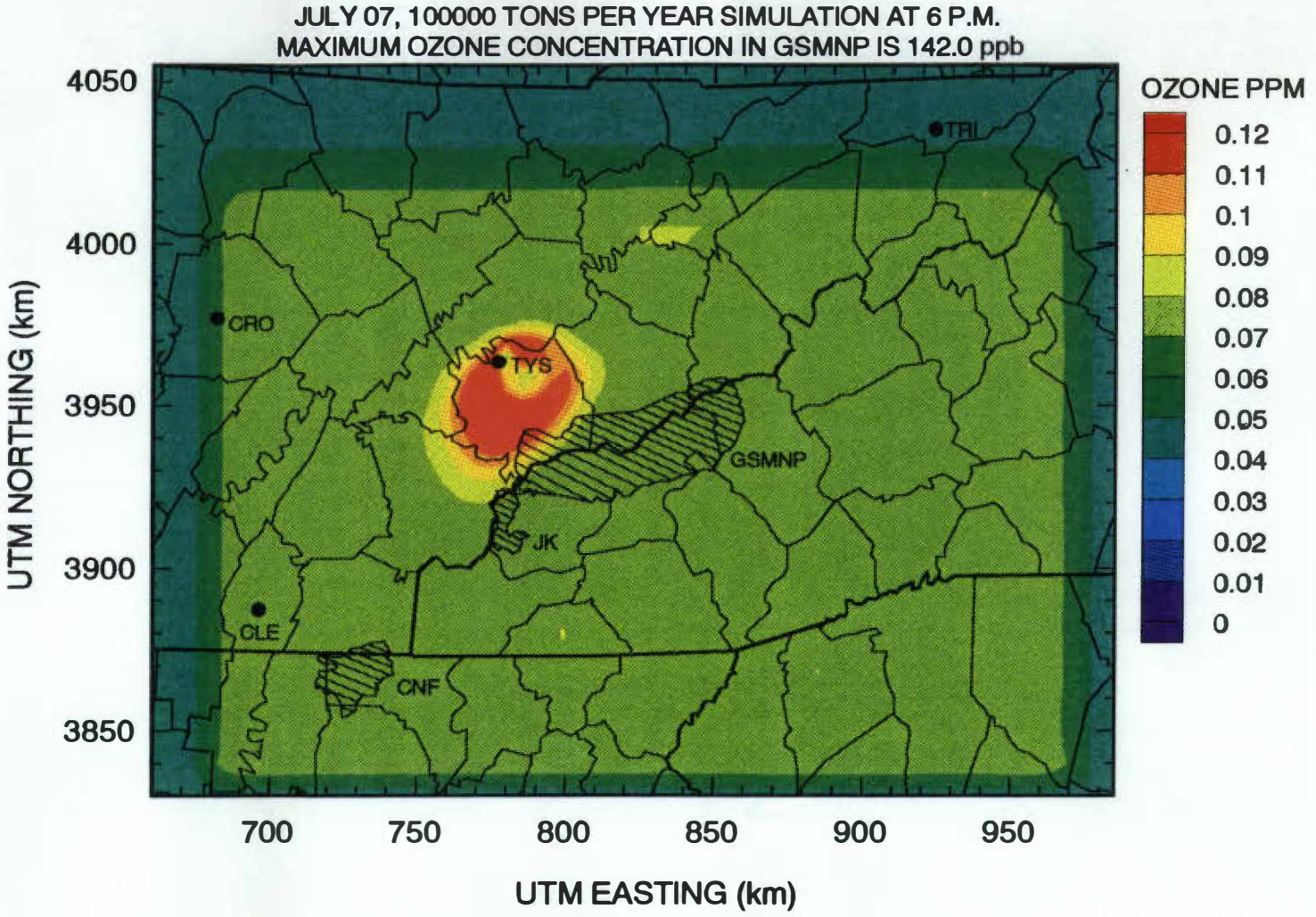


Figure 5.7. July 07 Point Source Simulation (6 p.m.) Using NTVD Concentrations.

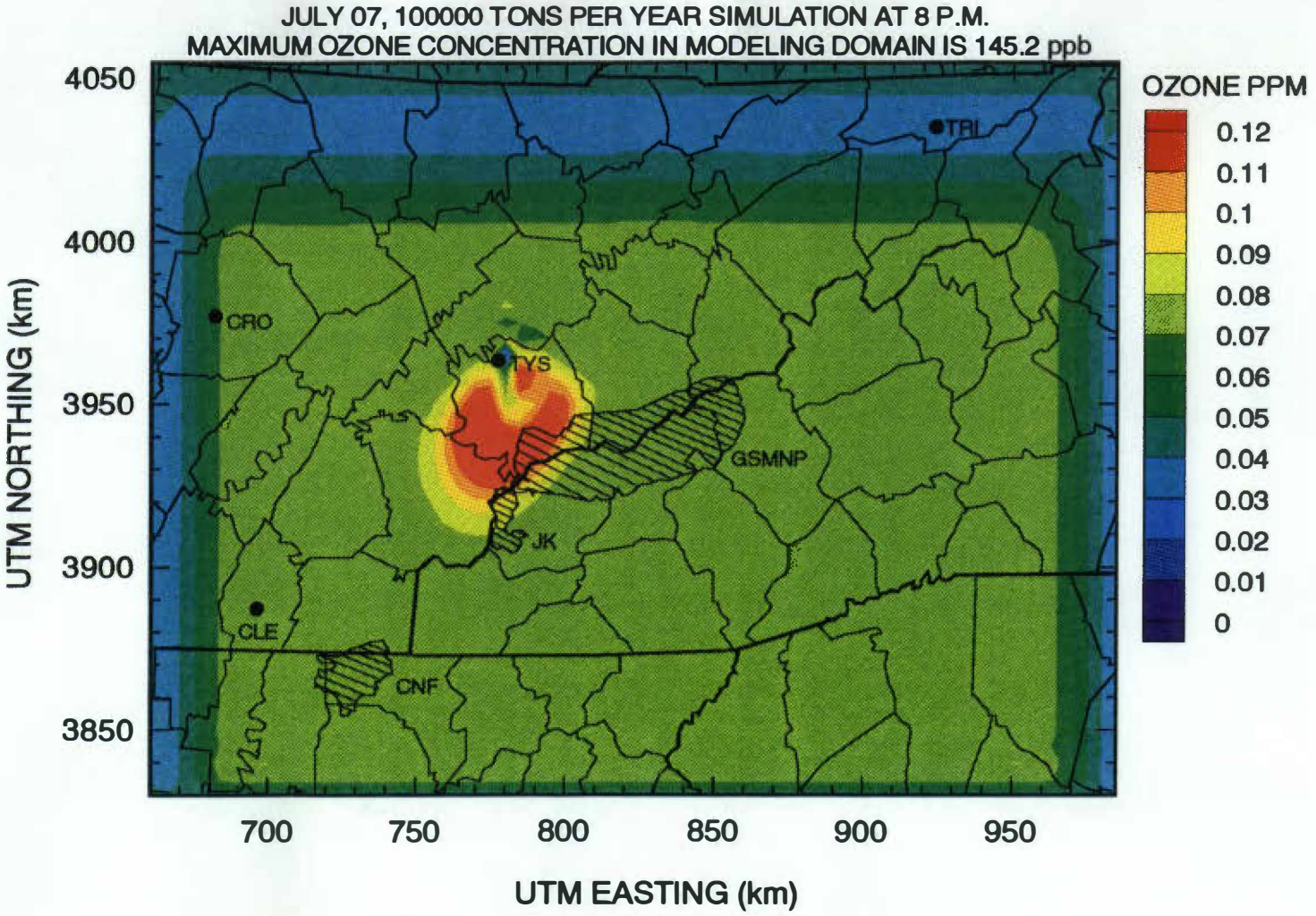


Figure 5.8. July 07 Point Source Simulation (8 p.m.) Using NTVD Concentrations.

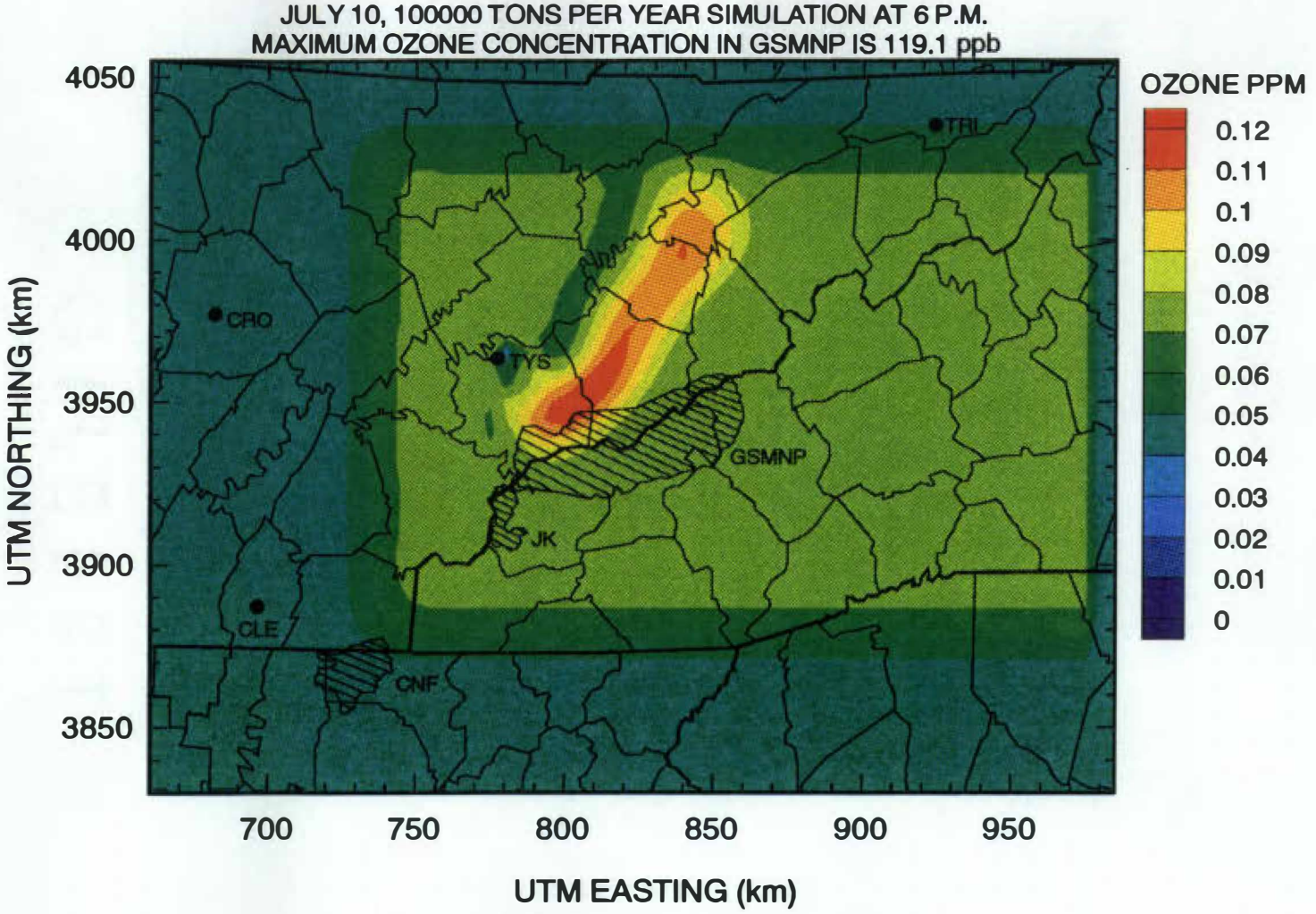


Figure 5.9. July 10 Point Source Simulation Using NTVD Concentrations.

concentrations. It would also have to occur sometime early to the middle of the day in order to affect the maximum ozone concentration predictions.

The isopleth maps for the July 07 simulation showed that the plume from the hypothetical source was never affected by the 'wave'. The isopleth maps of July 10 showed that the 'wave' did catch up to the plume at 9 p.m. that evening, but was too late to affect any maximum concentration predictions since the sun had already gone down and ozone scavenging was beginning to occur. The primary reason the plumes were not affected for these days was because the point source location (McGhee-Tyson airport) was located far enough away from the modeling domain boundary. Although the incremental ozone being formed within the modeling domain due to the hypothetical source on these two days did not appear to be affected by the NTVD boundary conditions, they show that it was a possibility.

5.3 June 30 Point Source Scenarios

The June 30 point source scenarios were conducted following the July 10 simulations. The location of the hypothetical NO_x source for these scenarios was Crossville, Tennessee. The results of these simulations predicted that there would be no impact on the ozone concentrations in the GSMNP due to any of the potential point source sizes. Referring back to the MAP-O3 results for this day, the ozone plume did not directly impact the park, but was considered because the edge of the ozone plume was within 22.5° from the edge of the GSMNP.

The maximum incremental ozone concentrations predicted within the modeling domain by the UAM for each source size were 56.7, 17.7, 0.72, and 0.0 ppb going from 100,000 tpy to 100 tpy source sizes respectively. These ozone increments occurred to the northwest of the GSMNP, which implies that if the wind profile had shifted a little to the south that day similar increments could have occurred within the park's boundary. Figure 5.10 is the isopleth map of the 100,000 tpy simulation at 5 p.m. when the maximum incremental ozone concentration occurs within the modeling domain.

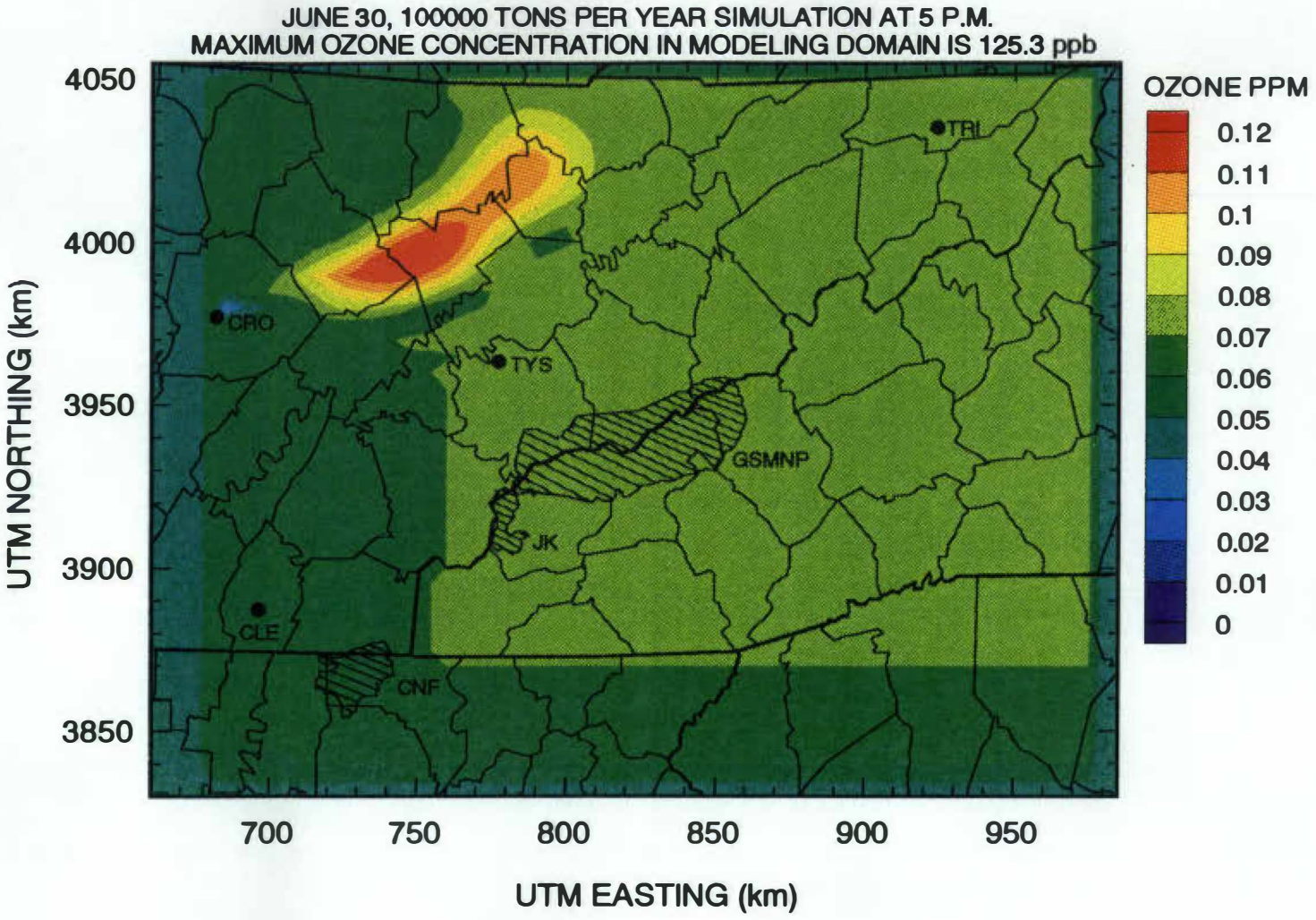


Figure 5.10. June 30 Point Source Simulation (5 p.m.) Using NTVD Concentrations.

Next, the point source isopleth maps were examined for each simulation to see if there was any interaction between the discrepancy wave and the emission plume. Analysis of the isopleth maps showed that the 'wave' reached the location of the point source early in the day, and by 3 p.m. the highest concentrations in the plume were surrounded by the wave. As can be seen on Figure 5.10, Crossville is located relatively close to the western edge of the modeling domain, which allows the discrepancy wave to interact with the point source emissions from that location. Figure 5.11 shows the discrepancy wave surrounding the hypothetical point source emission plume at 8 p.m., which is when the plume formed from the 100,000 tpy source was closest to the park and was recorded as a hit by MAP-O3.

5.4 June 14 Point Source Scenarios

The point source simulations for June 14 were the next to be conducted. The NO_x source location for this day's simulations was planned to be the Chattanooga airport. However, after analyzing the isopleth maps for the first simulation, the location was changed because some of the emissions were being lost (i.e. being transported north-westward) to the boundary. This was because Chattanooga was located very close to the domain boundary and the wind patterns for this day were not conducive to the site location. The morning winds were calm for the first few hours of the simulation. The next hour the wind blew to the northwest, transporting the emissions out of the modeling domain. Therefore the point source location was shifted from the edge of the boundary and re-located at Cleveland, Tennessee.

Once these changes were made, the point source simulations were conducted using surface meteorological data from Lovell Field airport in Chattanooga. The maximum predicted ozone increments within the modeling domain for each source size were 61.6, 18.7, 3.9, and 0.65 ppb. These increments occurred at 6 p.m. for the 100,000 tpy source, 3 p.m. for the 10,000 tpy source, and at 1 p.m. for the 1,000 and 100 tpy

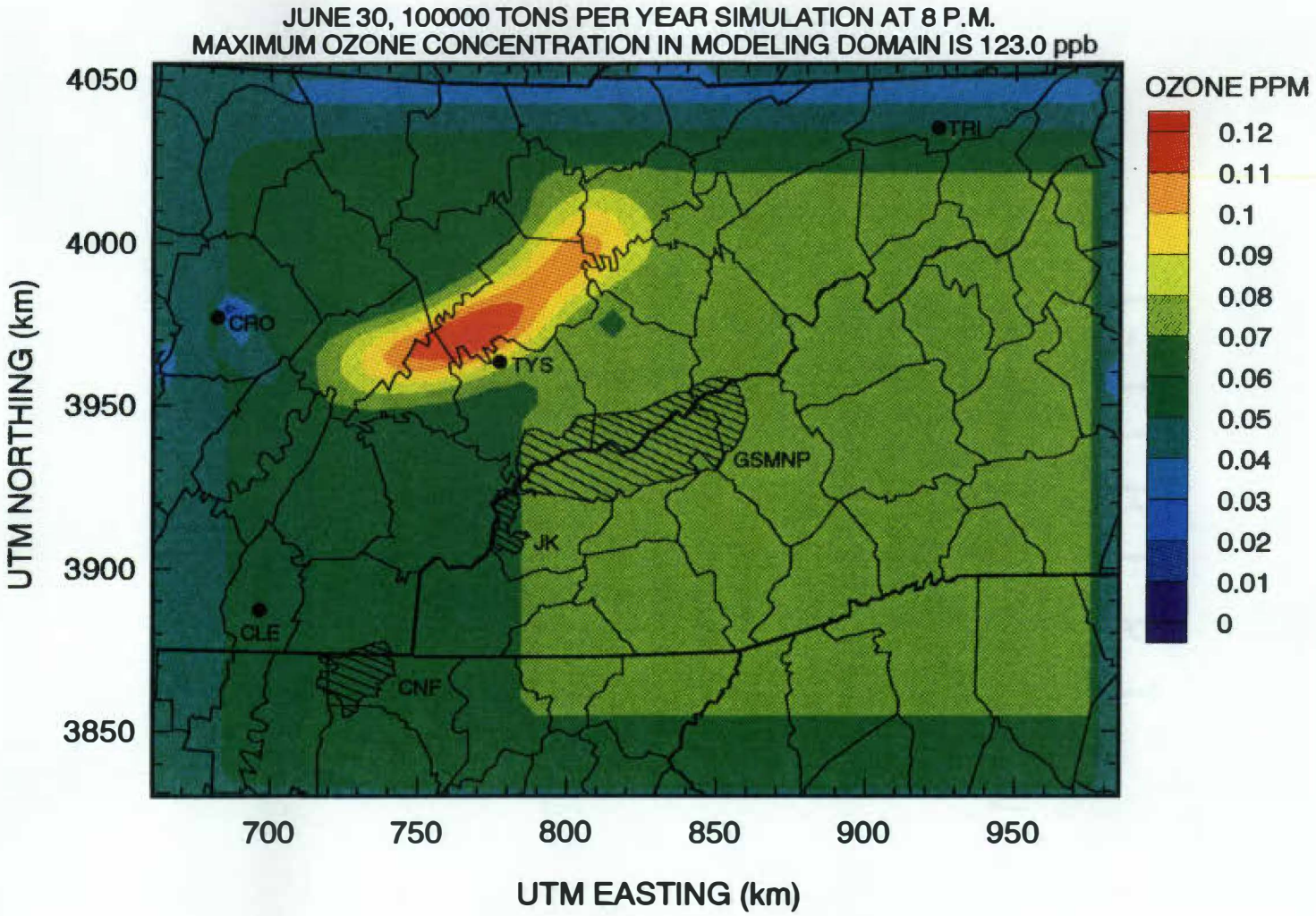


Figure 5.11. June 30 Point Source Simulation (8 p.m.) Using NTVD Concentrations.

sources. Figure 5.12 is the isopleth map of the 100,000 tpy simulation at 6 p.m. when the maximum increment occurs in the domain.

Later in the day, the ozone plumes from each source directly impacted the GSMNP. The resulting incremental ozone concentrations in the park were 59.7, 14.9, 1.56, and 0.34 ppb due to the four source sizes from largest to smallest. The largest two source sizes impacted the park at 8 p.m. and the smaller two impacted the park at 7 p.m.

Analyzing the isopleth maps constructed for these scenarios showed that the discrepancy wave formed by the NTVD boundary conditions appeared to overtake the source location at 2 p.m. and move east behind the emissions plume toward the GSMNP. The major portion of the plume was never in contact with the discrepancy wave, even when it impacted the park at 8 p.m. It appeared that the discrepancy wave did not catch up to the plume enough to affect maximum ozone predictions in the domain or in the park. Figure 5.13 shows the isopleth map for the 100,000 tpy source impacting the GSMNP at 8 p.m., as well as the discrepancy wave trailing behind the emission plume.

5.5 July 25 Point Source Scenarios

The final scenarios to be conducted were the July 25 point source simulations. The NO_x source location and surface meteorological station used for this day was the Tri-Cities airport. The wind file for this day gave an arching trajectory from the airport to the park, heading west southwest early in the morning and then mainly southwest later in the day at almost a straight line to the GSMNP resulting in a direct impact by the emission plume. The maximum predicted ozone concentrations in the modeling domain due to the four source sizes from largest to smallest were 48.9, 11.1, 0.87, and 0.0 ppb respectively. The increment due to the sources occurred at 5 p.m., 4 p.m., and 6 p.m. respectively. Figure 5.14 is the isopleth map of the 100,000 tpy simulation at 5 p.m. when the maximum incremental concentration occurred.

The maximum incremental ozone concentrations predicted to impact the GSMNP due to the four source sizes were 45.7, 8.2, 0.77, and 0.0 ppb respectively. The time that

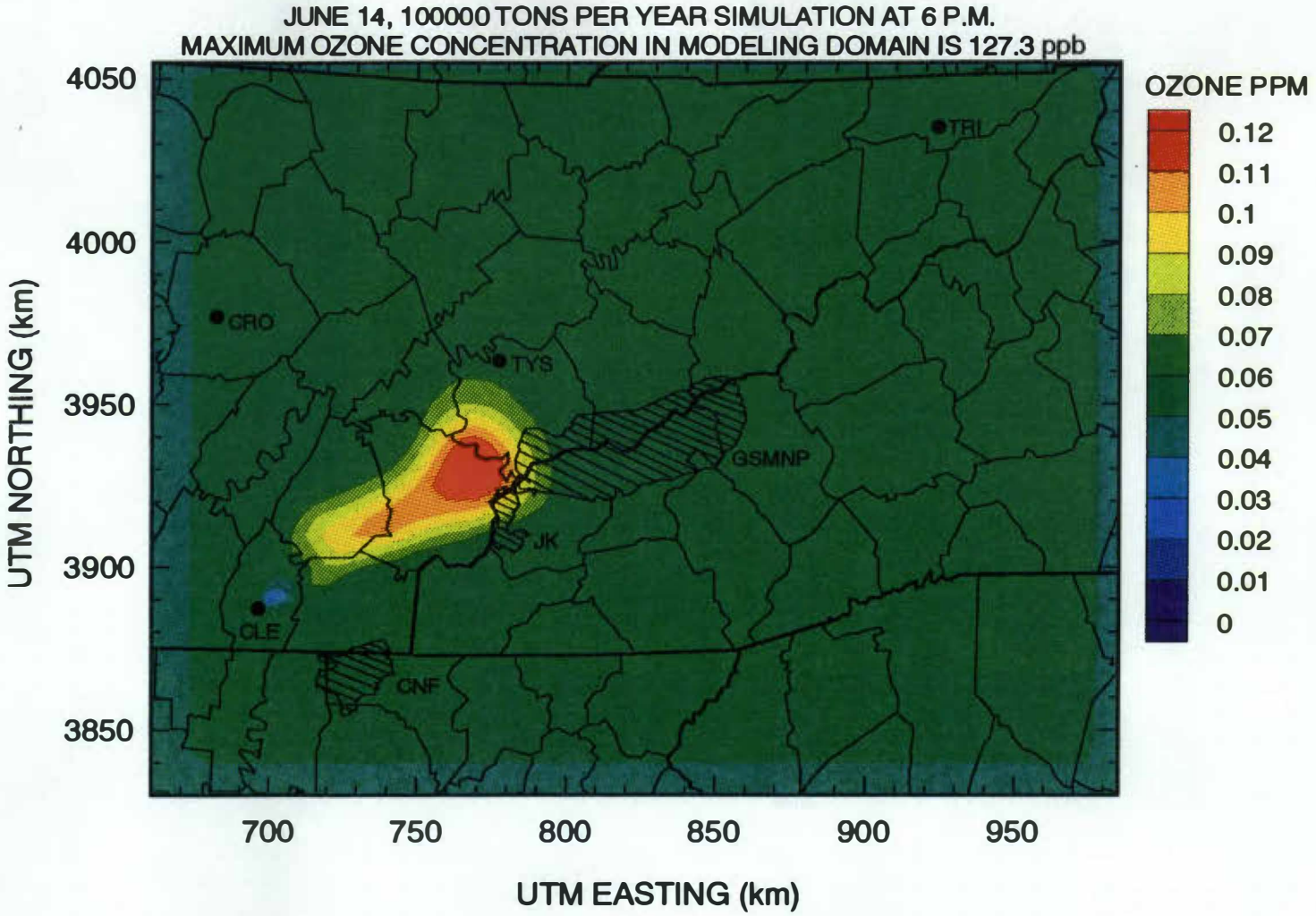


Figure 5.12. June 14 Point Source Simulation (6 p.m.) Using NTVD Concentrations.

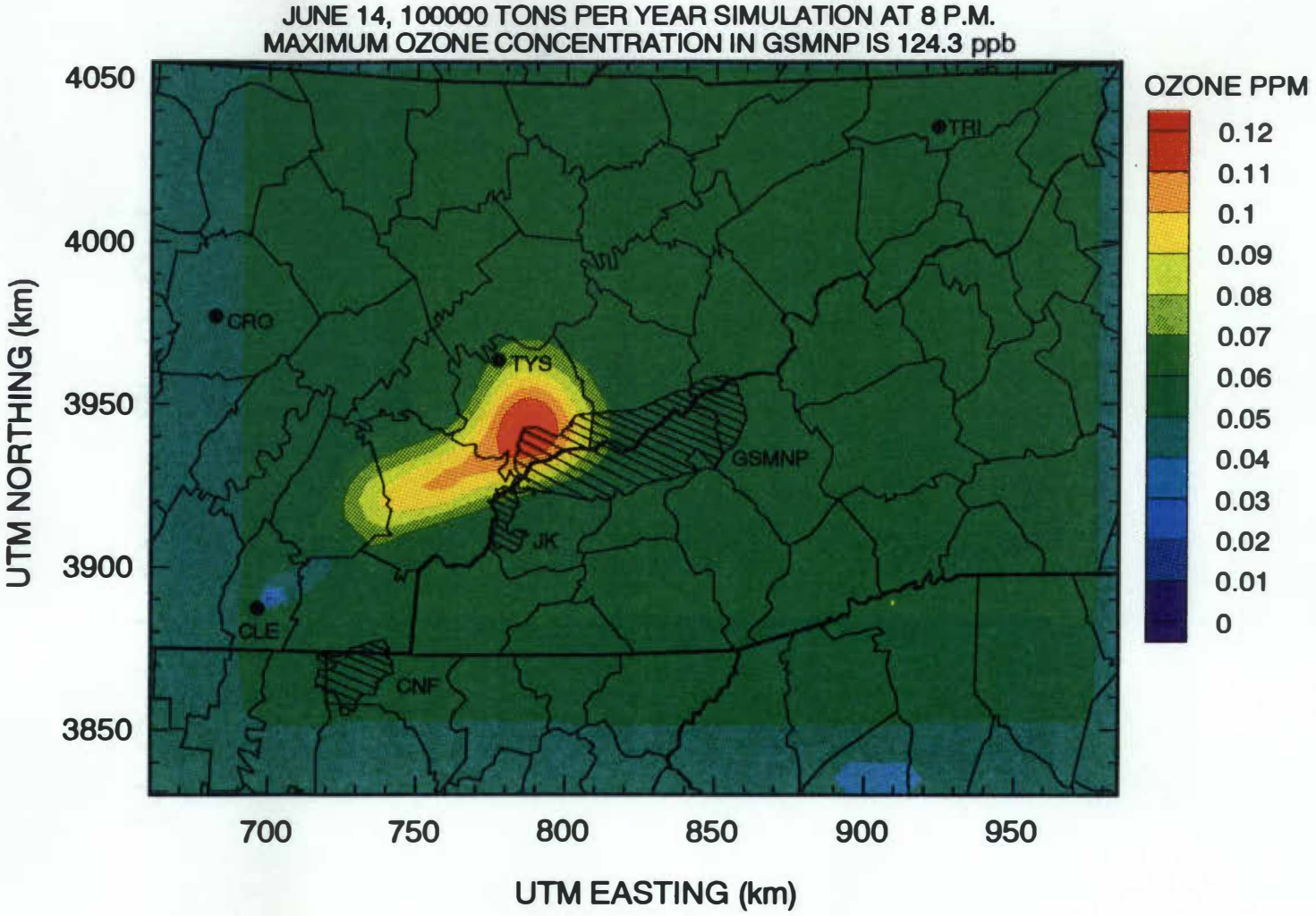


Figure 5.13. June 14 Point Source Simulation (8 p.m.) Using NTVD Concentrations.

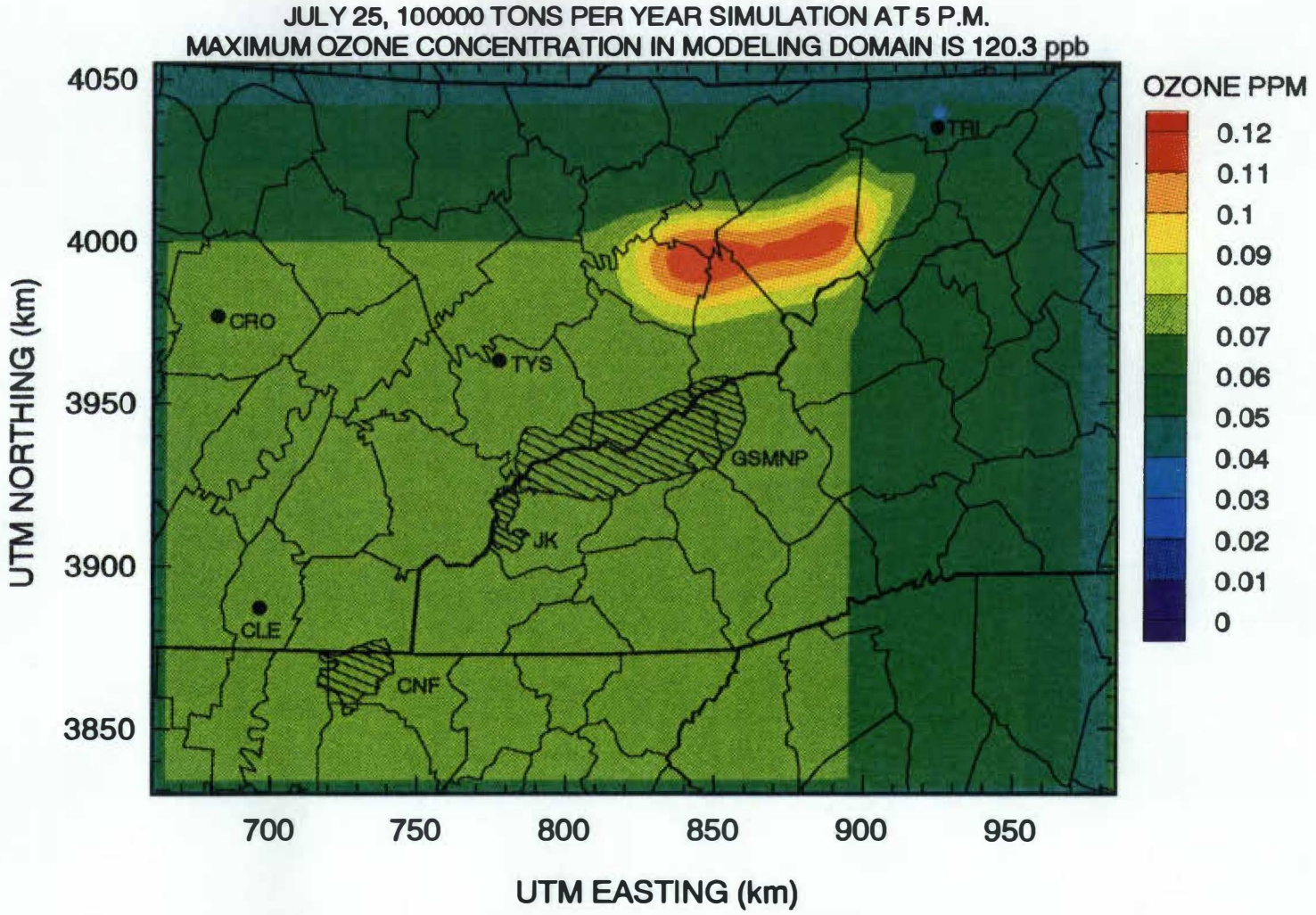


Figure 5.14. July 25 Point Source Simulation (5 p.m.) Using NTVD Concentrations.

these maximum increments occurred was 8 p.m. for each source size. Figure 5.15 is the isopleth map of the 100,000 tpy source showing the impact on the park at 8 p.m.

The isopleth maps constructed for this day showed that the discrepancy wave reached the location of the point source by 1 p.m. Consequently, the ozone plume hitting the park at 8 p.m. was surrounded by the 'wave'. Therefore, it was possible that the incremental ozone concentrations predicted in modeling domain for these simulations were affected by the discrepancy wave caused by the NTVD boundary concentrations.

5.6 TVP Method

To find out if the interference of the discrepancy wave on the point source emission plumes had an affect on predicted ozone increments in the domain, a method of minimizing the effect of boundary conditions on predicted ozone concentrations within the modeling domain was developed. This method was a two step process. The first step required that the basecase scenario for a day be executed using the same input data as previously described, including the NTVD concentrations for the boundary file. Once the simulation was completed and isopleth maps were constructed for each hour, a grid cell was selected that was not affected by boundary effects. The cell that was chosen had to be located sufficiently within the modeling domain such that it was representative of the basecase ozone and precursor concentrations formed by emissions and photochemical reactions occurring during the simulation period. This cell also had to be unaffected by boundary concentrations for all hours of the simulation.

The isopleth maps constructed for each basecase scenario were used to select a cell that was unaffected by boundary concentrations for each simulation. The cell for each day was identified by examining the isopleth map for each hour of a simulation in order. A rectangular box was then drawn on the final isopleth map, showing the edges within the domain which the discrepancy wave did not cross. Two lines were then drawn from one corner of the box to the other making an X in the box. The cell in which the

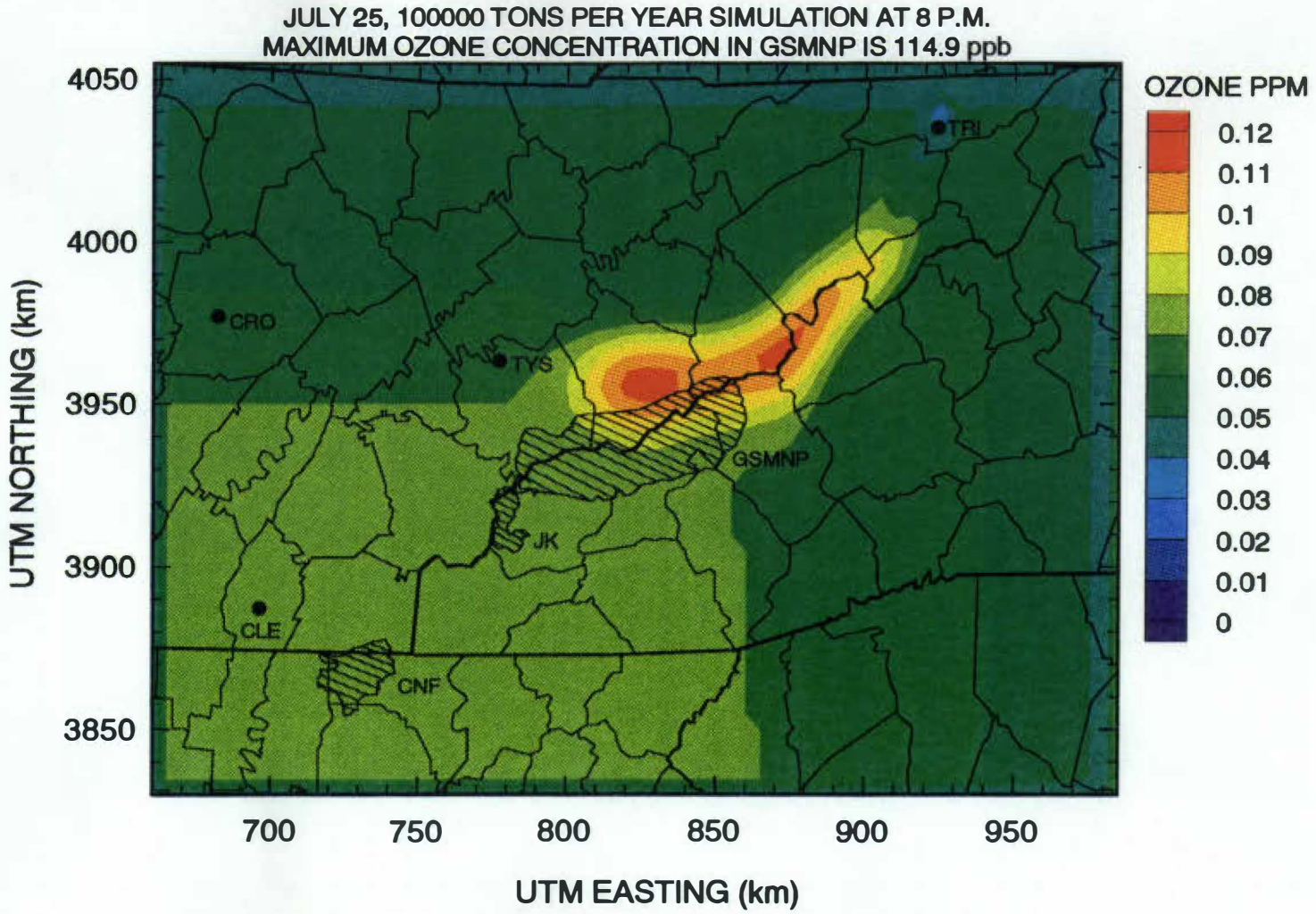


Figure 5.15. July 25 Point Source Simulation (8 p.m.) Using NTVD Concentrations.

lines crossed was chosen as the representative cell for the simulation. This cell was located in the center of the unaffected modeling domain.

The next step in minimizing the effect of boundary conditions was to extract the concentrations of all species from the single grid cell that was chosen, for each hour of the simulation. These concentrations were then input as the boundary concentrations for each cell along the modeling domain boundary for each hour. These species concentrations were referred to as the temporally varying predicted (TVP) concentrations and were used as the boundary input file to re-run that particular day's basecase as well the hypothetical point source simulations. These new TVP boundary conditions should be more representative (than NTVD conditions) of ozone and VOC precursor concentrations likely to occur at the domain boundary due to biogenic emissions and photochemical reactions occurring in areas adjacent to the modeling domain.

The output generated using these TVP concentrations along the boundary should be free of artificial effects caused by the NTVD concentrations. The results of the two simulations were then compared to see whether the NTVD concentrations affected the results of the preliminary runs.

6. FINAL RESULTS

The final results summarized in this chapter will address two questions. The first being whether the TVP concentrations used for boundary concentrations result in more appropriate ozone predictions within the modeling domain than those predicted using the NTVD concentrations. The second being whether ozone concentrations predicted using the MAP-O3 model are comparable to ozone concentrations predicted using the UAM, and do these concentrations occur in the GSMNP.

All modeling scenarios described in Chapter 5 were executed a second time using TVP boundary concentrations as described by section 5.5. The results of these simulations were compared to both the preliminary results and the MAP-O3 results in order to address the two questions. Tables 1-5 in Appendix B show the preliminary and final ozone concentration predictions for all simulations using the UAM.

6.1 TVP Basecase Results

July 07 was the first basecase scenario to be simulated using the new boundary concentrations. The maximum predicted ozone concentration in the domain for the TVP simulation decreased by 2.79 ppb from the NTVD simulation to a value of 79.02 ppb. Overall, the hourly results for this simulation were very similar to those from the preliminary simulation. The main difference between the results of the two simulations was that the discrepancy wave, which can be seen in Figure 5.2 for the NTVD simulation, was not present in the isopleth maps constructed for the TVP simulation. Figure 6.1 is the isopleth map of this final simulation at the same hour as Figure 5.2. As can be seen in Figure 6.1, the UAM predicted consistent background ozone values throughout the modeling domain for each hour of the simulation.

The basecase scenarios for the final four days were conducted next and isopleth maps were constructed for each. The isopleth maps for these runs are for the same hour as the preliminary simulations and can be seen in Figures 6.2 through 6.5. Comparing the TVP isopleth maps with the NTVD isopleth maps showed that the discrepancy wave was

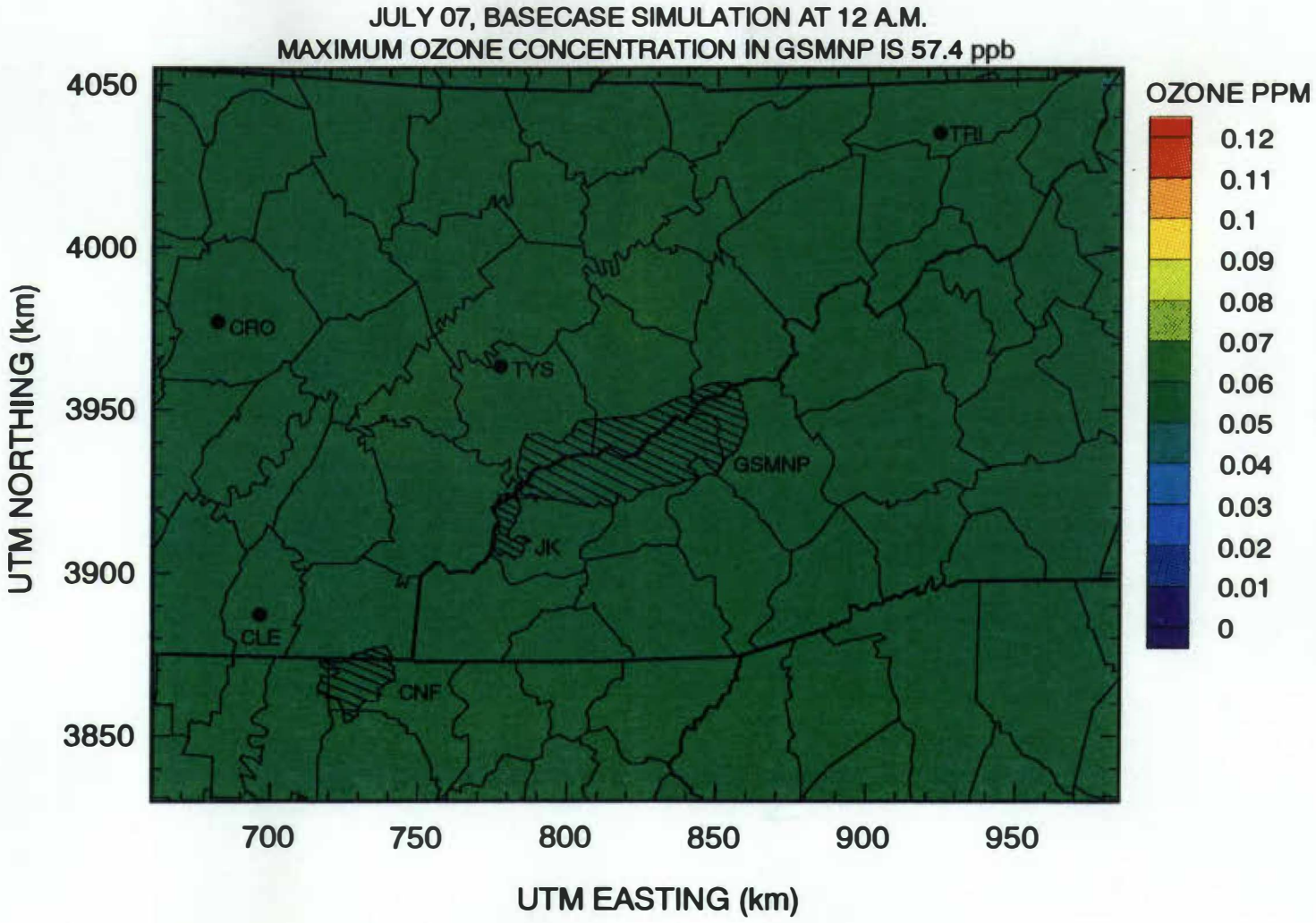


Figure 6.1. July 07 Basecase Simulation Using TVP Concentrations.

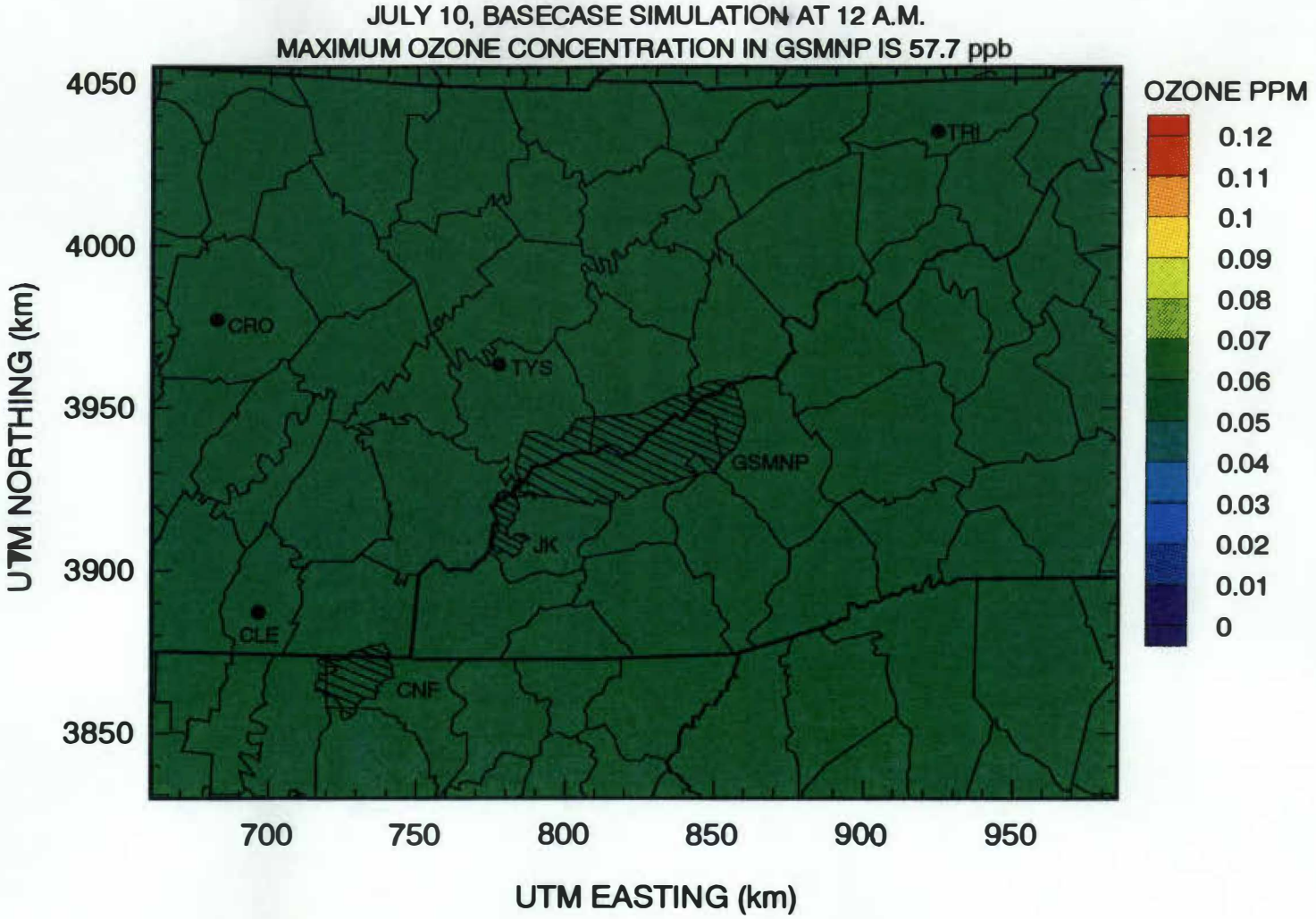


Figure 6.2. July 10 Basecase Simulation Using TVP Concentrations.

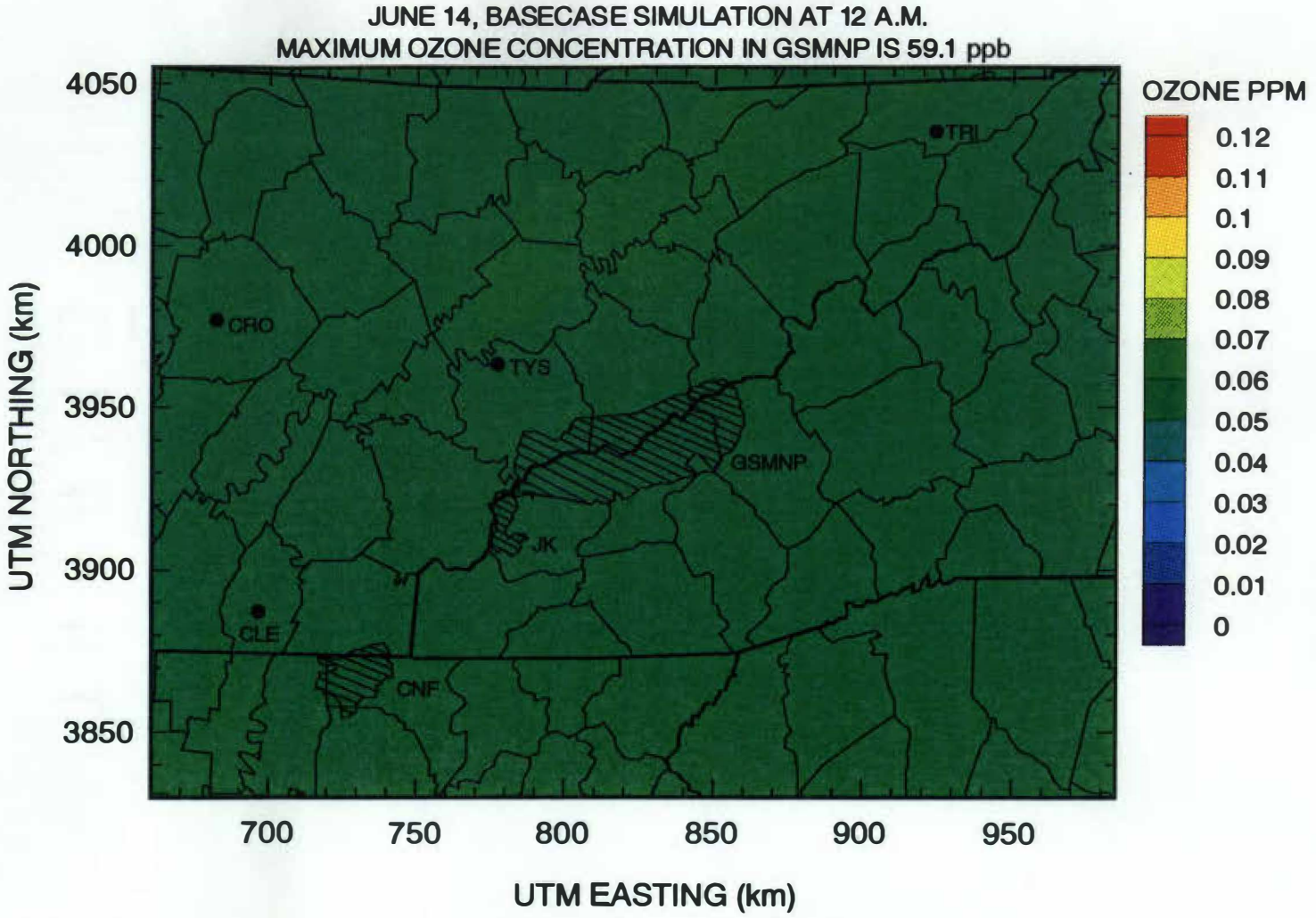


Figure 6.3. June 14 Basecase Simulation Using TVP Concentrations.

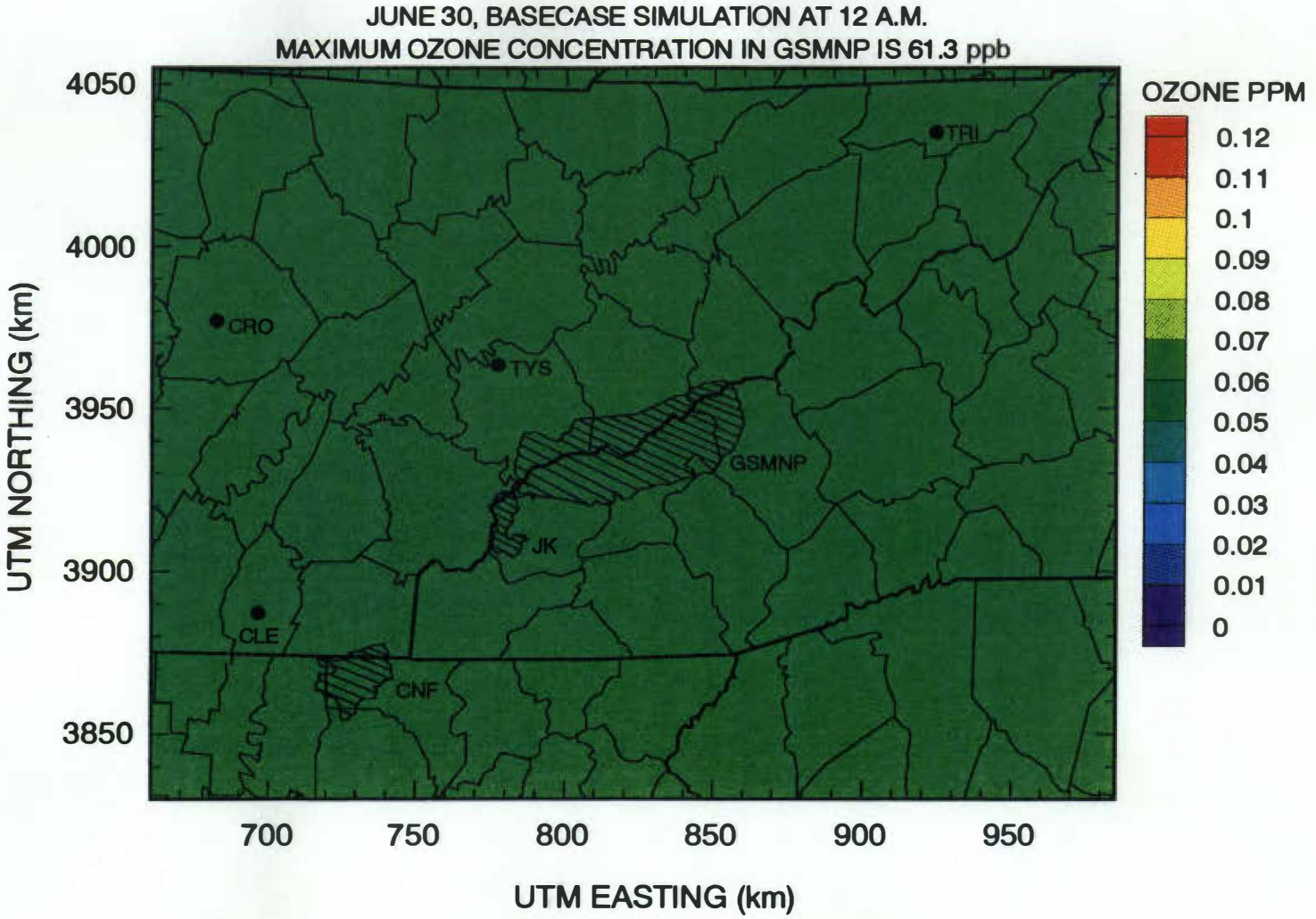


Figure 6.4. June 30 Basecase Simulation Using TVP Concentrations.

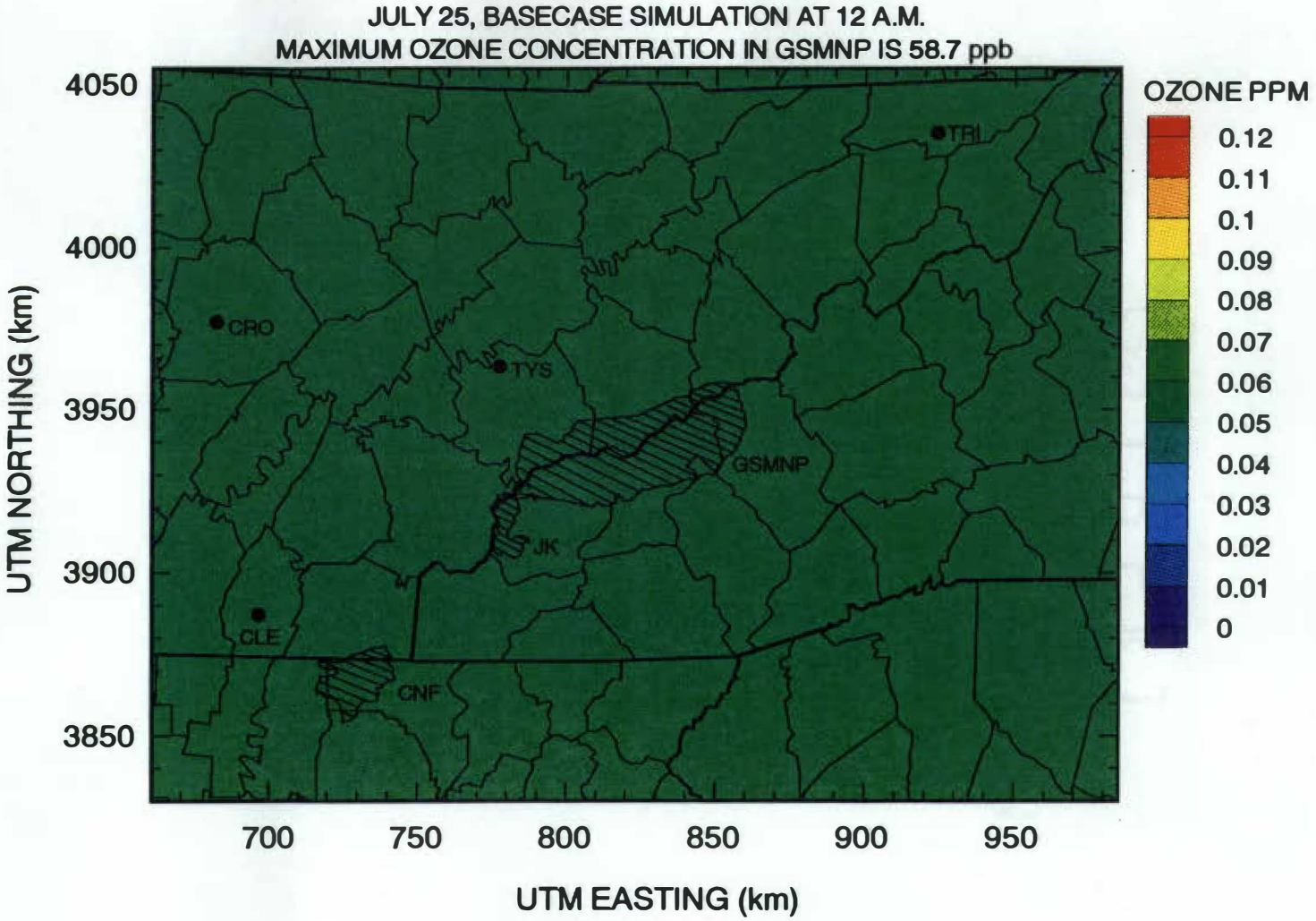


Figure 6.5. July 25 Basecase Simulation Using TVP Concentrations.

removed in each. Also, for each of the days, the TVP basecase simulations predicted consistent ozone values with the ozone concentrations that were predicted within the unaffected portion of the modeling domain from the preliminary runs.

The maximum predicted ozone concentration for the July 10 TVP simulation was 1.31 ppb lower than the value predicted for the NTVD simulation, and the maximum concentration for the June 14 TVP concentration increased 0.19 ppb above the NTVD predicted value. The maximum predicted ozone concentrations for June 30 and July 25 did not change from the NTVD to the TVP simulations. Table 6.1 shows the maximum predicted ozone concentrations in the domain for each of the basecase scenarios, as well as the differences between the NTVD and TVP simulations for each day.

Table 6.1. Results from the NTVD and TVP Basecase Simulations.

1 Date	2 Boundary Condition Method	3 Maximum Ozone Predicted in Modeling Domain (ppb)	4 Boundary Condition Method	6 Maximum Ozone Predicted in Modeling Domain (ppb)	7 Difference (6-3)	8 % Difference
Jul 07	NTVD	81.81	TVP	79.02	-2.79	3.5
Jul 10	NTVD	73.60	TVP	72.29	-1.31	1.8
Jun 14	NTVD	68.06	TVP	68.25	0.19	0.3
Jun 30	NTVD	73.25	TVP	73.25	0.0	0.0
Jul 25	NTVD	72.59	TVP	72.59	0.0	0.0

6.2 July 07 & July 10 TVP Scenarios

The discrepancy wave did not appear to interfere with the point source emissions or affect the predicted incremental ozone concentrations in the modeling domain or impacting the GSMNP in either the July 07 or July 10 preliminary simulations. In order to see if this was in fact the case, the point source simulations for these days were re-run

using the TVP boundary concentrations and the results compared to the preliminary results for each day.

The maximum predicted ozone concentration in the modeling domain for the July 07 100,000 tpy TVP simulation increased by 0.5 ppb from the NTVD simulation up to a value of 145.7 ppb. The maximum predicted ozone concentration impacting the GSMNP for this simulation increased by 0.4 ppb from the preliminary simulation to a value of 142.4 ppb. For the July 10 100,000 tpy TVP simulation, the maximum predicted ozone concentration in the domain increased by 0.2 ppb from the NTVD simulation up to a value of 119.3 ppb. This maximum value also occurred within the boundary of the GSMNP. Table 6.2 shows the maximum predicted ozone concentrations in the modeling domain and in the GSMNP for the 100,000 tpy NTVD and TVP simulations for July 07 and July 10 along with the resulting incremental concentrations and their differences.

Table 6.2. Maximum Predicted Ozone Concentrations for the July 07 and July 10 100,000 tpy NTVD and TVP Scenarios.

	NTVD Boundary		TVP Boundary				
1 Date	2 Maximum Ozone Predicted in Modeling Domain (ppb)	3 Incremental Ozone Occurring at 2. (ppb)	4 Maximum Ozone Predicted in Modeling Domain (ppb)	5 Incremental Ozone Occurring at 4. (ppb)	6 Difference (4-2) (ppb)	7 Difference (5-3) (ppb)	8 % Difference (5-3)
Jul 07	145.2	68.5	145.7	68.8	0.5	0.3	0.4
Jul 10	119.1	48.0	119.3	48.0	0.2	0.0	0.0
	NTVD Boundary		**TVP Boundary**				
9 Date	10 Maximum Ozone Predicted in GSMNP (ppb)	11 Incremental Ozone Occurring at 10. (ppb)	12 Maximum Ozone Predicted in GSMNP (ppb)	13 Incremental Ozone Occurring at 12. (ppb)	14 Difference (12-10) (ppb)	15 Difference (13-11) (ppb)	16 % Difference (13-11)
Jul 07	142.0	64.9	142.4	65.1	0.4	0.2	0.3
Jul 10	119.1	48.0	119.3	48.0	0.2	0.0	0.0

Figure 6.6 is the isopleth map of the July 07, 100,000 tpy simulation at 8 p.m. when the maximum incremental ozone concentration was predicted for the modeling domain and Figure 6.7 is the isopleth map of the same simulation at 6 p.m. when the maximum incremental ozone was predicted to occur within the park. Figure 6.8 is the isopleth map of the July 10, 100,000 tpy simulation at 6 p.m. when the maximum increment occurred in the park, which is also when the maximum increment was predicted within the domain.

6.3 June 14 TVP Scenarios

The isopleth maps for the June 14 NTVD simulations showed that the major portion of the plume was never in contact with the discrepancy wave. Although, as can be seen in Figures 5.11 and 5.12, the back half of the emission plume was surrounded by the discrepancy wave, it was the portion in front of the 'wave' which resulted in the maximum predicted ozone concentrations in the modeling domain and the GSMNP. Therefore, it was clear that the boundary conditions had no appreciable effect on the maximum predicted ozone concentrations for this day.

The simulations were re-run using the TVP boundary conditions and the results were compared with those from the preliminary simulations. The maximum predicted ozone concentrations did not change from the NTVD to the TVP runs in the modeling domain or within the GSMNP. However, the incremental ozone concentrations in the domain and in the park decreased by 0.1 ppb to values of 61.5 and 59.6 respectively. The maximum predicted ozone concentration occurred at 6 p.m. in the modeling domain, and the maximum predicted ozone concentration in the park occurred at 8 p.m. Figures 6.9 and 6.10 are the 6 p.m. and 8 p.m. isopleth maps of the June 14 100,000 tpy TVP simulation.

Table 6.3 shows the maximum predicted ozone concentrations in the modeling domain and in the GSMNP for the 100,000 tpy NTVD and TVP simulations for June 14 along with the resulting incremental concentrations and their differences.

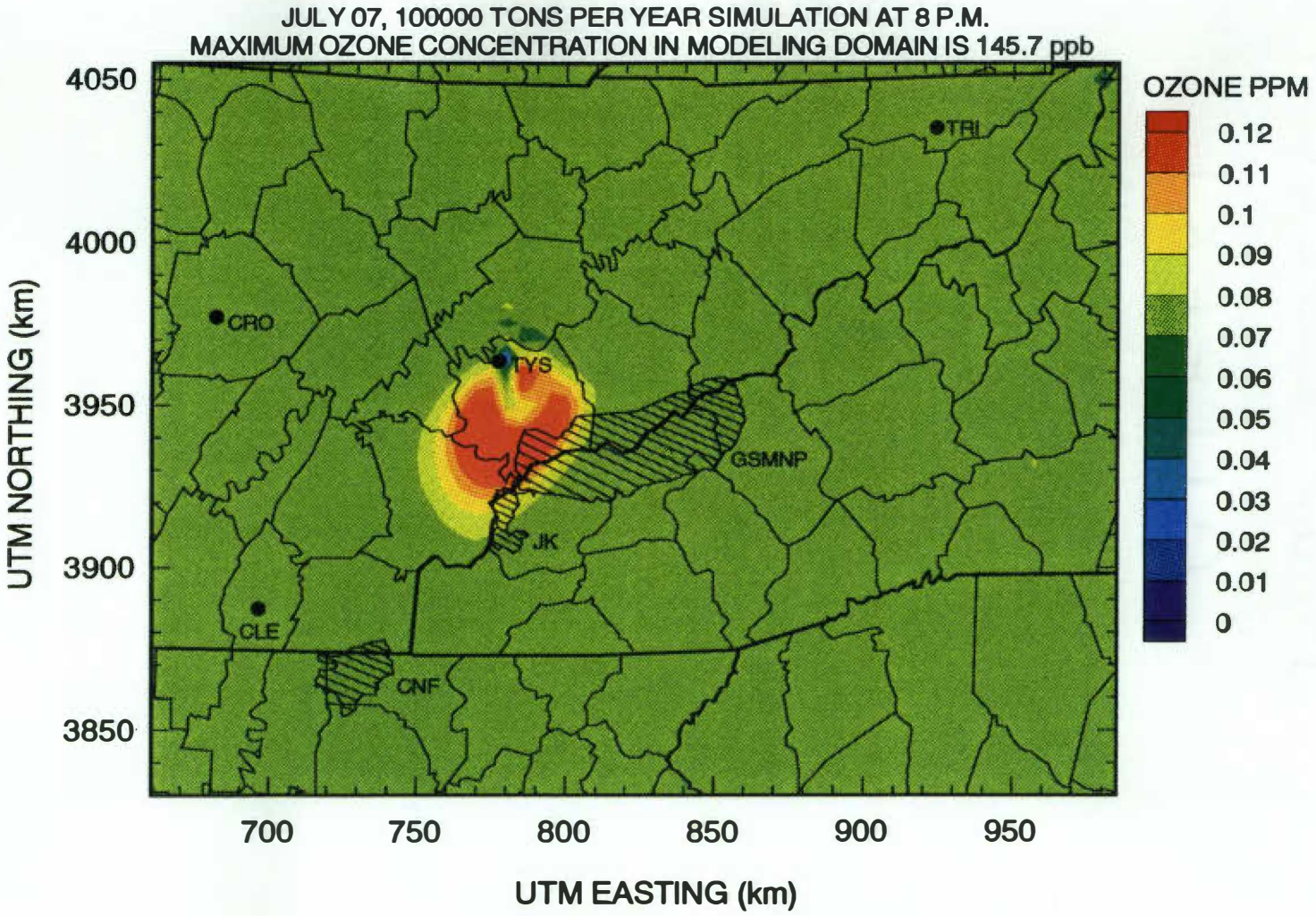


Figure 6.6. July 07 Point Source Simulation (8 p.m.) Using TVP Concentrations.

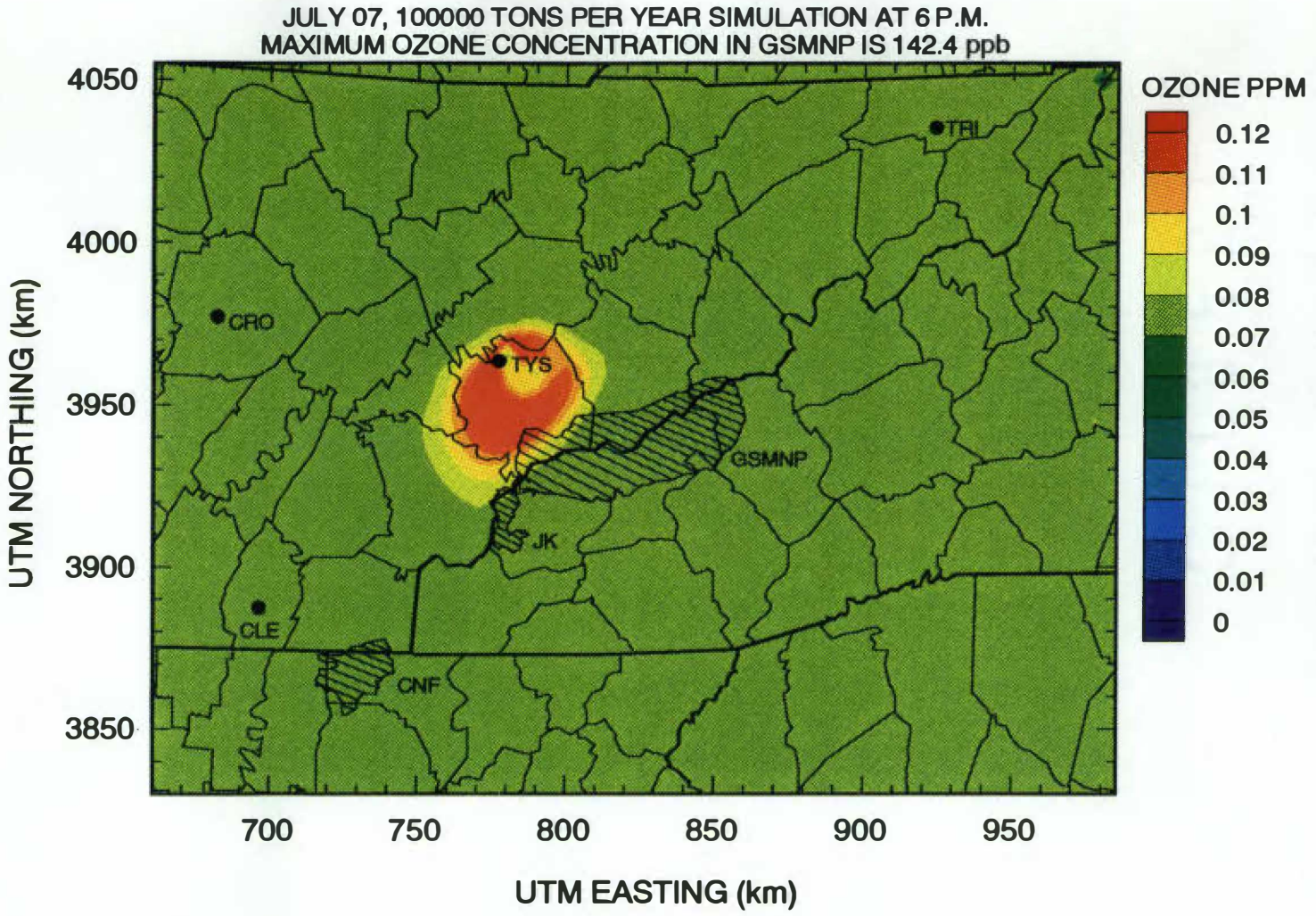


Figure 6.7. July 07 Point Source Simulation (6 p.m.) Using TVP Concentrations.

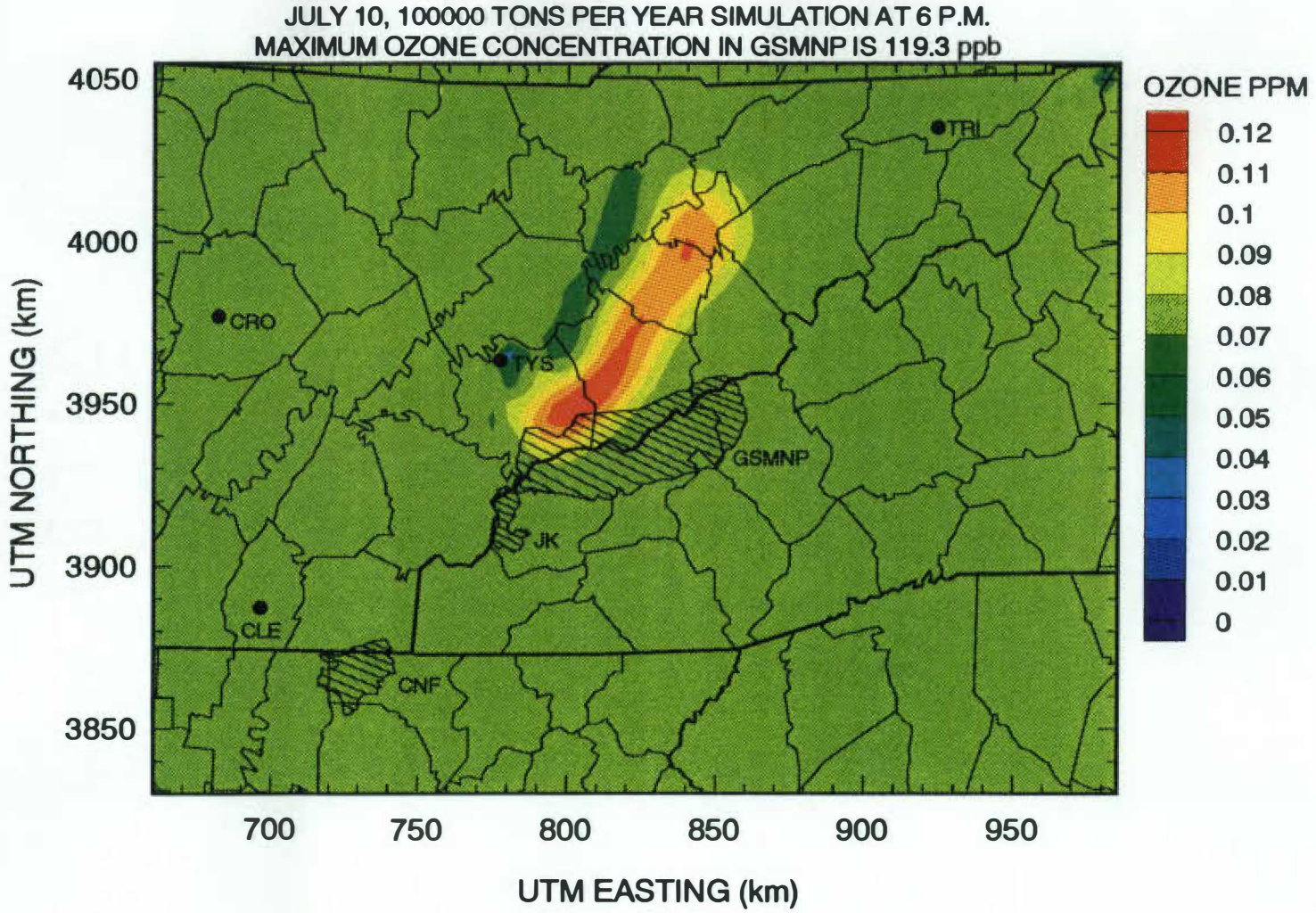


Figure 6.8. July 10 Point Source Simulation Using TVP Concentrations.

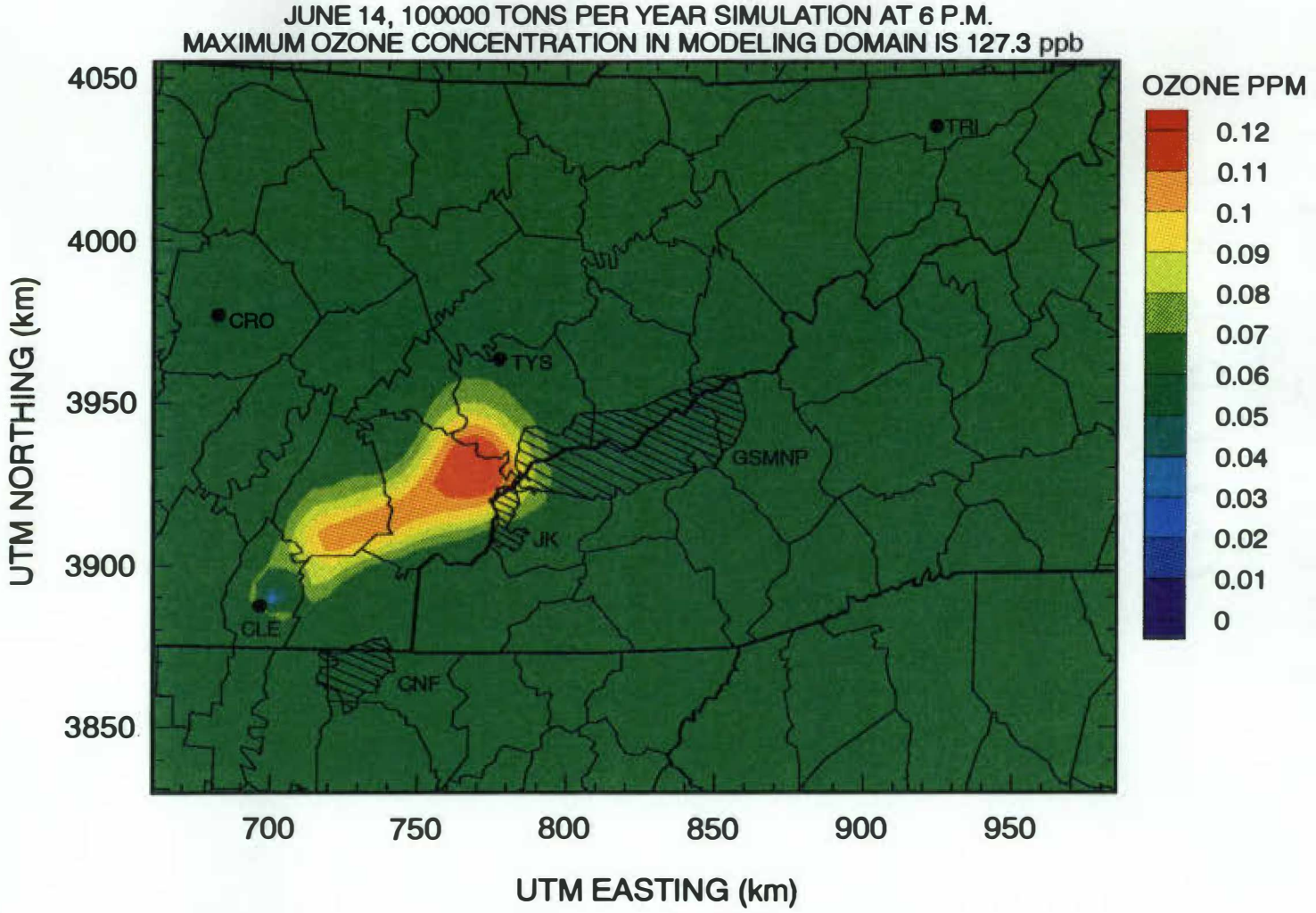


Figure 6.9. June 14 Point Source Simulation (6 p.m.) Using TVP Concentrations.

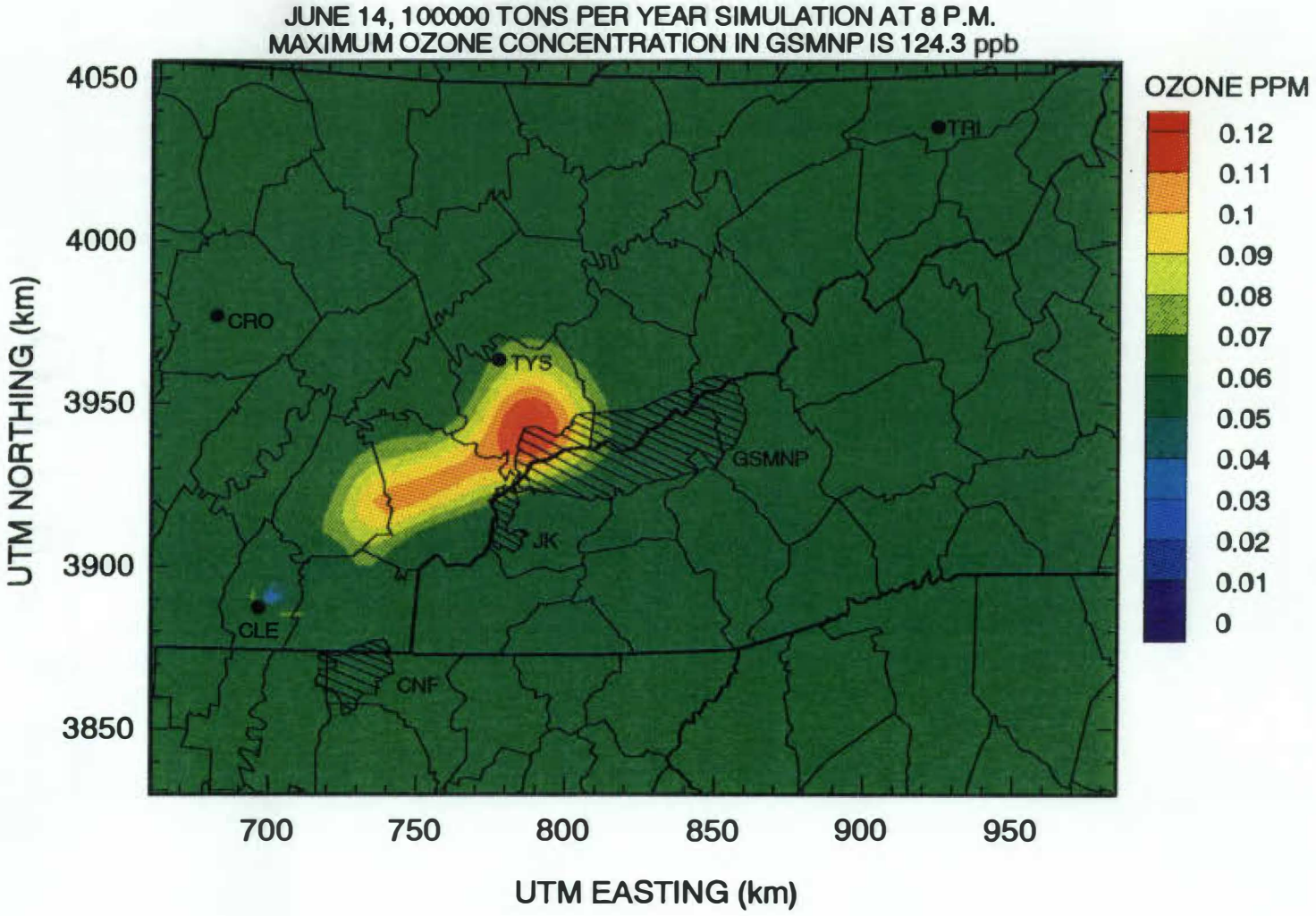


Figure 6.10. June 14 Point Source Simulation (8 p.m.) Using TVP Concentrations.

Table 6.3. Maximum Predicted Ozone Concentrations for the June 14 100,000 tpy NTVD and TVP Scenarios.

NTVD Boundary			TVP Boundary				
1 Date	2 Maximum Ozone Predicted in Modeling Domain (ppb)	3 Incremental Ozone Occurring at 2. (ppb)	4 Maximum Ozone Predicted in Modeling Domain (ppb)	5 Incremental Ozone Occurring at 4. (ppb)	6 Difference (4-2) (ppb)	7 Difference (5-3) (ppb)	8 % Difference (5-3)
Jun 14	127.3	61.6	127.3	61.5	0.0	-0.1	0.2
NTVD Boundary			**TVP Boundary**				
9 Date	10 Maximum Ozone Predicted in GSMNP (ppb)	11 Incremental Ozone Occurring at 10. (ppb)	12 Maximum Ozone Predicted in GSMNP (ppb)	13 Incremental Ozone Occurring at 12. (ppb)	14 Difference (12-10) (ppb)	15 Difference (13-11) (ppb)	16 % Difference (13-11)
Jun 14	124.3	59.7	124.3	59.6	0.0	-0.1	0.2

6.4 June 30 TVP Scenarios

The point source simulations for the June 30 scenario were the next to be conducted using the TVP boundary concentrations. This was the day in which preliminary modeling using the UAM predicted that the point source plume would miss the GSMNP just slightly to the north. Therefore, comparisons between the NTVD and TVP simulations for this day can only be based on the incremental ozone concentrations formed within the modeling domain at the hour of the maximum predicted concentration.

Table 6.4 shows the maximum predicted ozone concentrations formed within the modeling domain for the 100,000 tpy NTVD and TVP simulations with their resulting increments and differences. As can be seen in this table, the incremental ozone predicted for the 100,000 tpy simulation using the TVP concentrations increased by 1.32 ppb from the NTVD simulations to a value of 58.02 ppb at the hour and cell of maximum ozone predicted concentrations. The maximum predicted concentration from the NTVD

simulation increased by 4.9 ppb to a value of 130.2 ppb for the TVP simulation, but due to the effects of the discrepancy wave on basecase ozone concentrations, the incremental ozone formed increased by only 1.32 ppb. Figure 6.11 is the isopleth map of the June 30 100,000 tpy simulation using TVP concentrations at 5 p.m. when the maximum ozone concentration occurred.

Table 6.4. Maximum Predicted Ozone Concentrations for the June 30 100,000 tpy NTVD and TVP Scenarios.

	NTVD Boundary		TVP Boundary				
1 Date	2 Maximum Ozone Predicted in Modeling Domain (ppb)	3 Incremental Ozone Occurring at 2. (ppb)	4 Maximum Ozone Predicted in Modeling Domain (ppb)	5 Incremental Ozone Occurring at 4. (ppb)	6 Difference (4-2) (ppb)	7 Difference (5-3) (ppb)	8 % Difference (5-3)
Jun 30	125.3	56.70	130.2	58.02	4.9	1.32	2.28

6.5 July 25 TVP Scenarios

The final point source simulations to be conducted were the July 25 TVP scenarios. From the preliminary results, it was anticipated that the NTVD boundary concentrations may have interacted with emissions from the point source located at the Tri-Cities airport, and in turn altered the predicted ozone concentrations in the modeling domain as well as in the GSMNP. The comparisons of the TVP and NTVD simulations showed that using the NTVD concentrations did influence the maximum concentration and predicted incremental ozone being formed in the modeling domain as well as in the park. There was a substantial increase in maximum ozone concentrations and incremental ozone concentrations in the modeling domain, whereas, the increase of these values within the park were much smaller.

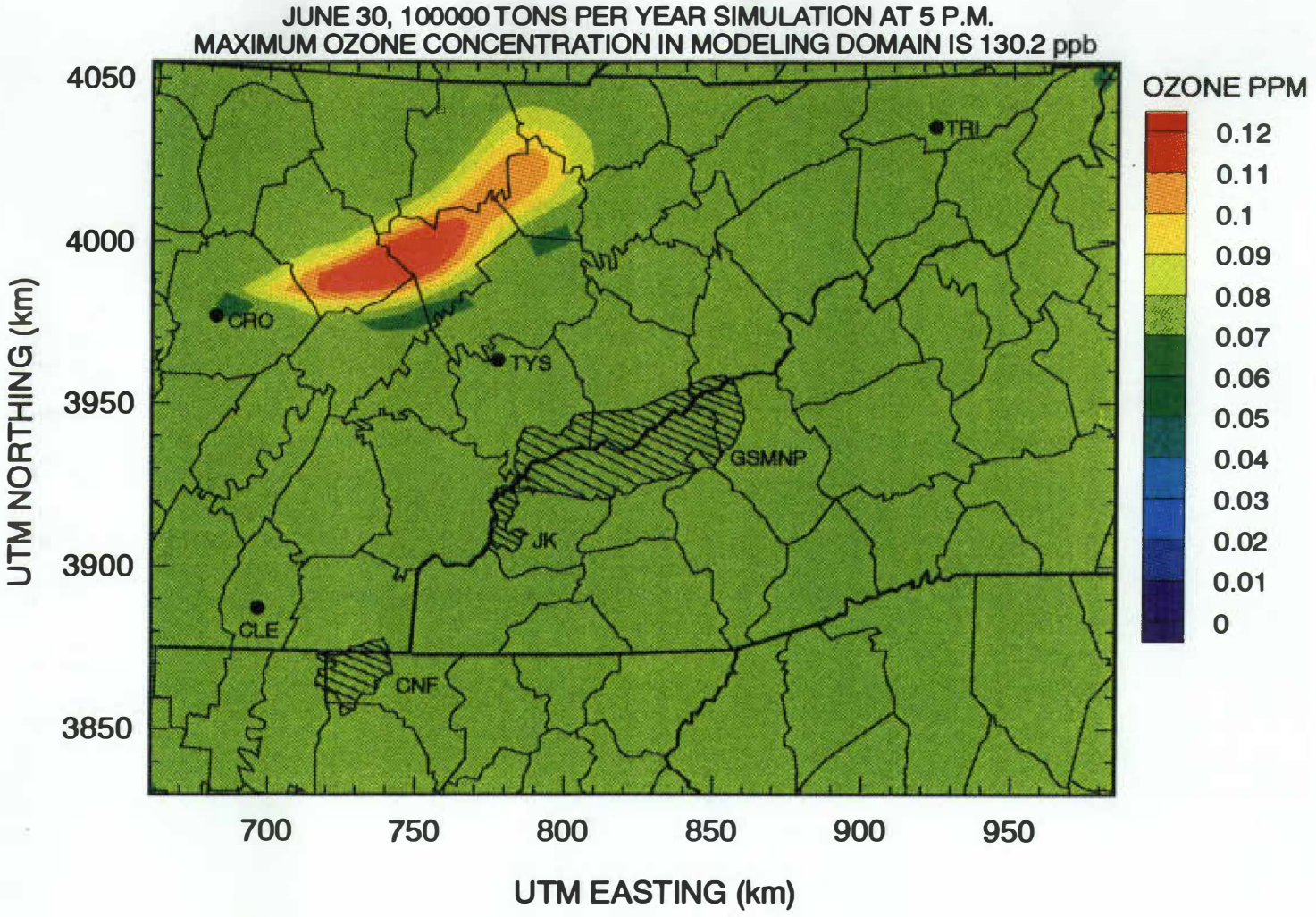


Figure 6.11. June 30 Point Source Simulation Using TVP Concentrations.

Table 6.5 shows the maximum predicted ozone concentrations in the modeling domain and in the GSMNP for the 100,000 NTVD and TVP simulations with their resulting increments and differences. As can be seen in the table, the results of the TVP run for July 25 showed an increase to the incremental ozone concentration at the hour of maximum ozone concentrations of 2.61 ppb up to a value of 51.51 ppb within the domain. The maximum predicted ozone concentration in the domain increased 2.55 ppb over the preliminary results for this simulation to a value of 122.86 ppb. Figure 6.12 is the isopleth map of the 100,000 tpy TVP simulation for July 25 at 7 p.m. when the maximum predicted ozone concentration occurs in the domain.

Table 6.5 also shows that the maximum predicted ozone concentration within the park for the TVP simulation increased 0.6 ppb over the NTVP concentration to a value of 115.5 ppb. The resulting increment, however only increased 0.1 ppb from the NTVD simulation. Figure 6.13 is the isopleth map of the July 25 100,000 tpy TVP simulation at 8 p.m. when the maximum predicted ozone concentration occurs in the GSMNP.

Table 6.5. Maximum Predicted Ozone Concentrations for the July 25 100,000 tpy NTVD and TVP Scenarios.

	NTVD Boundary		TVP Boundary				
1 Date	2 Maximum Ozone Predicted in Modeling Domain (ppb)	3 Incremental Ozone Occurring at 2. (ppb)	4 Maximum Ozone Predicted in Modeling Domain (ppb)	5 Incremental Ozone Occurring at 4. (ppb)	6 Difference (4-2) (ppb)	7 Difference (5-3) (ppb)	8 % Difference (5-3)
Jul 25	120.3	48.90	122.9	51.51	2.6	2.61	5.1
	NTVD Boundary		**TVP Boundary**				
9 Date	10 Maximum Ozone Predicted in GSMNP (ppb)	11 Incremental Ozone Occurring at 10. (ppb)	12 Maximum Ozone Predicted in GSMNP (ppb)	13 Incremental Ozone Occurring at 12. (ppb)	14 Difference (12-10) (ppb)	15 Difference (13-11) (ppb)	16 % Difference (13-11)
Jul 25	114.9	45.70	115.5	45.80	0.6	0.1	0.2

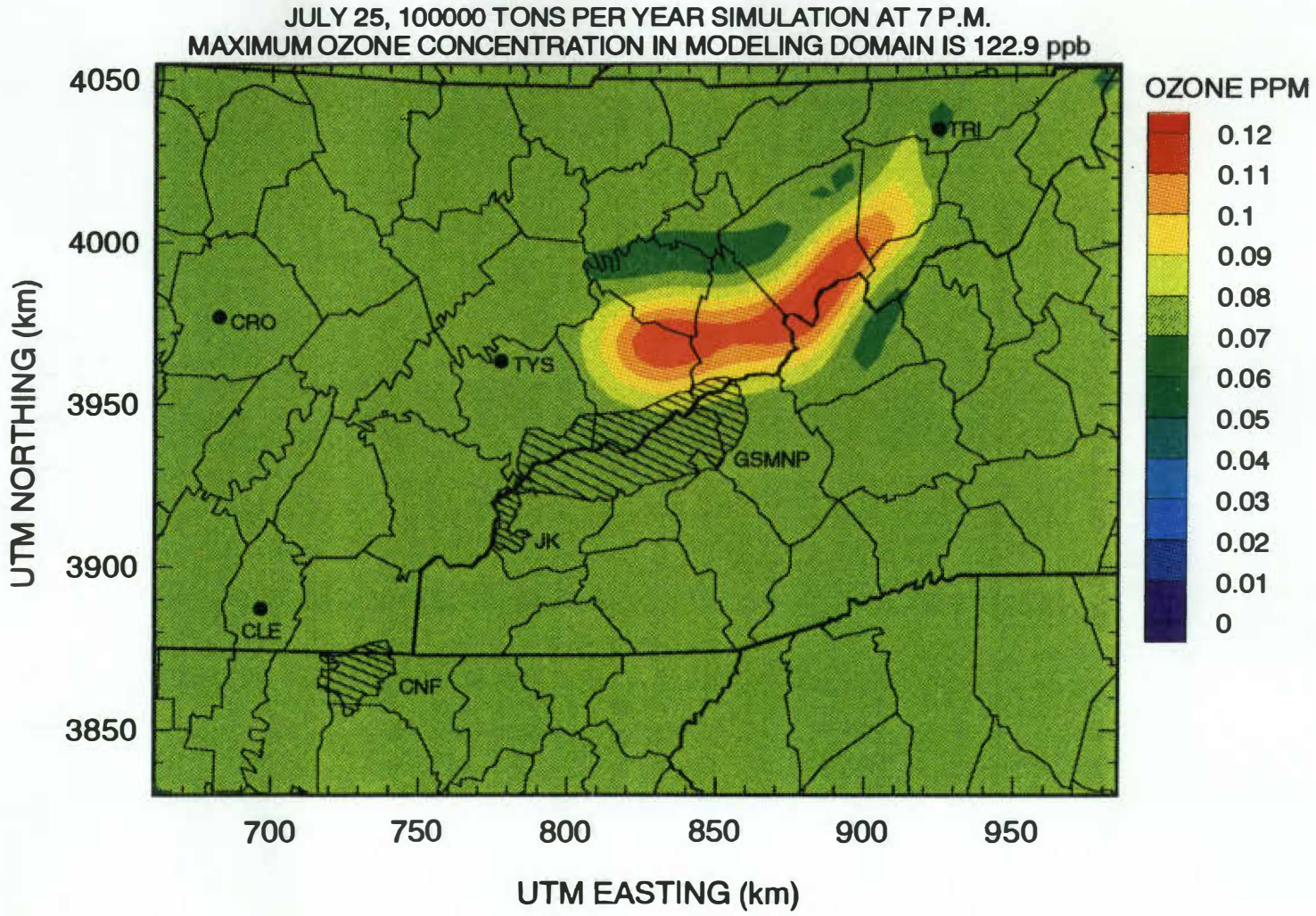


Figure 6.12. July 25 Point Source Simulation (7 p.m.) Using TVP Concentrations.

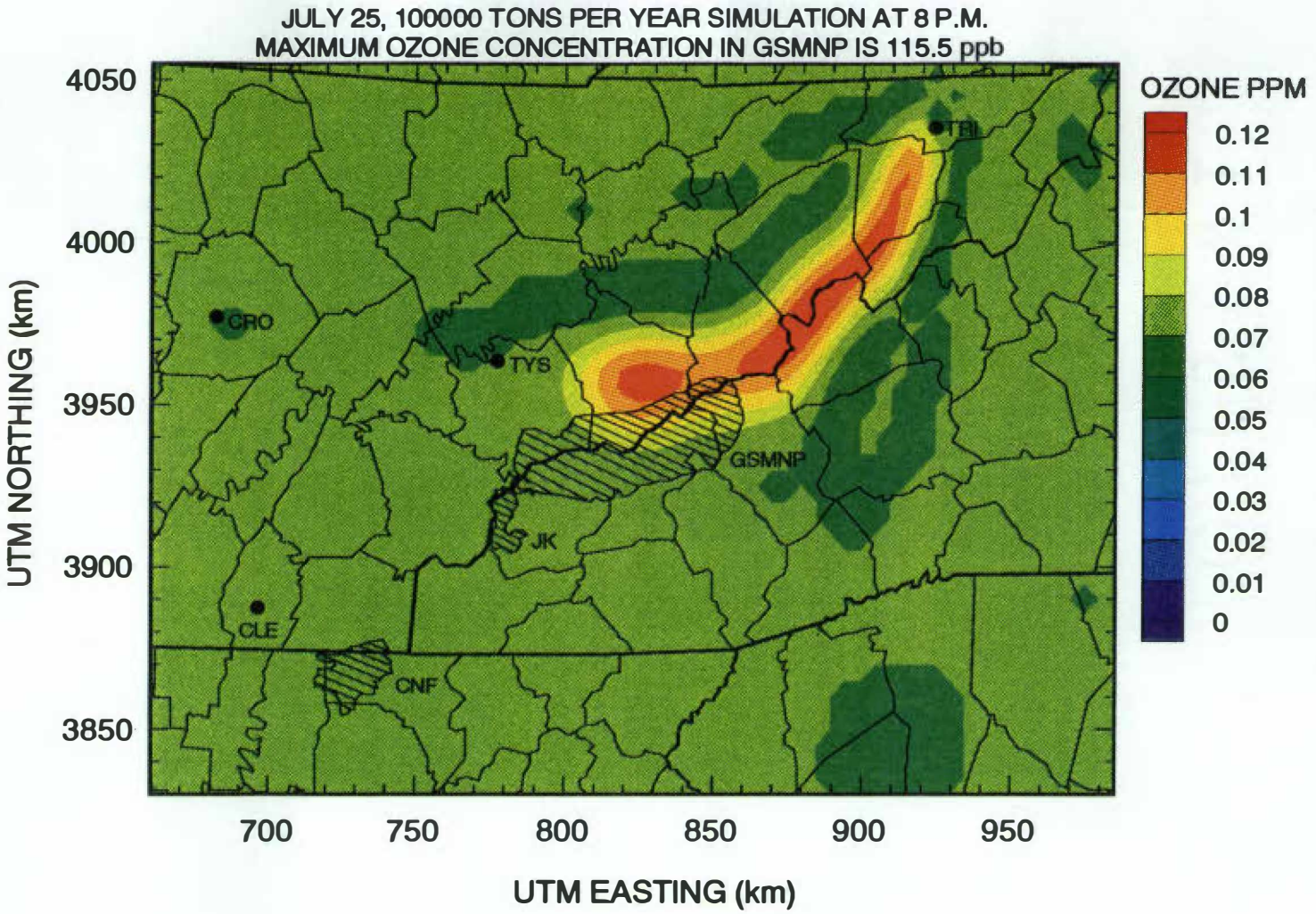


Figure 6.13. July 25 Point Source Simulation (8 p.m.) Using TVP Concentrations.

6.6 Comparison to MAP-O3 Results.

In selecting a screening model to pick the days to model with the UAM, a few criteria need to be met. First of all, the screening model should identify the days when meteorological conditions correspond with high ozone occurrences. Secondly, the screening model should pick from these days, the days that the plume from a source (hypothetical source), located somewhere in the domain, will impact a designated location in the domain (target). For this study there were four hypothetical source locations, and one target (GSMNP). The final criteria in selecting a proper screening model is that it should model the worst case scenarios, tending to over-predict ozone concentrations compared to those predicted using the more refined UAM model.

Since the MAP-O3 model was believed to possess these criteria, it was used as the screening model for selecting days to model with the UAM. Table 6.6 shows the results of the MAP-O3's prediction of incremental ozone in the GSMNP along with the UAM's prediction of incremental ozone for the five modeling scenarios.

Table 6.6 Maximum Incremental Ozone Concentrations Impacting the GSMNP.

Day	Source Size (tpy)	MAP-O3 Results (ppb)	UAM Results (ppb)	Difference (ppb)	% Difference
July	10,000	53.0	44.5	8.5	19.1
	1,000	8.0	8.6	-0.6	7.0
	100	0.90	0.77	0.13	16.9
July	10,000	53.0	12.4	40.6	327.4
	1,000	8.0	1.59	6.41	403.1
	100	0.75	0.16	0.59	368.8
June	10,000	20.0	17.8	2.2	12.4
	1,000	3.0	2.8	0.2	7.0
	100	0.35	0.0	0.35	---
June	10,000	36.0	14.8	21.2	143.2
	1,000	6.4	2.2	4.2	190.9
	100	0.74	0.26	0.48	184.6
July	10,000	19.0	8.2	10.8	131.7
	1,000	3.4	0.49	2.91	593.9
	100	0.4	0.0	0.4	---

Figure 6.14 is a graph comparing the predicted ozone concentrations by the MAP-O3 and UAM models for the scenarios summarized above. The ozone concentrations in Table 6.6 are plotted with the MAP-O3 values along the Y-axis and the UAM values along the X-axis. The straight line on the graph is where the data points would fall if both models predicted the same concentrations.

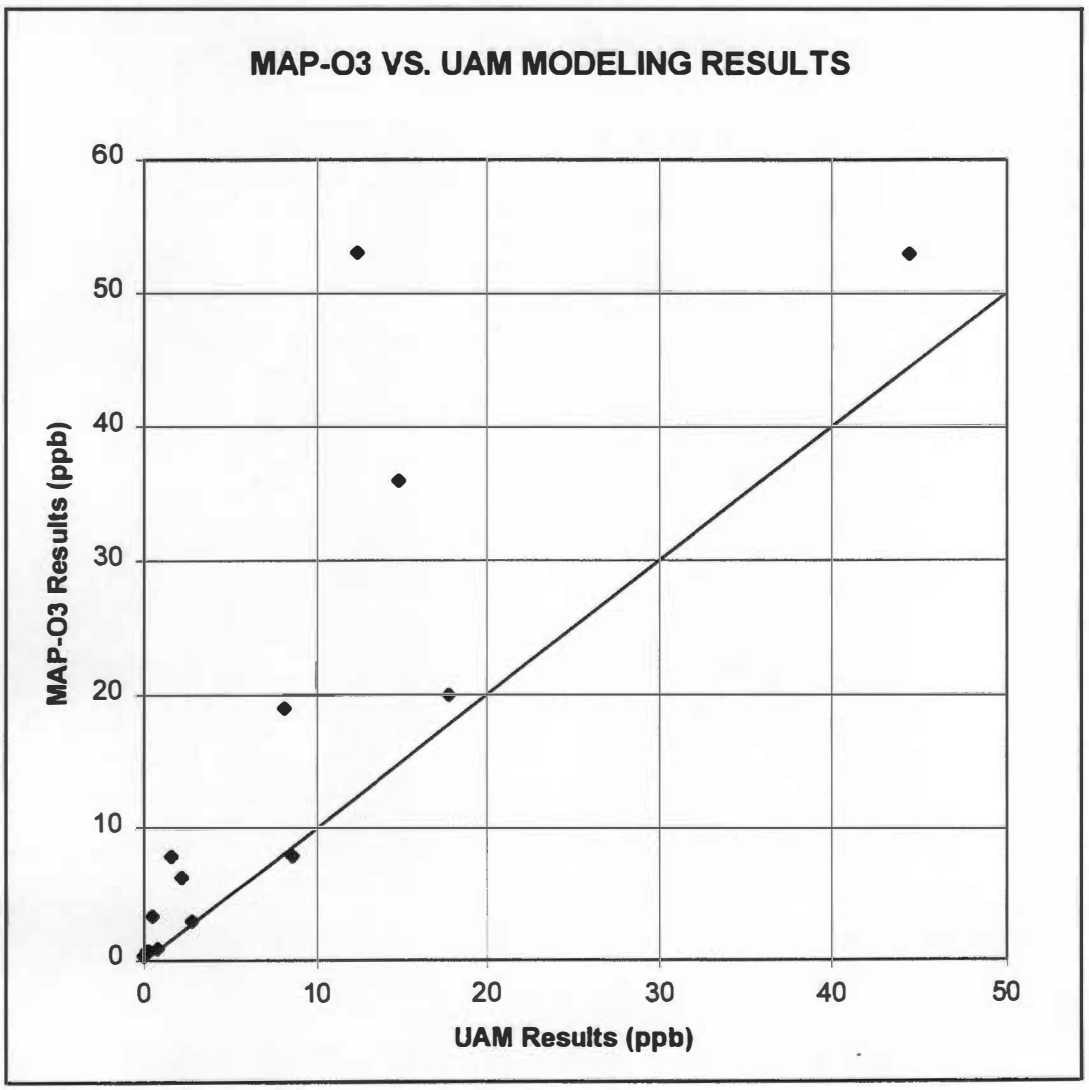


Figure 6.14. Comparison of MAP-O3 and UAM Ozone Concentration Predictions.

In all cases, as can be seen in Table 6.6 and Figure 6.14, the MAP-O3 model predicted a greater or equivalent ozone concentration than did the UAM. In order for the MAP-03 model to be considered an appropriate screening tool for the UAM this trend was necessary.

7. CONCLUSIONS

Summarized in this chapter are the comparisons of the NTVD and TVP scenario results as well as the TVP and MAP-O3 results. These comparisons resulted in accomplishing the project's goals. As stated previously, these goals were to determine whether temporally varying predicted (TVP) boundary concentrations give more appropriate results than do the non-temporally varying default boundary concentrations (NTVD), and whether MAP-O3 is an effective screening model for selecting dates to be further modeled by the UAM.

7.1 Basecase Scenarios

When the isopleth maps of the NTVD basecase scenarios were analyzed, the presence of a discrepancy wave was seen in each. The scenarios were therefore re-run using TVP boundary concentrations in an effort to minimize the effect of the boundary conditions and therefore remove the 'wave'.

From the data in Table 6.1, and by comparing the basecase isopleth maps using NTVD concentrations (Figures 5.2-5.6) with those using TVP concentrations (Figures 6.1-6.5) for each day, the effects of the boundary conditions in either case appear to be minimal. The ozone concentrations within the unaffected portion of the modeling domain for the NTVD scenarios were consistent throughout the day with the predicted ozone concentrations from the TVP scenarios, and there was no discrepancy wave in any of the TVP scenario isopleth maps. The results of the comparisons of the NTVD and TVP basecase scenarios, support the use of the TVP boundary concentrations rather than the NTVD boundary concentrations.

7.2 July 07 and July 10 Point Source Scenarios

The point source location for the July 07 and July 10 scenarios was the McGhee-Tyson airport. This airport is located a substantial distance (90 km from northern edge, and 130 km from western edge) from the closest edges of the modeling domain boundary. This enabled the incremental ozone concentrations attributed to the point source emissions being modeled at the airport to be free of any interference that could have occurred by interacting with the discrepancy wave that was being advected into the domain from the boundary during the NTVD simulations. Therefore the predicted ozone concentrations within the modeling domain and the park for these days were unchanged (less than 1%) from the NTVD to the TVP simulations. Using the TVP concentrations, did however, remove the discrepancy waves from the isopleth maps for all point source simulations for the two days and gave them a more reasonable appearance. Therefore, the use of the TVP concentrations was supported by the results of these scenarios.

7.3 June 14 Point Source Scenarios

The point source location for this day was Cleveland, Tennessee. Even though this location is relatively close to the southern and western edges of the modeling domain, the effects of the discrepancy wave on predicted ozone concentrations in the NTVD simulations ended up being minimal. There was only a 0.2% decrease in the maximum predicted ozone increments in the modeling domain and park from the NTVD to TVP 100,000 tpy simulations.

What was essentially occurring during these simulations was that the emissions that were in contact with the discrepancy wave in the NTVD simulations did not contribute to maximum ozone being formed. The emissions in the front of the plume resulted in the maximum ozone concentrations in the modeling domain and the park. Therefore the UAM predicted the same maximum ozone concentrations for both the NTVD and TVP scenarios. As with the July 07 and July 10 scenarios, using the TVP concentrations worked in minimizing the effects of the boundary conditions for this day's

scenarios and removed the discrepancy wave from the isopleth maps and was therefore supported to be the preferred method for determining boundary conditions.

7.4 June 30 Point Source Scenarios

The point source location for this day was Crossville, Tennessee. It is located very close to the western edge of the modeling domain boundary. Although the UAM did not predict the plume to impact the GSMNP on this day, it did come close. From comparing the results of the 100,000 tpy NTVD and TVP simulations and their isopleth maps, it was found that the discrepancy wave, in the NTVD simulation, interacted with the emissions and caused the UAM to underpredict the maximum ozone concentration and resulting incremental ozone concentration in the domain. The maximum ozone concentration predicted using the TVP concentrations was 4.9 ppb higher than for the NTVD simulation. The resulting ozone concentration increment was 1.32 ppb higher for the TVP simulation than for the NTVD simulation.

It was very apparent that using the TVP concentrations along the boundary for this day corrected the effects that the discrepancy wave had on the maximum predicted ozone concentrations. These results were highly supportive of using the TVP concentrations, and also eliminated the discrepancy wave in the modeling and graphical representations of the modeling.

7.5 July 25 Point Source Scenarios

The point source location for these scenarios was the Tri-Cities airport which is very close to the modeling domain boundary. The isopleth maps constructed for the NTVD simulations showed that the emission plume was in contact with the discrepancy wave for much of the day, and the possibility of it influencing the ozone concentrations formed seemed likely. The results of comparing the preliminary and final simulations were similar to the results for the Crossville simulations. The maximum predicted ozone concentrations from the NTVD to the TVP simulations for this day increased. The

increase for the 100,000 tpy simulation was 2.55 ppb and was due to the effect of the discrepancy wave on the emissions during the NTVD simulation.

The incremental ozone predicted also increased by 2.61 ppb from the NTVD to the TVP simulation. This was an increase of 5.1%. Therefore the results of the simulations for this day also support the use of the TVP concentrations along the boundary.

7.6 Evaluation of MAP-O3 as an Appropriate Screening Model

As stated previously, in order to determine whether the MAP-O3 model was successful in selecting the appropriate days for the UAM to model, two things were considered. The first of which was how the incremental ozone concentrations predicted by the MAP-O3 model compared to those predicted by the UAM for each simulation. In order for the MAP-O3 model to be an effective screening model, it should not underpredict ozone concentrations that the UAM predicts. As was seen in Table 6.6 and Figure 6.14, the MAP-O3 model consistently predicted greater incremental ozone concentrations than the UAM. For only one simulation did the UAM predict a greater incremental concentration of ozone to impact the GSMNP than did the MAP-O3 model (July 07, 1,000 tpy simulation) and it was by only 0.6 ppb, and considered to be and insignificant difference.

The second thing considered for determining whether the MAP-O3 model was successful in selecting appropriate days for the UAM to model was whether the UAM would also predict increased ozone concentrations in the GSMNP due to the source being modeled. The isopleth maps which were constructed following each UAM simulation showed that the MAP-O3 model was proficient in this aspect. These maps showed the emission plume being formed at the location of the source early in the day and eventually be transported by wind to impact the park sometime later in the day. Figures 7.1 - 7.5 show a typical plume progression from early in the morning, to the hour of maximum impact in the park for one of the days selected by MAP-O3 and modeled by the UAM.

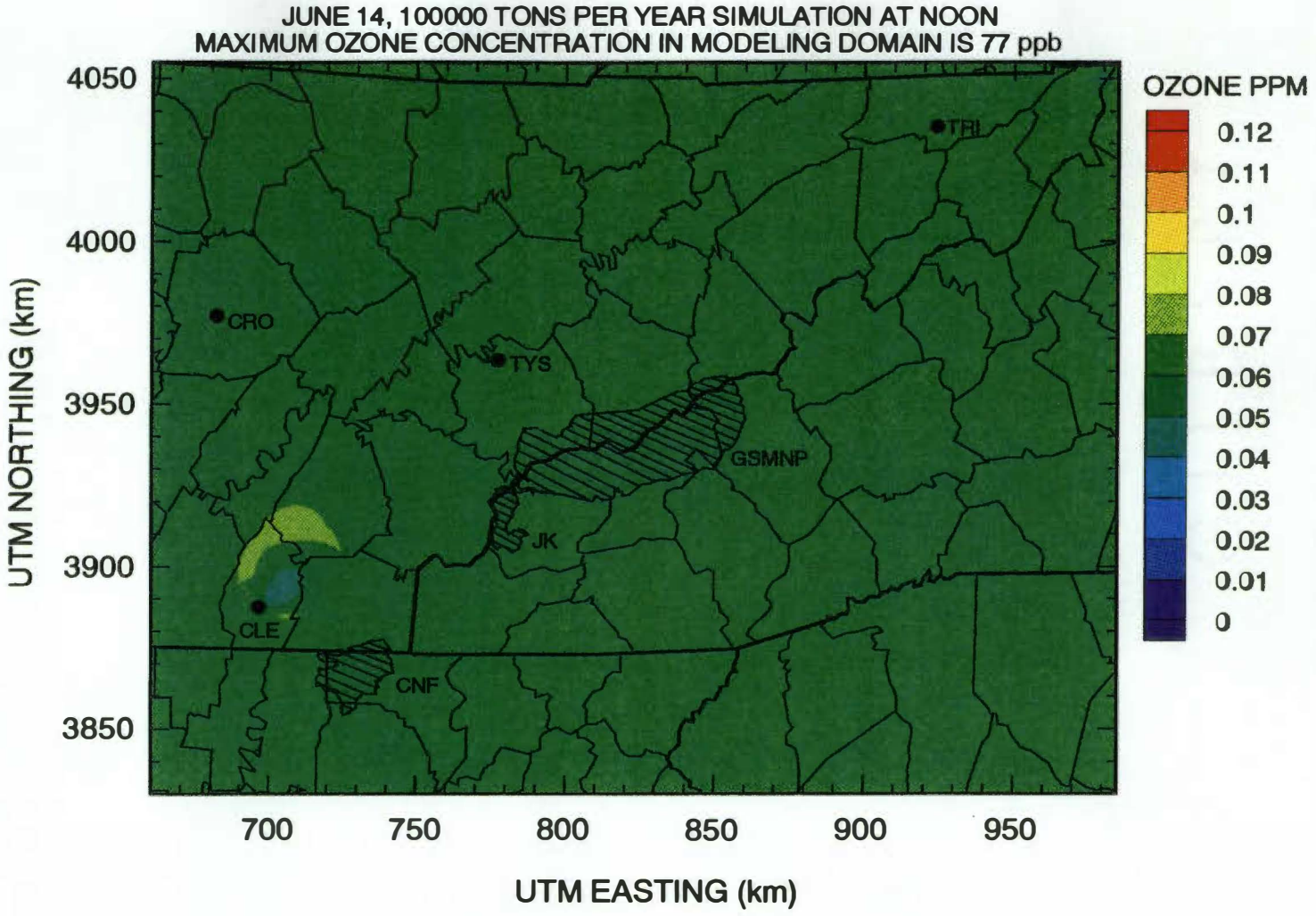


Figure 7.1. June 14 Point Source Simulation Showing Plume Progression at Noon.

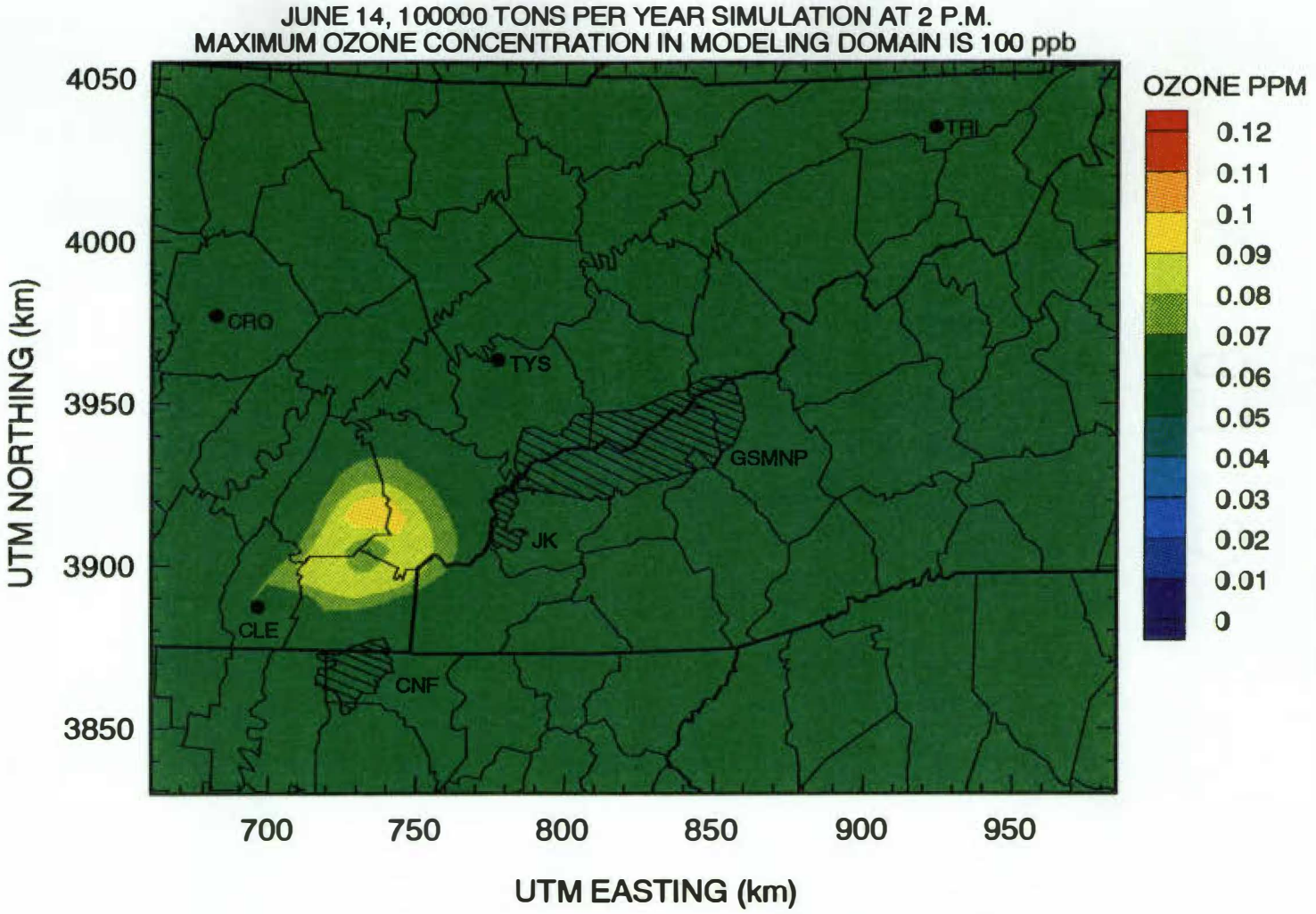


Figure 7.2. June 14 Point Source Simulation Showing Plume Progression at 2 P.M.

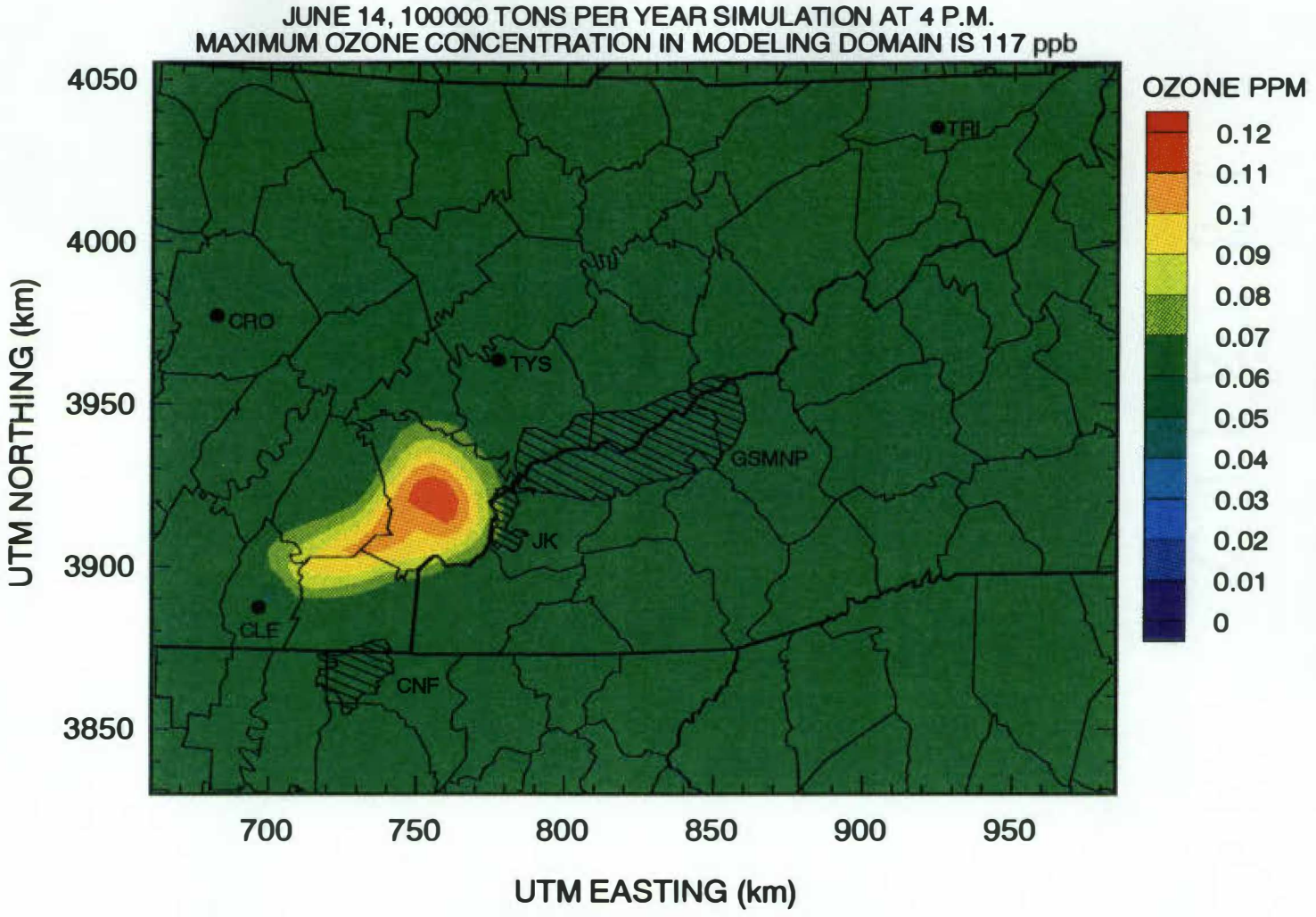


Figure 7.3. June 14 Point Source Simulation Showing Plume Progression at 4 P.M.

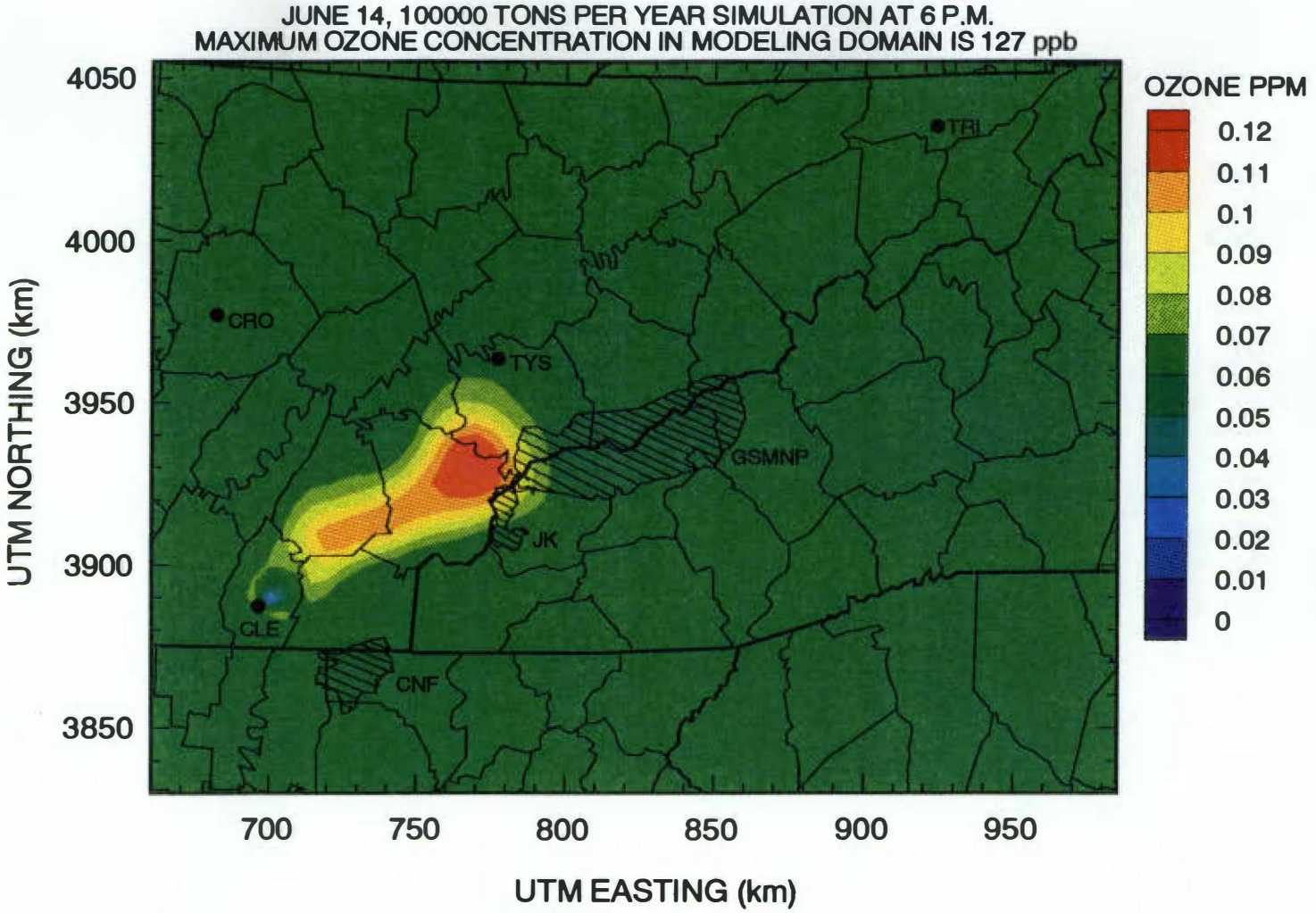


Figure 7.4. June 14 Point Source Simulation Showing Plume Progression at 6 P.M.

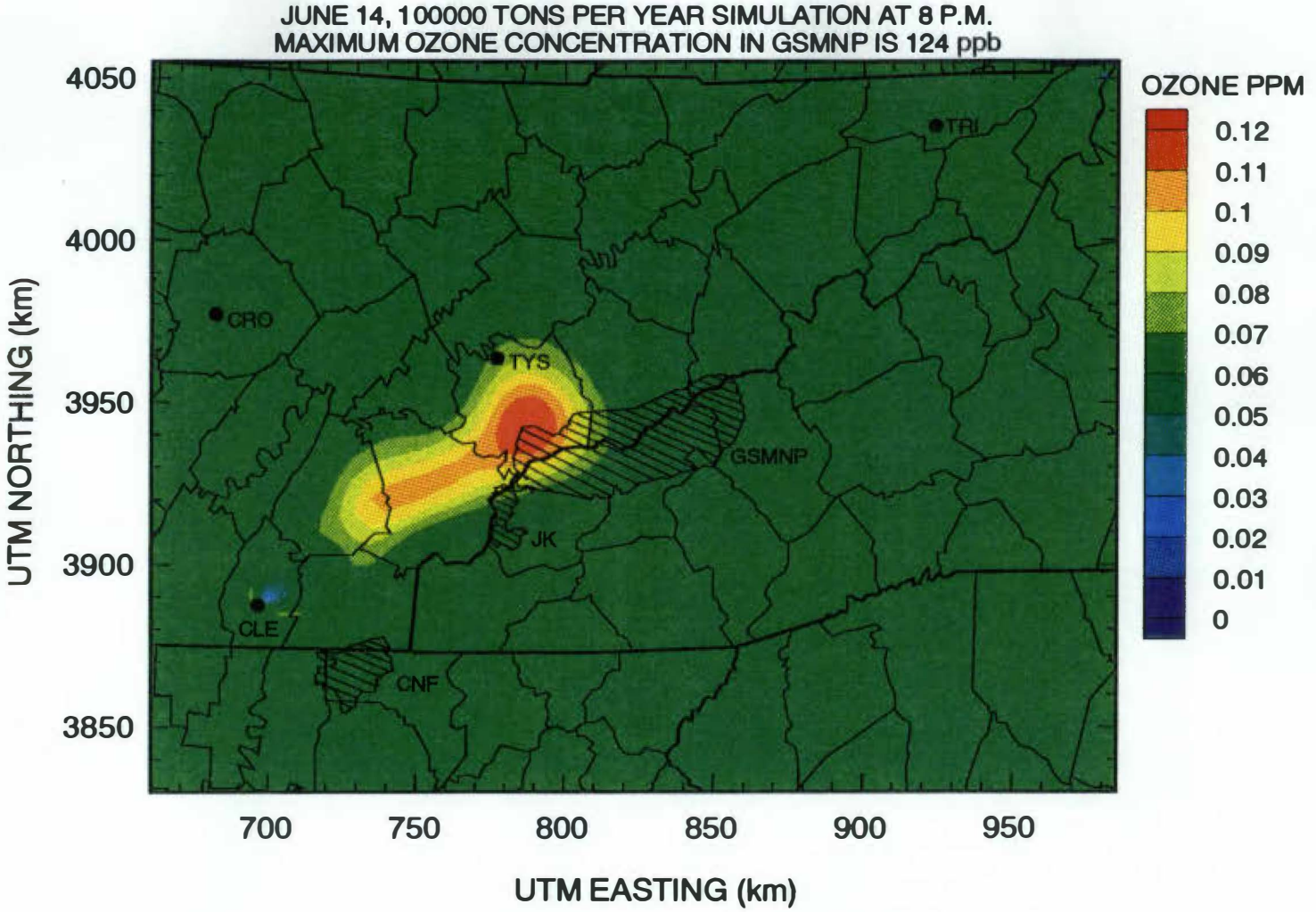


Figure 7.5. June 14 Point Source Simulation Showing Plume Progression at 8 P.M.

On only one occurrence did the MAP-O3 model predict a hit from a source that the UAM did not (June 30). Therefore, the MAP-O3 model was considered to be an appropriate screening model to predict the days to be modeled by the UAM.

REFERENCES

REFERENCES

Aneja, V.P., S. Businger, Z. Li, C. Claiborn, and A. Murthy, "Ozone Climate at Mt. Mitchell, North Carolina, and It's Association with Synoptic Episodes", Presented at the 82nd Annual Air & Waste Management Association Meeting, Anaheim, CA, 1989.

Bunyak, John, "Permit Application Guidance for New Air Pollution Sources", Natural Resources Report NPS / NRAQD / NRR-93 / 09, March, 1993.

Butala, Reshmi, Temporal Resolution of Ozone Precursor Emissions for the Middle Tennessee Modeling Domain, Thesis: The University of Tennessee, Knoxville, 1994.

Cawfield, Jo Ellen, Spatial Resolution of Ozone Precursor Emissions for a Selected Area in Middle Tennessee, 1990, Thesis: The University of Tennessee, Knoxville, 1994.

Chameides, W.L., and Ellis B. Cowling, The State of the Southern Oxidants Study (SOS): Policy-Relevant Findings in Ozone Pollution Research 1988-1994, Southern Oxidants Study, College of Forest Resources, North Carolina State University, April, 1995.

Chappelka, Arthur H., Elisabeth Hilderbrand, John M. Skelly, Deborah Mangis, and James R. Renfro, "Effects of Ambient Ozone Concentrations on Mature Eastern Hardwood Trees Growing in Great Smoky Mountains National Park and Shenandoah National Park", Presented at the 85th Annual Air & Waste Management Association Meeting, Kansas City, MO, 1992.

Cooper, D.C., and F.C. Alley, Air Pollution Control: A Design Approach, Waveland Press, Prospect Heights, Illinois, 1986.

Davis, Donald D., Russell J. Hutnik, and James R. McClenahen, "Evaluation of Vegetation Near Coal-Burning Power Plants in Southwestern Pennsylvania. II. Ozone Injury on Foliage of Hybrid Poplar", Journal of the Air and Waste Association, Vol. 43, No. 5, 1993.

Early, Andrea, The Significance of NOx Emissions from Coal-Fired Power Plants in the Middle Tennessee Area on Tropospheric Ozone, Thesis: University of Tennessee, Knoxville, 1994.

Edwards, Pamela J., William A. Jackson, and Alan Iskra, "Characterization of Ozone Symptoms on Native Vegetation at the Dolly Sods and Otter Creek Wildernesses", paper in Tropospheric Ozone and the Environment II: Effects, Modeling, and Control, Air and Waste Management Association, ISSN 1040-8177; No. 20, 1992.

Finlayson-Pitts, B.J., and J.N. Pitts, Jr., "Atmospheric Chemistry of Tropospheric Ozone Formation: Scientific and Regulatory Implications", Journal of the Air and Waste Management Association, Vol. 43, No. 8, 1993.

Gilliam, Frank S., and Nicole L. Turrill, "Temporal Patterns of Ozone Pollution in West Virginia: Implications for High-Elevation Hardwood Forests", Journal of the Air and Waste Management Association, Vol. 45, No. 8, 1995.

Hacker, W. David, James R. Renfro, Howard S. Neufeld, and David Silsbee, "Ozone in Great Smoky Mountains National Park: Dynamics and Effects on Plants", paper in Tropospheric Ozone and the Environment II: Effects, Modeling, and Control, Air and Waste Management Association, ISSN 1040-8177; No. 20, 1992.

Flores, M.I., D.R. Mangis, D.B. Joseph, and K.W. Stolte, "Tropospheric Ozone Exposures and Ozone Injury on Sensitive Pine Species in the Sierra Nevada of California", paper in Tropospheric Ozone and the Environment II: Effects, Modeling, and Control, Air and Waste Management Association, ISSN 1040-8177; No. 20, 1992.

Foley, Janell K., and Allen S. Lefohn, "Establishing Relevant Ozone Standards to Protect Vegetation and Human Health: Exposure / Dose-Response Considerations", Journal of the Air and Waste Management Association, Vol. 43, No.1, 1993.

Lefohn, Allen S., Robert C. Musselman, and Patrick M. McCool, "Ozone Descriptors for an Air Quality Standard to Protect Vegetation", Journal of the Air and Waste Management Association, Vol. 44, No. 12, 1994.

Kaminski, Mark, Urban Airshed Modeling of the Middle Tennessee Modeling Domain: Model Performance Evaluation, Thesis: University of Tennessee, Knoxville, 1994.

Krupa, Sagar V., and William J. Manning, "Atmospheric Ozone: Formation and Effects on Vegetation", Environmental Pollution, Vol. 50, 1988.

Maniero, Tonnie G., Christine L. Shaver, and Kathy A. Tonnessen, "Clearing the Air at Great Smoky Mountains National Park", Ecological Applications, Vol. 4, No. 4, 1994.

McIlvaine, Cindy, Development of the MAP-O3 Model for Predicting Seasonal Average Ozone Concentrations Due to Large Point Source NO_x Emissions, Dissertation: The University of Tennessee, Knoxville, 1994.

McIlvaine, Cindy, and Terry L. Miller, "Development and Application of a Screening Model for Predicting Ozone Formation Due to Major Point Source Emissions in East Tennessee", report submitted to Tennessee Department of Health and Environment Division of Air Pollution Control, 1996.

Morris, R.E., T.C. Myers, and J.L. Haney, User's Guide for the Urban Airshed Model, Volume I: User's Manual for UAM (CB-IV), EPA-450/4-90-007A, U.S. Environmental Protection Agency, Research Triangle Park, NC (NTIS No.: PB91- 131227), 1990.

Morris, R.E., T.C. Myers, E.L. Carr, M.C. Causley, S.G. Douglas and J.L. Haney, User's Guide for the Urban Airshed Model, Volume II: User's Manual for the UAM (CB-IV) Modeling System, EPA-450/4-90-007B, U.S. Environmental Protection Agency, Research Triangle Park, NC (NTIS No.: PB91-131235), 1990.

National Research Council, (NRC), Rethinking the Ozone Problem in Urban and Regional Air Pollution, National Academy Press, Washington, D.C., 1991.

Renfro, James R., "Air and Water Quality Monitoring Program at Great Smoky Mountains National Park", U.S. Department of Interior, National Park Service, Resources Management and Science Division, Uplands Field Research Laboratory, Gatlinburg, Tennessee, 1990.

Tang, R.T., S.C. Gerry, J.S. Newsom, A.R. Van Meter, R.A. Wayland, J.M. Godowitch, and K.L. Schere, User's Guide for the Urban Airshed Model, Volume V: Description and Operation of the ROM-UAM Interface Program System, EPA-450/4-90-007E, U.S. Environmental Protection Agency, Research Triangle Park, NC (NTIS No.: PB91-131268), 1990.

U.S. EPA, Guideline for Regulatory Application of the Urban Airshed Model, Office of Air Quality Planning and Standards, EPA-450/4-91-013, July 1991.

Wark, K., and C. Warner, Air Pollution: It's Origin and Control, Second Edition, Harper and Row Publishers, 1981.

APPENDICES

APPENDIX A

MEMORANDUM OF UNDERSTANDING

BETWEEN

THE TENNESSEE DIVISION OF AIR POLLUTION CONTROL

AND

THE U. S. DEPARTMENT OF THE INTERIOR

The parties to this Memorandum of Understanding are the Tennessee Division of Air Pollution Control (the "Division") and the United States Department of the Interior (the "DOI"). The Division, through its Technical Secretary has the authority, inter alia, pursuant to the Tennessee Air Pollution Control Act and state regulations, to issue permits, known as Prevention of Significant Deterioration (PSD) permits, within the State of Tennessee for the construction of new or modified major air pollution sources. The Department of the Interior, through its bureau, the National Park Service (the "NPS"), has the responsibility, inter alia, for preserving and protecting all National Parks, and all NPS administered mandatory Class I areas under the Clean Air Act, 42 U.S.C. § 7401 et seq. The federal official charged with the direct responsibility for management of a National Park is the Park Superintendent, and the Federal Land Manager (FLM) is the DOI's Assistant Secretary for Fish and Wildlife and Parks. The Clean Air Act and state laws charge the FLM and Park Superintendent with the "affirmative responsibility" to protect air quality related values ("AQRVs"), including visibility, by reviewing proposed PSD permits for sources which may impact Class I areas.

This document sets out procedures to assure the coordination between the Division and the NPS, so that all reasonable efforts

will be made to protect Class I areas from the harmful effects of air pollution in accordance with the Federal Clean Air Act and Tennessee Air Pollution Control Act and regulations. It is not the intent of this document to constitute rule-making but, instead, to explain policies and to articulate points of coordination and guidelines to be followed in permitting PSD sources that may affect Class I areas.

In accordance with these understandings, the parties agree to the following:

A. The Division agrees that, when it is first notified that a potential PSD source is planning a new or modified source within 100 km of a Class I area (or at a greater distance if it is a large PSD source), the Division will provide written notification to the NPS Air Quality Division (AQD). The Division will distribute to PSD sources publications titled, "General Air Quality Modeling Requirements Tennessee Division of Air Pollution Control," and "Federal Land Manager Guidance for the Analysis of Source Impacts on Class I Areas." In addition, the Division will distribute to these sources the most current version of a NPS publication titled, "Permit Application Guidance for New Air Pollution Sources." Other guidance materials furnished by the NPS will also be distributed to PSD sources, when made available.

B. The Division agrees to require a FLM defined AQRV analysis as part of a "complete" permit application for every PSD source that may impact a Class I area. The AQRV analysis will address the AQRVs identified in the publications listed in paragraph A, above, unless the NPS identifies additional AQRV considerations to the Division and submits such in writing. After

receiving a permit application, the Division agrees to consult with the NPS AQD prior to making a completeness determination concerning AQRVs. (While the process set out in this Memorandum of Understanding concerns the impacts that PSD sources may have on AQRVs at Class I areas administered by the NPS, nothing herein is intended to limit the DOI's or NPS's ability to comment on other aspects of permit applications.) The Division will inform the applicant that the applicant must send a copy of the permit application and any amendments or supplements to the NPS AQD at the same time the applicant sends the application to the Division. It is understood that the Division currently has thirty (30) days in which to make a completeness determination; therefore, the NPS response concerning completeness must be received by the Division within that thirty (30) day time period.

C. The NPS will furnish to the Division any currently applicable "screening level" impact values for AQRVs for each PSD permit application which may affect a Class I area. The Division will require the applicant to perform preliminary modeling and/or analyses to assess the impacts of the source on AQRVs. If the preliminary modeling and/or analyses indicates a possible impact equal to or greater than the screening level value, the Division will require the applicant to perform more refined modeling and/or analyses in order to better determine whether a potential adverse impact exists.

D. If the FLM preliminarily determines that a new or modified source may cause an adverse impact on specified AQRVs, the Division and the NPS will consult. During this consultation, the Division and the NPS will discuss the preliminary adverse impact

determination. After consultation, if the FLM makes a final adverse impact determination, it will be submitted in writing to the Division in a timely manner and will include an analysis and rational basis for the determination. The adverse impact determination will also include the screening levels for those parameters which are indicators of adverse impacts to the identified AQRVs.

E. If the Division disagrees with the adverse impact determination, the Division will offer an opportunity for a meeting or further consultation with the NPS, and, if disagreement persists, the Division will respond in writing to the adverse impact determination, providing an analysis and rational basis for the rejection. If the Division continues to disagree, it will issue the permit. The DOI will have any and all rights of appeal pursuant to T.C.A. § 68-201-101, et seq.

F. If the Division agrees with the FLM's adverse impact determination, the Division will deny the permit, unless it can be demonstrated by the source that measures will be implemented to mitigate the adverse impact. The Division will include such measures as enforceable conditions to the permit.

G. The Division and the DOI jointly recognize that post-construction monitoring has importance in certain permit reviews.

H. The Division will support the creation of an "offsets market" through its participation in SAMI or other regional organizations in which the State is a member.

I. The Division will inform all PSD applicants through the publications listed in paragraph A, above, that the NPS is

available to offer assistance and encourage applicants to consult with the FLM as early as possible regarding Class I issues.

J. It is the intention of the parties that this Memorandum be consistent with current federal and state law and regulations and with current EPA policy. Any conflicts between the provisions of this Memorandum and federal and state law and regulations and EPA policy are to be resolved by interpreting the provision in question so that it is consistent with the applicable law, regulation or policy. If new laws, regulations or EPA policies are enacted and/or properly adopted so that they are in effect within the State, this Memorandum, to the fullest extent possible, will be interpreted to be consistent with the new law, regulation or policy and, if necessary, will be revised so that consistency is achieved.

In consideration of the foregoing, the parties, by their authorized representatives, hereby bind themselves to this Memorandum of Understanding by executing it in duplicate on this 27th day of April, 1995.

TENNESSEE DIVISION OF AIR POLLUTION CONTROL

By: John Walton
JOHN WALTON
Technical Secretary

U. S. DEPARTMENT OF THE INTERIOR

By: George T. Frampton, Jr.
GEORGE T. FRAMPTON, JR.
Assistant Secretary for Fish and Wildlife and Parks

APPENDIX B

14-Jun Cleveland (prelim)	1 Max Conc due to Source	2 Time 1 Occurs	3 Location 1 Occurs	4 Background Conc @ 3&4	5 Difference (1-4)	6 Max Conc due to Srce in Park	7 Time 6 Occurs	8 Location 6 Occurs	9 Background Conc @ 7&8	10 Difference (6-9)
100,000	127.3	12	1343	65.7	61.6	124.3	14	1547	64.6	59.7
10,000	85.5	9	1074	66.8	18.7	79.5	14	1479	64.6	14.9
1,000	71.6	7	937	67.65	3.9	67	13	1412	65.44	1.56
100	68.3	7	937	67.65	0.65	65.78	13	1412	65.44	0.34
basecase	68.06	7	2480			67.61	8	1420		

	11 Dif. Max Conc	12 Time 11 Occurs	13 Location 11 Occurs	14 Background Conc@ 12&13	15 Max Conc @ 12&13	16 Dif Max in Park	17 Time 16 Occurs	18 Location 16 Occurs	19 Background @ 17 & 18	20 Max Conc @ 17&18
100,000	66.2	14	1205	27.18	93.4	59.7	14	1547	64.6	124.3
10,000	42.1	18	1406	17.74	59.84	15.0	14	1478	64.6	79.6
1,000	34.6	18	1406	17.74	52.3	8.1	18	1280	50.37	58.47
100	34.6	18	922	18.5	53.1	8.37	18	1280	50.37	58.74

14-Jun Cleveland (second)	1 Max Conc due to Source	2 Time 1 Occurs	3 Location 1 Occurs	4 Background Conc @ 3&4	5 Difference (1-4)	6 Max Conc due to Srce in Park	7 Time 6 Occurs	8 Location 6 Occurs	9 Background Conc @ 7&8	10 Difference (6-9)
100,000	127.3	12	1343	65.81	61.5	124.3	14	1545	64.7	59.6
10,000	85.5	9	1074	66.93	18.5	79.5	14	1748	64.75	14.77
1,000	71.6	7	937	67.84	3.73	67	14	1478	64.75	2.21
100	68.3	7	937	67.84	0.46	65	14	1478	64.75	0.26
basecase	68.25	7	2480			67.79	8	1420		

	11 Dif. Max Conc	12 Time 11 Occurs	13 Location 11 Occurs	14 Background Conc@ 12&13	15 Max Conc @ 12&13	16 Dif Max in Park	17 Time 16 Occurs	18 Location 16 Occurs	19 Background @ 17 & 18	20 Max Conc @ 17&18
100,000	61.51	12	1343	65.81	127.3	59.54	14	1545	64.7	124.3
10,000	18.55	9	1074	66.93	85.5	14.77	14	1478	64.75	79.52
1,000	5.05	5	867	62.89	67.94	2.21	14	1478	64.75	66.96
100	0.935	5	867	62.89	63.83	0.26	14	1478	64.75	65.01

30-Jun Crossville (prelim)	1 Max Conc due to Source	2 Time 1 Occurs	3 Location 1 Occurs	4 Background Conc @ 3&4	5 Difference (1-4)	6 Max Conc due to Srce in Park	7 Time 6 Occurs	8 Location 6 Occurs	9 Background Conc @ 7&8	10 Difference (6-9)
100,000	125.3	11	2197	68.61	56.7	no impact				
10,000	84.9	11	2129	67.21	17.7					
1,000	73.36	12	2470	72.64	0.72					
100	73.25	12	2148	73.25	0					
basecase	73.25	12	2148							

	11 Dif. Max Conc	12 Time 11 Occurs	13 Location 11 Occurs	14 Background Conc@ 12&13	15 Max Conc @ 12&13	16 Dif Max in Park	17 Time 16 Occurs	18 Location 16 Occurs	19 Background @ 17 & 18	20 Max Conc @ 17&18
100,000	57.2	11	2196	67.89	125.1	0.22	18	1614		
10,000	17.68	11	2129	67.21	84.9	0				
1,000	3.11	9	2058	66.52	69.63	0				
100	0.35	6	1987	62.09	62.44	0				

30-Jun Crossville (second)	1 Max Conc due to Source	2 Time 1 Occurs	3 Location 1 Occurs	4 Background Conc @ 3&4	5 Difference (1-4)	6 Max Conc due to Srce in Park	7 Time 6 Occurs	8 Location 6 Occurs	9 Background Conc @ 7&8	10 Difference (6-9)
100,000	130.2	11	2196	72.18	58.02	no impact				
10,000	90	11	2129	72.18	17.82					
1,000	74.94	11	2129	72.18	2.76					
100	73.25	12	2148	73.25	0					
basecase	73.25	12	2148							

	11 Dif. Max Conc	12 Time 11 Occurs	13 Location 11 Occurs	14 Background Conc@ 12&13	15 Max Conc @ 12&13	16 Dif Max in Park	17 Time 16 Occurs	18 Location 16 Occurs	19 Background @ 17 & 18	20 Max Conc @ 17&18
100,000	58	11	2196	72.18	130.2					
10,000	18.1	9	2057	71.44	89.54					
1,000	3.05	9	2058	71.46	74.51					
100	0.35	6	1987	67.23	67.58					

7-Jul Knoxville (prelim)	1 Max Conc due to Source	2 Time 1 Occurs	3 Location 1 Occurs	4 Background Conc @ 3&4	5 Difference (1-4)	6 Max Conc due to Srce in Park	7 Time 6 Occurs	8 Location 6 Occurs	9 Background Conc @ 7&8	10 Difference (6-9)
100,000	145.2	14	1476	76.7	68.5	142	12	1544	77.1	64.9
10,000	123.3	12	1676	77.3	46	120.9	14	1544	76.5	44.4
1,000	86.5	12	1676	77.3	9.2	85	14	1544	76.5	8.5
100	78.38	12	1676	77.32	1.06	77.94	13	1544	77.14	0.8
basecase	81.81	13	192			77.55	13	1685		

	11 Dif. Max Conc	12 Time 11 Occurs	13 Location 11 Occurs	14 Background Conc@ 12&13	15 Max Conc @ 12&13	16 Dif Max in Park	17 Time 16 Occurs	18 Location 16 Occurs	19 Background @ 17 & 18	20 Max Conc @ 17&18
100,000	68.5	14	1476	76.7	145.2	64.9	12	1544	77.1	142
10,000	46	12	1676	77.3	123.3	44.4	14	1544	76.5	120.9
1,000	9.2	12	1676	77.3	86.5	8.5	14	1544	76.5	85
100	1.06	12	1676	77.32	78.38	0.97	14	1544	76.5	77.47

7-Jul Knoxville (second)	1 Max Conc due to Source	2 Time 1 Occurs	3 Location 1 Occurs	4 Background Conc @ 3&4	5 Difference (1-4)	6 Max Conc due to Srce in Park	7 Time 6 Occurs	8 Location 6 Occurs	9 Background Conc @ 7&8	10 Difference (6-9)
100,000	145.7	14	1476	76.9	68.8	142.4	12	1544	77.26	65.14
10,000	123.5	12	1676	77.52	46	121.1	14	1544	76.65	44.45
1,000	86.74	12	1676	77.52	9.22	85.16	14	1544	76.65	8.51
100	78.58	12	1676	77.52	1.06	78.13	13	1544	77.33	0.8
basecase	79.02	13	1949			77.74	13	1685		

	11 Dif. Max Conc	12 Time 11 Occurs	13 Location 11 Occurs	14 Background Conc@ 12&13	15 Max Conc @ 12&13	16 Dif Max in Park	17 Time 16 Occurs	18 Location 16 Occurs	19 Background @ 17 & 18	20 Max Conc @ 17&18
100,000	68.81	14	1476	76.9	145.7	65.1	12	1544	77.26	142.36
10,000	46.03	12	1676	77.52	123.55	44.4	14	1544	76.65	121.1
1,000	9.22	12	1676	77.52	86.74	8.5	14	1544	76.65	85.15
100	1.06	12	1676	77.52	78.58	0.97	14	1544	76.65	77.62

10-Jul Knoxville (prelim)	1 Max Conc due to Source	2 Time 1 Occurs	3 Location 1 Occurs	4 Background Conc @ 3&4	5 Difference (1-4)	6 Max Conc due to Srce in Park	7 Time 6 Occurs	8 Location 6 Occurs	9 Background Conc @ 7&8	10 Difference (6-9)
100,000	119.1	12	1614	71.1	48	119.1	12	1614	71.1	48
10,000	84.9	10	1743	71.7	13.2	83.5	12	1614	71.1	12.4
1,000	73.4	12	1741	71.5	1.9	72.7	12	1614	71.1	1.6
100	71.48	13	1808	71.25	0.23	71.27	12	1614	71.11	0.16
basecase	73.6	10	1075			72.07	9	1284		

	11 Dif. Max Conc	12 Time 11 Occurs	13 Location 11 Occurs	14 Background Conc@ 12&13	15 Max Conc @ 12&13	16 Dif Max in Park	17 Time 16 Occurs	18 Location 16 Occurs	19 Background @ 17 & 18	20 Max Conc @ 17&18
100,000	48	12	1614	71.1	119.1	47.96	12	1614	71.11	119.1
10,000	13.24	10	1743	71.7	84.9	12.36	12	1614	71.11	83.5
1,000	2.14	13	1808	71.25	73.39	1.61	12	1614	71.11	72.7
100	0.234	13	1808	71.25	71.48	0.16	12	1614	71.11	71.27

10-Jul Knoxville (second)	1 Max Conc due to Source	2 Time 1 Occurs	3 Location 1 Occurs	4 Background Conc @ 3&4	5 Difference (1-4)	6 Max Conc due to Srce in Park	7 Time 6 Occurs	8 Location 6 Occurs	9 Background Conc @ 7&8	10 Difference (6-9)
100,000	119.3	12	1614	71.31	48	119.3	12	1614	71.11	48.2
10,000	85.1	10	1743	71.86	13.24	83.7	12	1614	71.11	12.59
1,000	73.75	10	1743	71.86	1.89	72.9	12	1614	71.11	1.79
100	72.25	11	2280	72.15	0.1	71.47	12	1614	71.11	0.36
basecase	72.29	10	2017			72.1	10	1286		

	11 Dif. Max Conc	12 Time 11 Occurs	13 Location 11 Occurs	14 Background Conc@ 12&13	15 Max Conc @ 12&13	16 Dif Max in Park	17 Time 16 Occurs	18 Location 16 Occurs	19 Background @ 17 & 18	20 Max Conc @ 17&18
100,000	48	12	1614	71.31	119.3	48	12	1614	71.11	119.1
10,000	13.24	10	1743	71.86	85.1	12.4	12	1614	71.11	83.51
1,000	2.14	13	1808	71.43	73.57	1.61	12	1614	71.11	72.72
100	0.234	13	1808	71.43	71.66	0.16	12	1614	71.11	71.27

25-Jul Tri-Cities (prelim)	1 Max Conc due to Source	2 Time 1 Occurs	3 Location 1 Occurs	4 Background Conc @ 3&4	5 Difference (1-4)	6 Max Conc due to Srce in Park	7 Time 6 Occurs	8 Location 6 Occurs	9 Background Conc @ 7&8	10 Difference (6-9)
100,000	120.31	11	2216	71.42	48.9	114.86	14	1685	69.13	45.7
10,000	82.51	10	2350	71.39	11.1	77.34	14	1685	69.13	8.2
1,000	73.05	12	1950	72.18	0.87	70.5	14	1617	69.73	0.77
100	72.59	11	1947	72.59	0	70.2	14	1213	70.2	0
basecase	72.59	11	1947							

	11 Dif. Max Conc	12 Time 11 Occurs	13 Location 11 Occurs	14 Background Conc@ 12&13	15 Max Conc @ 12&13	16 Dif Max in Park	17 Time 16 Occurs	18 Location 16 Occurs	19 Background @ 17 & 18	20 Max Conc @ 17&18
100,000	49.18	13	1884	70.84	120	45.93	15	1552	66.92	112.85
10,000	12.47	10	2491	67.88	80.4	9	16	1626	61.87	70.87
1,000	2.44	6	2819	65.69	68.1	1.18	17	1691	57.05	58.23
100	0.29	5	2821	61.02	61.3	0				

25-Jul Tri-Cities (second)	1 Max Conc due to Source	2 Time 1 Occurs	3 Location 1 Occurs	4 Background Conc @ 3&4	5 Difference (1-4)	6 Max Conc due to Srce in Park	7 Time 6 Occurs	8 Location 6 Occurs	9 Background Conc @ 7&8	10 Difference (6-9)
100,000	122.86	13	2092	71.35	51.51	115.5	14	1685	69.7	45.8
10,000	84.5	11	2491	71.87	12.63	77.9	14	1685	69.7	8.2
1,000	73.51	11	2558	71.98	1.53	72.1	13	1691	71.61	0.49
100	72.61	12	1947	72.59	0.02					0
basecase	72.59	12	1947			72.5	12	1547		

	11 Dif. Max Conc	12 Time 11 Occurs	13 Location 11 Occurs	14 Background Conc@ 12&13	15 Max Conc @ 12&13	16 Dif Max in Park	17 Time 16 Occurs	18 Location 16 Occurs	19 Background @ 17 & 18	20 Max Conc @ 17&18
100,000	51.53	14	2026	69.53	121.06	46.1	15	1552	67.71	113.81
10,000	12.64	11	2491	71.87	84.51	9.1	16	1625	65.16	74.26
1,000	2.44	6	2819	65.84	68.28	0.49	13	1691	71.61	72.1
100	0.29	5	2821	61.03	61.32	0				

VITA

Donald William Brew was born in Davenport, Iowa on August 24, 1972. Soon after, he and his family moved to Milan, Tennessee. He grew up there and graduated from Milan High School in 1990. He attended college at Christian Brothers University in Memphis, Tennessee where he received a Bachelor of Science degree in Civil Engineering the spring of 1994. That fall he enrolled in the Environmental Engineering graduate program at the University of Tennessee, Knoxville. He worked in the Air Pollution Control Lab at the University his final three semesters before receiving his Master of Science degree in the spring of 1996.